

Response to RC1

(responses in blue)

Mutz et al. look to use paleoclimate GCMs to identify drivers of past geomorphic change. This is a topic for which I hold great interest, and I feel that the authors have crafted a very useful set of model results that they leave underutilized. As such, I feel inclined to accept the paper on the basis of the useful results, but to request major revisions such that they do their own work justice.

My major concerns, which will become clear in the line-by-line comments (please feel free to respond to similar comments en masse) are as follows: 1. The paper is motivated by denudation rates and landscape evolution, but really includes this as a speculative wrapper that is not substantiated. I suggest that instead you propose testable hypotheses surrounding your findings.

2. Related to #1, much of the text is a litany of "temperature was X here ...". I find such statements of results useful only insofar as they expand upon a figure (associated with a supplementary data set) that presents the results. While these sections are written clearly, I would suggest that the authors focus on a set of geomorphic questions (if this be their motivation) and how the model-data set informs those questions.

3. Many of the discussions of model results are of ice-covered regions, yet no consideration of direct glacial erosion is given. Furthermore, no reference to the changes in the statistics of discharge or catchment area in ice-covered regions is given. This seems a disservice to this relatively high-resolution paleoclimate AGCM: the geologic setting *must* be considered, otherwise it seems that the authors' pushing on the modeling end has not been matched by a simple geological history sanity check. I would suggest that either significantly glaciated regions and the catchments that they feed be masked out, or that glacial erosion and its associated processes be included in the discussion.

4. (Discussed only here): You have not compared your models against any data. I understand that this may be simply a modeling exercise that you do compare to other models. However, I think that such a comparison could assuage skepticism about your results and lend support to your case, especially if you include it as part of a local case study (see the third point below). The core of these three points is that, with a bit more care, I think your results could say something really useful to the geomorphic community. Currently, the paper seems to be more a statement of, "this is important to geomorphology", followed by a long list of the model results. I challenge the authors to demonstrate (rather than simply stating) the importance of their work to geomorphology in a way that includes how it may impact the way scientists view Quaternary landscape evolution. Ideas include:

- Changes in means (done)
- Changes in statistical distributions of temperature and precipitation – think extreme events, frost-cracking window, etc.
- A focus on a few iconic regions while *explicitly* ignoring significantly ice-covered domains (I think this would be easiest, though obviously would be thrilled if you decided to tackle glacial processes)
- Using this focus to build a template for how to use paleoclimate GCM outputs to advance the field of geomorphology. Currently, I think that the work is acceptable following changes for internal consistency and geological accuracy (see #1 and #3), but I think that you could be selling yourselves short if you don't dig just a tiny bit deeper to investigate your forcings and their impact on geomorphology. I hope that you find these comments helpful in continuing to craft an insightful piece of work out of what seems to be a strong modeling approach.

We thank Prof. Andrew Wickert for his highly valuable review of our manuscript. Many important points were raised in the review and we hope that our appreciation for the input is sufficiently reflected in the revisions we made in response to it. We also encourage him to see our response to the second reviewer, where we provide additional geologic relevance of this study by now including a comparison of available terrestrial proxy data to our model results. We also explain throughout our response to the 2nd reviewer why an application of the predicted climate change to predict denudation rate changes is a large undertaking that can not be meaningfully conducted in this paper, but warrants more detailed applications of the models to individual areas (a topic of ongoing work/application for us). We refrain from using the model predicted runoff in the global GCM (even though it's conducted at relatively high resolution compared to previous work) to calculate changes in fluvial incision. This would be better done by mapping the predicted precipitation changes onto higher resolution (<90 m) DEMs and solving the kinematic wave equation for each fluvial erosion in each catchment, for

the changes in precipitation. However, as we repeatedly mention above, this is not possible to include in this manuscript without first characterising how the precipitation has changed in each region (the current manuscript goals). Work in progress we are conducting is trying to apply the kinematic wave equation and palaeoprecipitation to selected areas, but it's proving difficult to implement meaningfully without temporally continuous (e.g. LGM to present) simulations of precipitation change. We hope this brings to the reviewers attention the complications associated with doing full erosion history calculations based on these results. We have expanded the last paragraph in the instruction to convey the above perspective better, and more clearly articulate (and justify) the scope and limitations of the manuscript.

We appreciate the importance of addressing specific sets of geomorphic questions and hypotheses (1 & 2) and we are currently taking an in-depth look at quantifying the potential for erosion by a variety of processes. These include different methods of quantifying frost cracking intensity and extreme precipitation events and how these changed over time. However, in order to include those in this manuscript, we fear that would have to seriously compromise the thoroughness with which we investigate these questions at the moment. Instead, we hope that we can convey the usefulness of our consistently set up palaeoclimate simulations as a framework for addressing any of these particular questions in detail, and have modified sections of this manuscript accordingly. This includes, but is not restricted to, extensive compilations of proxy-based precipitation reconstructions for our two larger study sites (South Asia and western South America) and comparison of this data to our model output. With this, we hope that we were also able to address the concerns raised in point 4. In order to address the important point raised about glaciated areas (3), we added an ice cover layer on all of our difference plots, included global maps of ice extent (as used for our simulations) in the supplementary material, and discussed where the large differences in temperature and precipitation we highlight in the manuscript are accompanied by changes in ice cover. Thus we hope to prevent that interpretations of the implications of our results are made without consideration of changes in ice cover (and consequently shifts in the process domain).

Line-by-line:

23. US Pacific Northwest Pacific → drop second "Pacific"

This has been corrected. Thank you for catching that.

29. future observational studies interested in quantifying → future observational studies that quantify (studies can't be interested in things, strictly speaking)

That is right of course. It has been corrected as suggested.

53. orogen scale → orogen-scale

It has been corrected as suggested.

~57. A couple of recent studies from the climate science community shed light on the impacts of the Andes (first ref below) and continents in general (second ref below). In case these are interesting to you, I'm pasting the bibliographic information here:

Maroon, E. A., D. M. W. Frierson, and D. S. Battisti (2015), The tropical precipitation response to Andes topography and ocean heat fluxes in an aquaplanet model, *J. Clim.*, 28(1), 381–398, doi:10.1175/JCLI-D-14-00188.1.

Maroon, E. A., D. M. W. Frierson, S. M. Kang, and J. Scheff (2016), The precipitation response to an idealized subtropical continent, *J. Clim.*, 29(12), 4543–4564, doi:10.1175/JCLI-D-15-0616.1.

Many thanks for the references. These are indeed of much interest to us and we included them in the revised manuscript.

73-75. "Furthermore, recent controversy exists concerning the spatial and temporal scales over which geologic and geochemical observations can record climate-driven changes in weathering and erosion [e.g. Whipple, 2009; von Blanckenburg et al., 2015; Braun, 2016].": I see that you do not return to this point later, so could you describe the controversy for those who are not familiar with it?

Thank you for pointing this out. We described the controversy briefly for those unfamiliar with it after the sentence quoted above.

81. I see that later you discuss a little about what an AOGCM may do, but I will be looking for justification

about how an AGCM may suffice. Is this in part because you prescribe the b.c.'s and you are running it for 17 years only? If so, could you discuss potential systematic variations between this and an AOGCM?

We prescribe sea surface temperature reconstructions (SSTs) boundary conditions, which allows us to bypass the computationally expensive coupled simulations. Because these are fixed climatologies (though with seasonality preserved), the simulation of fewer years suffices. As a consequence, however, we do not expect to see decadal scale variability as we would in case of coupled models or prescribed SSTs that vary from year to year (such as present day simulations using AMIP SST's). We discuss this in the revised manuscript.

89. "PLIO to the Last Glacial Maximum": as you include no time-slices between these, I suggest making these part of the list and dropping the "to the".

This has been corrected as suggested.

147. "This section describes the clustering method used in this study." You could drop this sentence – the section title should be enough for even an inattentive reader!

We followed this suggestion and dropped that sentence.

176-178. I was wondering how you picked the number of clusters: I am glad to see that you performed a thorough search.

Thank you. We added some text explaining this. We systematically increased the number of clusters from 3 to 10 and assessed the distinctiveness or similarities of resulting climate clusters. Once the increase in the number of cluster no longer resulted in the addition of another cluster that was distinctly different from the others, we used this as a cut off point and used the cluster number of the previous iteration as the optimal cluster number.

Section 3: Much of this is information that I find better communicated through figures than with text. It is clearly written, however, and I am reluctant to suggest a rewrite for brevity in a length-unconstrained journal so long as the text can be co-located with the figure.

190-192. I see you have another "This section describes..." sentence. If this is your preferred way to write, you may keep it; here, the second sentence is not such a good topic-sentence replacement.

Thank you. We kept the sentence in this instance as it also immediately draws attention to the relevant figures, which may also serve in addressing the previous point you raised.

197-198. i.e. over the ice sheets. (This applies to other regions as well, and should be important to point out if you are going to then discuss fluvial processes in orogens)

Many thanks for pointing this out. We are more mindful of this in the revised discussion.

203-paragraph: Also because of local ice loss, presumably. So I think that the two prior paragraphs could have a new summary that "The greatest changes in temperature is observed where the greatest change in local ice extent occurs."

Thank you. We followed your suggestion.

214-215. Have you considered discussions of the African Humid Period?

We had not considered discussion of precipitation changes in North Africa, since it lies outside the regions we focus on. However, we appreciate that Holocene precipitation changes in the region are important and may be of interest to many readers. We therefore included a short discussion of Holocene precipitation changes in Northern Africa in the revised manuscript.

373-374. If you are looking at the influence of temperature and precipitation on erosion, and you are not including subglacial erosion, then your preceding text must indicate where your changes really are indicative of ice extent – both as a separate process domain and as a driver of fluvial processes and potential changes in the statistics of river discharge.

Thank you. We are more mindful of this in our discussion.

Section 4.1. Your first paragraph (weathering) differs from the content (comparing your model results with those published). These should be in different subsections, and the weathering paragraph may need to be expanded. Your "weathering and erosion" paragraph also neglects direct effects of glaciers, ice caps, and ice sheets, which were globally significant.

Thank you for this suggestion. We re-structured this section as suggested and took ice extent into consideration in the erosion section.

Section 4.2. Once again, your discussion is often of formerly (or currently) ice-covered regions without explicitly acknowledging that this is a different process domain. In addition, as with the previous section, the body paragraphs are mostly about model comparison and regional changes with sparse link to the landscape-evolution factors indicated in the topic paragraph.

As above, we restructured this section, took ice extent into account and chose a more fitting section title.

416-423. Please discuss the direct influence of glaciers on the erosion orogens in the context of changing precipitation (and therefore mass balance). Is it significant or not?

Although it is challenging to sufficiently quantify changes in glacier-related erosion due to differences in precipitation, we now include this point in our discussion.

433-434. "Coastal North America"? Doesn't look like it: seems to be most of NA south of the ice margin.

That is correct. We revised our descriptions accordingly.

Section 4.3. The authors describe the results here, but I find the connection to erosion rates to be insufficiently described compared to how they are highlighted in the topic sentence, as well as in the abstract. I would like you to go one step beyond "ought to be considered" and actually posit how you expect the erosion rates – and therefore, the balance between erosion and exhumation and perhaps the equilibrium shapes of the mountains and their rivers – to vary. Otherwise, you are suggesting future work rather than actually describing the possible geomorphic significance – and I think underutilizing your results in a paper that is clearly targeted towards geomorphologists.

As described in our response above, we believe that trying to address specific problems such as these or quantifying how differences would be expressed as erosion rates would be beyond the scope of this manuscript and come at the cost of not being able to address these as thoroughly as we are currently attempting in other ongoing work.

498. "which may favour frost driven weathering during glacial climate states" – the St. Elias range was covered by glaciers! Yes, there can be some frost-cracking around the ice, but don't you think this is important too? http://instaar.colorado.edu/groups/QGISL/ak_paleoglacier_atlas/gallery/index.html

Thank you for drawing our attention to this. We consider this in our discussion now and revised the manuscript accordingly.

508. "enhanced sediment production driven by frost processes" – same as above. Glaciers were there. Consider them.

As for the comment above, we also considered glaciers here in the revised manuscript.

Conclusions: Comparison to other models: is this match surprising or no? Did you (mostly) use the same inputs and simply increase the grid resolution? If so, could you comment on how the improved grid and possible variations in inputs and use of them ocean as a boundary condition may have affected (or not) your results as compared to those of earlier studies? This would be more useful to include in the discussion than a simple list of "Our temperature in place Y was T_0 , and X et al. wrote that they found it was T_1 , which is close to T_0 . Think big-picture, in both process and numerics!

Due to model-specific parameterisation, deviation is possible. In the revised manuscript, we comment on this as well as on the model resolution and implications of using ocean as boundary conditions instead of an ocean model.

533. Did your 8-10 degC changes occur significantly over areas that would be affected by hillslope or fluvial processes? (i.e. unglaciated areas?)

Some unglaciated areas experience large differences in temperature, but the maxima of 8-10 degC geographically coincide with ice cover changes. We acknowledge and discuss this in the revised manuscript.

1 Revised Manuscript

2 **Where is Late Cenozoic climate change most likely to impact** 3 **denudation?**

4
5 Sebastian G. Mutz¹, Todd A. Ehlers¹, Martin Werner², Gerrit Lohmann², Christian Stepanek²,
6 Jingmin Li^{1,3}

7 ¹Department of Geosciences, University Tübingen, D-72074 Tübingen, Germany

²Department of Paleoclimate Dynamics, Alfred Wegener Institute, Helmholtz Centre for Polar and Marine Research, D-
27570 Bremerhaven, Germany

8 ³[now at](#) Institute for Geography and Geology, University of Würzburg, Würzburg, D-97074 Germany

9 *Correspondence to:* Sebastian G. Mutz (sebastian.mutz@uni-tuebingen.de)

10

11 **Abstract**

12 The denudation history of active orogens is often interpreted in the context of modern climate and vegetation gradients.
13 Here we address the validity of this approach and ask the question: what are the spatial and temporal variations in
14 palaeo-climate for a latitudinally diverse range of active orogens? We do this using high-resolution (T159, ca. 80 x 80
15 km at the equator) palaeo-climate simulations from the ECHAM5 global Atmospheric General Circulation Model and a
16 statistical cluster analysis of climate over different orogens (Andes, Himalaya, SE Alaska, Pacific NW USA). Time
17 periods and boundary conditions considered include the Pliocene (PLIO, ~3 Ma), the Last Glacial Maximum (LGM,
18 ~21 ka), Mid Holocene (MH, ~6 ka) and Pre-Industrial (PI, reference year 1850). The regional simulated climates of
19 each orogen are described by means of cluster analyses based on the variability of precipitation, 2m air temperature, the
20 intra-annual amplitude of these values, and monsoonal wind speeds where appropriate. Results indicate the largest
21 differences to the PI climate ~~are observed~~ existed for the LGM and PLIO climates in the form of widespread cooling and
22 reduced precipitation in the LGM and warming and enhanced precipitation during the PLIO. The LGM climate shows
23 the largest deviation in annual precipitation from the PI climate, and shows enhanced precipitation in the temperate
24 Andes, and coastal regions for both SE Alaska and the US Pacific Northwest [Pacific](#). Furthermore, LGM precipitation
25 is reduced in the western Himalayas and enhanced in the eastern Himalayas, resulting in a shift of the wettest regional
26 climates eastward along the orogen. The cluster-analysis results also suggest more climatic variability across latitudes
27 east of the Andes in the PLIO climate than in other time-slice experiments conducted here. Taken together, these results
28 highlight significant changes in Late Cenozoic regional climatology over the last ~3 Ma. [Comparison of simulated](#)
29 [climate with proxy-based reconstructions for the MH and LGM reveal satisfactory to good performance of the model in](#)

30 | [reproducing precipitation changes, although in some cases discrepancies between neighbouring proxy observations](#)
31 | [highlight contradictions between proxy observations themselves](#). Finally, we document regions where the largest
32 | magnitudes of Late Cenozoic changes in precipitation and temperature occur and offer the highest potential for future
33 | observational studies ~~interested in quantifying~~ that quantify the impact of climate change on denudation and weathering
34 | rates.

35

36 | **Keywords:** Cenozoic climate, ECHAM5, Last Glacial Maximum, Mid-Holocene, Pliocene, cluster analysis, Himalaya,
37 | Tibet, Andes, Alaska, Cascadia

38

39 | 1. Introduction

40 | Interpretation of orogen denudation histories in the context of climate and tectonic interactions is often hampered
41 | by a paucity of terrestrial palaeo-climate proxy data needed to reconstruct spatial variations in palaeo-climate. [While it](#)
42 | [is self-evident that palaeoclimate changes could influence palaeodenudation rates, it is not always self-evident what the](#)
43 | [magnitude of climate change over different geologic time scales is, or what geographic locations offer the greatest](#)
44 | [potential to investigate palaeoclimate impacts on denudation](#). Palaeoclimate reconstructions are particularly beneficial
45 | when denudation rates are determined using geo- and thermo-chronology techniques that integrate over timescales of
46 | 10^3 - 10^6 years (e.g. cosmogenic radionuclides or low-temperature thermochronology) [e.g., Kirchner et al., 2001;
47 | Schaller et al., 2002; Bookhagen et al., 2005; Moon et al., 2011; Thiede and Ehlers, 2013; Lease and Ehlers, 2013].
48 | However, few studies using denudation rate determination methods that integrate over longer timescales have access to
49 | information about past climate conditions that could influence these palaeo-denudation rates. Palaeo-climate modelling
50 | offers an alternative approach to sparsely available proxy data for understanding the spatial and temporal variations in
51 | precipitation and temperature in response to changes in orography [e.g. Takahashi and Battisti, 2007a, b; Insel et al.,
52 | 2010; Feng et al., 2013] and global climate change events [e.g. Salzmann, 2011; Jeffery et al., 2013]. In this study, we
53 | characterize the climate at different times in the [Late](#) Cenozoic, and the magnitude of climate change for a range of
54 | active orogens. Our emphasis is on identifying changes in climate parameters relevant to weathering and catchment
55 | denudation to illustrate the potential importance of various global climate change events on surface processes.

56 | Previous studies of orogen-scale climate change provide insight into how different tectonic or global climate
57 | change events influence regional climate change. For example, sensitivity experiments demonstrated significant
58 | changes in regional and global climate in response to landmass distribution and topography of the Andes, including
59 | changes in moisture transport, [the north-south asymmetry of the Intertropical Convergence Zone and the north-south](#)
60 | [asymmetry of the Inter-Tropical Convergence Zone](#) [e.g. Takahashi and Battisti, 2007a, ; Insel et al., 2010] [and](#)

61 [\(tropical\) precipitation](#) [Maroon et al., 2015, ; ~~Maroon et al.~~ 2016]. [Another example is the regional](#) and global climate
62 changes induced by the Tibetan Plateau surface uplift due to its role as a ~~cold-temperature island and~~ physical obstacle
63 to circulation [Raymo and Ruddiman, 1992; Kutzbach et al., 1993; Thomas, 1997; Bohner, 2006; Molnar et al., 2010;
64 Boos and Kuang, 2010]. The role of tectonic uplift in long term regional and global climate change remains a focus of
65 research and continues to be assessed with geologic datasets [e.g. ~~Zhisheng, 2001~~; Dettman et al., 2003; [Caves et al.,](#)
66 [2017](#); [Kent-Corson et al., 2006](#); [Lechler et al., 2013](#); [Lechler and Niemi, 2011](#); [Licht et al., 2016](#);
67 [Methner et al., 2016](#); [Mulch et al., 2015, 2008](#); [Pingel et al., 2016](#)] and climate modelling [e.g. Kutzbach et
68 al., 1989; Kutzbach et al., 1993; ~~Zhisheng, 2001~~; Bohner, 2006; Takahashi and Battisti, 2007a; Ehlers and Poulsen,
69 2009; Insel et al., 2010; Boos and Kuang, 2010]. Conversely, climate influences tectonic processes through erosion
70 [e.g. Molnar and England, 1990; Whipple et al., 1999; Montgomery et al., 2001; Willett et al., 2006; Whipple, 2009].
71 Quaternary climate change between glacial and interglacial conditions [e.g. Braconnot et al., 2007; Harrison et al.,
72 2013] resulted in not only the growth and decay of glaciers and glacial erosion [e.g. Yanites and Ehlers, 2012; Herman
73 et al., 2013; Valla et al., 2011] but also global changes in precipitation and temperature [e.g. Otto-Bliesner et al., 2006;
74 Li et al., 2017] that could influence catchment denudation in non-glaciated environments [e.g. Schaller and Ehlers,
75 2006; Glotzbach et al., 2013; Marshall et al., 2015]. These dynamics highlight the importance of investigating how
76 much climate has changed over orogens that are [the](#) focus of studies of climate-tectonic interactions and their impact on
77 erosion.

78 Despite recognition by previous studies that climate change events relevant to orogen denudation are prevalent
79 throughout the Late Cenozoic, few studies have critically evaluated how different climate change events may, or may
80 not, have affected the orogen climatology, weathering and erosion. Furthermore, recent controversy exists concerning
81 the spatial and temporal scales over which geologic and geochemical observations can record climate-driven changes in
82 weathering and erosion [e.g. Whipple, 2009; von Blanckenburg et al., 2015; Braun, 2016]. [For example, the previous](#)
83 [studies highlight that although palaeoclimate impacts on denudation rates are evident in some regions and measurable](#)
84 [with some approaches, they are not always present \(or detectable\) and the spatial and temporal scale of climate change](#)
85 [influences our ability to record climate sensitive denudation histories.](#) This study contributes to our understanding of
86 the interactions between climate, weathering, and erosion by bridging the gap between the palaeoclimatology and
87 surface processes communities by documenting the magnitude and distribution of climate change over tectonically
88 active orogens. ~~Our focus is on documenting the magnitude of paleoclimateclimate and climate change in different~~
89 ~~locations with the intent of informing past and ongoing paleodenudation studies of these regions. The application of~~
90 ~~these results to predicted changes in denudation rates is beyond the scope of this study and the focus of future work.~~

91 ~~We~~ [In this study, we](#) employ the ECHAM5 global Atmospheric General Circulation Model and document
92 climate [and climate](#) change for time slices ranging between the Pliocene (PLIO, ~3 Ma) to pre-industrial (PI) times for

93 the St. Elias Range of South East Alaska, the US Pacific Northwest (Olympic and Cascade Range), western South
94 America (Andes) and South Asia (incl. parts of Central- and East Asia). Our approach is two-fold and includes:

95 | 1. An empirical characterizsation of palaeo-climates in these regions based on the covariance and spatial
96 clustering of monthly precipitation and temperature, the monthly change in precipitation and temperature magnitude,
97 and wind speeds where appropriate.

98 | 2. Identification of changes in annual mean precipitation and temperature in selected regions ~~over in the~~
99 ~~following time, specifically from the~~ for four time periods: (PLIO, ~~to the~~ Last Glacial Maximum (LGM), the Mid-
100 Holocene (MH) and PI): [and subsequent validation of the simulated precipitation changes for MH and LGM.](#)
101 Our focus is on documenting climate and climate change in different locations with the intent of informing past and
102 ongoing [palaeodenudation studies of these regions. The results presented here also provide a means for future work to](#)
103 [formulate testable hypotheses and investigations into whether or not regions of large palaeoclimate change produced a](#)
104 [measurable signal in denudation rates. In this study, we intentionally refrain from applying predicted palaeoclimate](#)
105 [changes to predict denudation rate changes. Such a prediction is beyond the scope of this study because a convincing](#)
106 [\(and meaningful\) calculation of climate-driven transients in fluvial erosion \(e.g. via the kinematic wave equation\),](#)
107 [variations in frost cracking intensity, or changes in hillslope sediment production and transport at the large regional](#)
108 [scales considered here is not tractable within a single manuscript, and instead is the focus of our ongoing work. Instead,](#)
109 [our emphasis lies on addressing the first question we are confronted with in our own research into denudation rate](#)
110 [studies around world, namely - where is Late Cenozoic climate change most likely to impact denudation?](#)

111

112 | 2. Methods: Climate modellng and cluster analyses for climate characteriszzation

113

114 2.1 ECHAM5 simulations

115 The global Atmospheric General Circulation Model ECHAM5 [Roeckner et al., 2003] has been developed at the
116 Max Planck Institute for Meteorology and is based on the spectral weather forecast model of the ECMWF [Simmons et
117 al., 1989]. In the context of palaeoclimate applications, the model has been used mostly at lower resolution (T31,
118 [approximately](#)ca. 3.75°x3.75°; [T63, ca. 1.9°x1.9° in case of Feng et al. \[2016\] and T106 in the case of Li et al. \[2016\]](#)
119 [and Feng and Poulsen \[2016\]](#)). The performed studies are not limited to the last millenium [e.g. Jungclaus et al., 2010]
120 but also include research in the field of both warmer and colder climates, at orbital [e.g. Gong et al., 2013; Lohmann et
121 al., 2013; Pfeiffer and Lohmann, 2016; Zhang et al., 2013a; Zhang et al., 2014; Wei and Lohmann, 2012] and tectonic
122 time scales [e.g. Knorr et al., 2011; Stepanek and Lohmann, 2012], and under anthropogenic influence [Gierz et al.,
123 2015].

124 Here, the ECHAM5 simulations were conducted at a T159 spatial resolution (horizontal grid size ca. 80 km x 80

125 km at the equator) with 31 vertical levels (between the surface and 10hPa). This high model resolution is admittedly not
126 required for [all of the climatological questions investigated in this study, and it should be noted that the skill of GCM's](#)
127 [in predicting orographic precipitation remains limited at this scale \[e.g. Meehl et al. 2007\]](#). However, simulations were
128 conducted at this resolution so that future work can apply the results [in combination with different dynamical and](#)
129 [statistical downscaling methods](#) to quantify changes at large catchment to orogen scales. [The output frequency is](#)
130 [relatively high \(1 day\) to enhance the usefulness of our simulations as input for landscape evolution and other models](#)
131 [that may benefit from daily input.](#)-The simulations were conducted for five different time periods: present-day (PD), PI,
132 MH, LGM and PLIO.

133 A PD simulation (not shown here) was used to establish confidence in the model performance before conducting
134 [palaeo-simulations](#) and has been compared with the following observation-based datasets: European Centre for
135 Medium-Range Weather Forecasts (ECMWF) re-analyses [ERA40, Uppala et al., 2005], National Centers for
136 Environmental Prediction and National Center for Atmospheric Research (NCEP/NCAR) re-analyses [Kalnay et al.,
137 1996; Kistler et al., 2001], NCEP Regional Reanalysis (NARR) [Mesinger et al., 2006], the Climate Research Unit
138 (CRU) TS3.21 dataset [Harris et al., 2013], High Asia Refined Analysis (HAR30) [Maussion et al., 2014] and the
139 University of Delaware dataset (UDEL v3.01) [Legates et al., 1990]. (See Mutz et al. [2016] for a detailed comparison
140 with a lower resolution model).

141 The PI climate simulation is an ECHAM5 experiment with PI (reference year 1850) boundary conditions. Sea
142 Surface Temperatures (SST) and Sea Ice Concentration (SIC) are derived from transient coupled ocean-atmosphere
143 simulations [Lorenz and Lohmann, 2004; Dietrich et al., 2013]. Following Dietrich et al. [2013], greenhouse gas
144 (GHG) concentrations ([CO₂: 280 ppm](#)) are taken from ice core based reconstructions of CO₂ [Etheridge et al., 1996],
145 CH₄ [Etheridge et al., 1998] and N₂O [Sowers et al., 2003]. Sea surface boundary conditions for MH originate from a
146 transient, low-resolution, coupled atmosphere-ocean simulation of the mid (6 ka) Holocene [Wei and Lohmann, 2012;
147 Lohmann et al, 2013], where the GHG concentrations ([CO₂: 280 ppm](#)) are taken from ice core reconstructions of
148 GHG's by Etheridge et al. [1996], Etheridge et al. [1998] and Sowers et al. [2003]. GHG's concentrations for the LGM
149 ([CO₂: 185 ppm](#)) have been prescribed following Otto-Bliesner et al. [2006]. Orbital parameters for MH and LGM are
150 set according to Dietrich et al. [2013] and Otto-Bliesner et al. [2006], respectively. LGM land-sea distribution and ice
151 sheet extent and thickness are set based on the PMIP III ([Palaeoclimate Modelling Intercomparison Project, phase 3](#))
152 guidelines (elaborated on by Abe-Ouchi et al [2015]). Following Schäfer-Neth and Paul [2003], SST and SIC for the
153 LGM are based on GLAMAP [Sarnthein et al. 2003] and CLIMAP [CLIMAP project members, 1981] reconstructions
154 for the [for the](#) Atlantic and Pacific/Indian Ocean, respectively. Global MH and LGM vegetation are based on maps of
155 plant functional types by the BIOME 6000 / Palaeovegetation Mapping Project [Prentice et al., 2000; Harrison et al.,
156 2001; Bigelow et al., 2003; Pickett et al., 2004] and model predictions by Arnold et al. [2009]. Boundary conditions for

157 | the PLIO simulation, including GHG concentrations ([CO2: 405](#)), orbital parameters and surface conditions (SST, SIC,
158 | sea land mask, topography and ice cover) are taken from the PRISM (Pliocene Research, Interpretation and Synoptic
159 | Mapping) project [Haywood et al., 2010; Sohl et al., 2009; Dowsett et al., 2010], [specifically PRISM3D](#). The PLIO
160 | vegetation boundary condition was created by converting the PRISM vegetation reconstruction to the JSBACH plant
161 | functional types as described by Stepanek and Lohmann [2012], [but the built-in land surface scheme was used](#).

162 | [SST reconstructions can be used as an interface between oceans and atmosphere \[e.g. Li et al. 2016\] instead of](#)
163 | [conducting the computationally more expensive fully coupled Atmosphere-Ocean GCM experiments. While the use of](#)
164 | [SST climatologies comes at the cost of capturing decadal-scale variability, and the results are ultimately biased towards](#)
165 | [the SST reconstructions the model is forced with, the simulated climate more quickly reaches an equilibrium state and](#)
166 | [the means of atmospheric variables used in this study do no change significantly after the relatively short spin-up](#)
167 | [period](#). The palaeoclimate simulations (PI, MH, LGM, PLIO) using ECHAM5 are [therefore](#) carried out for 17 model
168 | years, of which the first two years are used for model spin up. The monthly long-term averages (multi-year means for
169 | individual months) for precipitation, temperature, as well as precipitation and temperature amplitude, i.e. the mean
170 | difference between the hottest and coldest months, have been calculated from the following 15 model years for the
171 | analysis presented below.

172 | For further comparison between the simulations, the investigated regions were subdivided (Fig. 1). Western
173 | South America was subdivided into four regions: parts of tropical South America (80°-60° W, 23.5°-5° S), temperate
174 | South America (80°-60° W, 50°-23.5° S), tropical Andes (80°-60° W, 23.5°-5° S; high-pass filtered), i.e. most of the
175 | Peruvian Andes, Bolivian Andes and northernmost Chilean Andes, and temperate Andes (80°-60° W, 50°-23.5° S,
176 | high-pass filtered). South Asia was subdivided into three regions: tropical South Asia (40°-120°E, 0°-23.5°N),
177 | temperate South Asia (40°-120°E, 23.5°-60°N), and high altitude South Asia (40°-120°E, 0°-60°N; high-pass filtered).

178 | [Our approach of using a single GCM \(ECHAM5\) for our analysis is motivated by, and differs from, previous](#)
179 | [studies where inter-model variability exists from the use of different GCMs due to different parameterisations in each](#)
180 | [model. The variability in previous inter-model GCM comparisons exists despite the use of the same forcings \[e.g. see](#)
181 | [results highlighted in IPCC AR5\]. Similarities identified between these palaeoclimate simulations conducted with](#)
182 | [different GCMs using similar boundary conditions can establish confidence in the models when in agreement with](#)
183 | [proxy reconstructions. However, differences identified in inter-model GCM comparisons highlight biases by all or](#)
184 | [specific GCMs, or reveal sensitivities to one changed parameter, such as model resolution. Given these limitations of](#)
185 | [GCM modelling, we present in this study a comparison of a suite of ECHAM5 simulations to proxy-based](#)
186 | [reconstructions \(where possible\) and, to a lesser degree, comment on general agreement or disagreement of our](#)
187 | [ECHAM5 results with other modelling studies. A detailed inter-model comparison of our results with other GCMs is](#)
188 | [beyond the scope of this study, and better suited for a different study in a journal with a different focus and audience.](#)

189 [Rather, by using the same GCM and identical resolution for the time slice experiments, we reduce the number of](#)
190 [parameters \(or model parameterisations\) varying between simulations and thereby remove potential sources of error or](#)
191 [uncertainty that would otherwise have to be considered when comparing output from different models with different](#)
192 [parameterisations of processes, model resolution, and in some cases model forcings \(boundary conditions\).](#)
193 [Nevertheless, the reader is advised to use these model results with the GCM's shortcoming and uncertainties in](#)
194 [boundary condition reconstructions in mind. For example, precipitation results may require dynamical or statistical](#)
195 [downscaling to increase accuracy where higher resolution precipitation fields are required. Furthermore, readers are](#)
196 [advised to familiarise themselves with the palaeogeography reconstruction initiatives and associated uncertainties. For](#)
197 [example, while Pliocene ice sheet volume can be estimated, big uncertainties pertaining to their locations remain](#)
198 [\[Haywood et al. 2010\].](#)

199

200 **2.2 Cluster analysis to document temporal and spatial changes in climatology**

201 ~~This section describes the clustering method used in this study.~~ The aim of the clustering approach is to group
202 climate model surface grid boxes together based on similarities in climate. Cluster analyses are statistical tools that
203 allow elements (i) to be grouped by similarities in the elements' attributes. In this study, those elements are spatial units,
204 the elements' attributes are values from different climatic variables, and the measure of similarity is given by a
205 statistical distance. The four basic variables used as climatic attributes of these spatial elements are: near-surface (2m)
206 air temperature, seasonal 2m air temperature amplitude, precipitation rate, and seasonal precipitation rate amplitude.
207 Since monsoonal winds are a dominant feature of the climate in the South Asia region, near surface (10m) speeds of u-
208 wind and v-wind (zonal and meridional wind components, respectively) during the monsoon season (July) and outside
209 the monsoon season (January) are included as additional variables in our analysis of that region. Similarly, u-wind and
210 v-wind speeds during (January) and outside (July) the monsoon season in South America are added to the list of
211 considered variables to take into account the South American Monsoon System (SASM) in the cluster analysis for this
212 region. The long-term monthly means of those variables are used in a hierarchical clustering method, followed by a
213 non-hierarchical k-means correction with randomized re-groupment [Mutz et al., 2016; Wilks, 2011; Paeth, 2004;
214 Bahrenberg et al., 1992].

215 The hierarchical part of the clustering procedure starts with as many clusters as there are elements (ni), then
216 iteratively combines the most similar clusters to form a new cluster using centroids for the linkage procedure for
217 clusters containing multiple elements. The procedure is continued until the desired number of clusters (k) is reached.
218 One disadvantage of a pure hierarchical approach is that elements cannot be re-categorized once they are assigned to a
219 cluster, even though the addition of new elements to existing clusters changes the clusters' defining attributes and could
220 warrant a re-categorization of elements. We address this problem by implementation of a (non-hierarchical) k-means

221 clustering correction [e.g. Paeth, 2004]. Elements are re-categorized based on the multivariate centroids determined by
222 the hierarchical cluster analysis in order to minimize the sum of deviations from the cluster centroids. The
223 Mahalanobis distance [e.g. Wilks, 2011] is used as a measure of similarity or distance between the cluster centroids,
224 since it is a statistical distance and thus not sensitive to different variable units. The Mahalanobis distance also accounts
225 for possible multi-collinearity between variables.

226 The end results of the cluster analyses are subdivisions of the climate in the investigated regions into k
227 subdomains or clusters based on multiple climate variables. The region-specific k has to be prescribed before the
228 analyses. A large k may result in redundant additional clusters describing very similar climates, thereby defeating the
229 purpose of the analysis to identify and describe the dominant, distinctly different climates in the region and their
230 geographical coverage. Since it is not possible to know a priori the ideal number of clusters, k was varied between 3 and
231 10 for each region and the results presented below identify the optimal number of visibly distinctly different clusters
232 from the analysis. [Optimal \$k\$ was determined by assessing the distinctiveness and similarities between the climate
233 clusters in the systematic process of increasing \$k\$ from 3 to 10. Once an increase in \$k\$ no longer resulted in the addition
234 of another cluster that was climatologically distinctly different from the others, and instead resulted in at least two
235 similar clusters, \$k\$ of the previous iteration was chosen as the optimal \$k\$ for the region.](#)

236 [The cluster analysis ultimately results in a description of the geographical extent of a climate \(cluster\)
237 characterised by a certain combination of mean values for each of the variables associated with the climate. For
238 example, climate cluster 1 may be the most tropical climate in a region and thus be characterised by a high precipitation
239 values, high temperature values and low seasonal temperature amplitude. Each of the results \(consisting of the
240 geographical extent of climates and mean vectors describing the climate\) can be viewed as an optimal classification for
241 the specific region and time. It serves primarily as a means for providing an overview of the climate in each of the
242 regions at different times, reduces dimensionality of the raw simulation output, and identify regions of climatic
243 homogeneity that is difficult to notice by viewing simple maps of each climate variable. Its synoptic purpose is similar
244 to that of the widely known Köppen-Geiger classification scheme \[Peel et al., 2007\], but we allow for optimal
245 classification rather than prescribe classes, and our selection of variables is more restricted and made in accordance with
246 the focus of this study.](#)

247

248 3. Results

249 Results from our analysis are first presented for general changes in global temperature and precipitation for the
250 different time slices (Fig. 2, 3), which is then followed by an analysis of changes in the climatology of selected orogens.
251 A more detailed description of temperature and precipitation changes in our selected orogens is presented in subsequent
252 subsections (Fig. 4 and following). All differences in climatology are expressed relative to the PI control run. Changes

253 relative to the PI rather than PD conditions are presented to avoid interpreting an anthropogenic bias in the results and
254 focusing instead on pre-anthropogenic variations in climate. For brevity, near-surface (2m) air temperature and total
255 precipitation rate are referred to as temperature and precipitation.

256

257 **3.1 Global differences in mean annual temperature**

258 This section describes the differences between simulated MH, LGM, and PLIO annual mean temperature anom-
259 alies with respect to PI shown in Fig. 2b, and PI temperature absolute values shown in Fig. 2a. Most temperature differ-
260 ences between the PI and MH climate are within -1°C to 1°C . Exceptions to this are the Hudson Bay, Weddell Sea and
261 Ross Sea regions which experience warming of $1-3^{\circ}\text{C}$, $1-5^{\circ}\text{C}$ and $1-9^{\circ}\text{C}$ respectively. Continental warming is mostly
262 restricted to low-altitude South America, Finland, western Russia, the Arabian Peninsula ($1-3^{\circ}\text{C}$) and subtropical north
263 Africa ($1-5^{\circ}\text{C}$). Simulation results show that LGM and PLIO annual mean temperature deviate from the PI means the
264 most. The global PLIO warming and LGM cooling trends are mostly uniform in direction, but the magnitude varies re-
265 gionally. The strongest LGM cooling is concentrated in [regions where the greatest change in ice extent occurs \(as indic-](#)
266 [ated on Fig. 2\), i.e.](#) Canada, Greenland, the North Atlantic, Northern Europe and Antarctica. Central Alaska shows no
267 temperature changes, whereas coastal South Alaska experiences cooling of $\leq 9^{\circ}\text{C}$. Cooling in the US Pacific northwest
268 is uniform and between 11 and 13°C . Most of high-altitude South America experiences mild cooling of $1-3^{\circ}\text{C}$, $3-5^{\circ}\text{C}$ in
269 the central Andes and $\leq 9^{\circ}\text{C}$ in the south. Along the Himalayan orogen, LGM temperature values are $5-7^{\circ}\text{C}$ below PI
270 values. Much of central Asia and the Tibetan plateau cools by $3-5^{\circ}\text{C}$, and most of India, low-altitude China and south-
271 east Asia by $1-3^{\circ}\text{C}$.

272 In the PLIO climate, parts of Antarctica, Greenland and the Greenland Sea experience the greatest temperature
273 increase ($\leq 19^{\circ}\text{C}$). Most of southern Alaska warms by $1-5^{\circ}\text{C}$ and $\leq 9^{\circ}\text{C}$ near McCarthy, Alaska. The US Pacific northw-
274 est warms by $1-5^{\circ}\text{C}$. The strongest warming in South America is concentrated at the Pacific west coast and the Andes
275 ($1-9^{\circ}\text{C}$), specifically between Lima and Chiclayo, and along the Chilean-Argentinian Andes south of Bolivia ($\leq 9^{\circ}\text{C}$).
276 Parts of low-altitude South America to the immediate east of the Andes experience cooling of $1-5^{\circ}\text{C}$. The Himalayan
277 orogen warms by $3-9^{\circ}\text{C}$, whereas Myanmar, Bangladesh, Nepal, northern India and northeast Pakistan cool by $1-9^{\circ}\text{C}$.

278

279 **3.2 Global differences in mean annual precipitation**

280 Notable differences occur between simulated MH, LGM, PLIO annual mean precipitation anomalies with re-
281 spect to PI shown in Fig. 3b, and the PI precipitation absolute values shown in Fig. 3a. Of these, MH precipitation devi-
282 ates the least from PI values. The differences between MH and PI precipitation on land appear to be largest in northern
283 tropical Africa (increase ≤ 1200 mm/a) and along the Himalayan orogen (increase ≤ 2000 mm/a) and in central Indian
284 states (decrease) ≤ 500 mm. The biggest differences in western South America are precipitation increases in central Chile

285 between Santiago and Puerto Montt. The LGM climate shows the largest deviation in annual precipitation from the PI
286 climate, and precipitation on land mostly decreases. Exceptions are increases in precipitation rates in North American
287 coastal regions, especially in coastal South Alaska (≤ 2300 mm/a) and the US Pacific Northwest (≤ 1700 mm/a). Further
288 exceptions are precipitation increases in low-altitude regions immediately east of the Peruvian Andes (≤ 1800 mm/a),
289 central Bolivia (≤ 1000 mm/a), most of Chile (≤ 1000 mm/a) and northeast India (≤ 1900 mm/a). Regions of notable pre-
290 cipitation decrease are northern Brazil (≤ 1700 mm/a), southernmost Chile and Argentina (≤ 1900 mm/a), coastal south
291 Peru (≤ 700 mm/a), central India (≤ 2300 mm/a) and Nepal (≤ 1600 mm/a).

292 Most of the precipitation on land in the PLIO climate is higher than those in the PI climate. Precipitation is en-
293 hanced by ca. 100-200 mm/a in most of the Atacama desert, by ≤ 1700 mm/a south of the Himalayan orogen and by
294 ≤ 1400 mm/a in tropical South America. Precipitation significantly decreases in central Peru (≤ 2600 mm), southernmost
295 Chile (≤ 2600 mm) and from eastern Nepal to northernmost northeast India (≤ 2500 mm).

296

297 | 3.3 Palaeoclimate characterization from the cluster analysis and changes in regional climatology

298 In addition to the above described global changes, the PLIO to PI regional climatology changes substantially in
299 the four investigated regions of: South Asia (section 3.3.1), the Andes (section 3.3.2), South Alaska (section 3.3.3) and
300 the Cascade Range (section 3.3.4). Each climate cluster defines separate distinct climate that is characterized by the
301 mean values of the different climate variables used in the analysis. The clusters are calculated by taking the arithmetic
302 means of all the values (climatic means) calculated for the grid boxes within each region. The regional climates are
303 referred to by their cluster number C_1, C_2, \dots, C_k , where k is the number of clusters specified for the region. The clusters
304 for specific palaeo-climates are mentioned in the text as $C_{i(t)}$, where i corresponds to the cluster number ($i=1, \dots, k$) and
305 t to the simulation time period ($t=PI, MH, LGM, PLIO$). The descriptions first highlight the similarities and then the
306 differences in regional climate. The cluster means of seasonal near-surface temperature amplitude and seasonal
307 precipitation amplitude are referred to as temperature and precipitation amplitude. The median, 25th percentile, 75th
308 percentile, minimum and maximum values for annual mean precipitation are referred to as $P_{md}, P_{25}, P_{75}, P_{min}$ and P_{max}
309 respectively. Likewise, the same statistics for temperature are referred to as $T_{md}, T_{25}, T_{75}, T_{min}$ and T_{max} . These are
310 presented as boxplots of climate variables in different time periods. When the character of a climate cluster is described
311 as “high”, “moderate” and “low”, the climatic attribute’s values are described relative to the value range of the specific
312 region in time, thus high PLIO precipitation rates may be higher than high LGM precipitation rates. The character is
313 presented a raster plots, to allow compact visual representation of it. The actual mean values for each variable in every
314 time-slice and region-specific cluster are included in tables in the supplementary material.

315

316 | 3.3.1 Climate change and palaeoclimate characterization in South Asia, Central- and East Asia

317 This section describes the regional climatology of the four investigated Cenozoic time slices and how
318 precipitation and temperature changes from PLIO to PI times in tropical, temperate and high altitude regions. LGM and
319 PLIO simulations show the largest simulated temperature and precipitation deviations (Fig. 4b) from PI temperature and
320 precipitation (Fig. 4a) in the South Asia region. LGM temperatures are 1-7°C below PI temperatures and the direction
321 of deviation is uniform across the study region. PLIO temperature is mostly above PI temperatures by 1-7°C. The
322 cooling of 3-5°C in the region immediately south of the Himalayan orogen represents one of the few exceptions.
323 Deviations of MH precipitation from PI precipitation in the region are greatest along the eastern Himalayan orogeny,
324 which experiences an increase in precipitation (≤ 2000 mm/a). The same region experiences a notable decrease in
325 precipitation in the LGM simulation, which is consistent in direction with the prevailing precipitation trend on land
326 during the LGM. PLIO precipitation on land is typically higher than PI precipitation.

327 Annual means of precipitation and temperature spatially averaged for the regional subdivisions and the different
328 time slice simulations have been compared. The value range P_{25} to P_{75} of precipitation is higher for tropical South Asia
329 than for temperate and high altitude South Asia (Fig. 5 a-c). The LGM values for P_{25} , P_{md} and P_{75} are lower than for the
330 other time slice simulations, most visibly for tropical South Asia (ca. 100 mm/a). The temperature range (both $T_{75}-T_{25}$
331 and $T_{max}-T_{min}$) is smallest in the hot (ca. 21°C) tropical South Asia, wider in the high altitude (ca. -8°C) South Asia, and
332 widest in the temperate (ca. 2°C) South Asia region (Fig. 5 d-f). T_{md} , T_{25} and T_{75} values for the LGM are ca. 1°C, 1-2°C
333 and 2°C below PI and MH temperatures in tropical, temperate and high altitude South Asia respectively, whereas the
334 same temperature statistics for the PLIO simulation are ca. 1°C above PI and MH values in all regional subdivisions
335 (Fig. 5 d-f). With respect to PI and MH values, precipitation and temperature are generally lower in the LGM and
336 higher in the PLIO in tropical, temperate and high altitude South Asia.

337 In all time periods, the wettest climate cluster C_1 covers an area along the southeastern Himalayan orogen (Fig. 6
338 a-d) and is defined by the highest precipitation amplitude (dark blue, Fig. 6 e-h). $C_{5(PI)}$, $C_{3(MH)}$, $C_{4(LGM)}$ and $C_{5(PLIO)}$ are
339 characterized by (dark blue, Fig. 6e-h) the highest temperatures, u-wind and v-wind speeds during the summer monsoon
340 in their respective time periods, whereas $C_{4(PI)}$, $C_{5(MH)}$, and $C_{6(LGM)}$ are defined by low temperatures and highest
341 temperature amplitude, u-wind and v-wind speeds outside the monsoon season (in January) in their respective time
342 periods (Fig. 6 e-h). The latter 3 climate classes cover much of the more continental, northern landmass in their
343 respective time periods and represents a cooler climate affected more by seasonal temperature fluctuations (Fig. 6 a-d).
344 The two wettest climate clusters C_1 and C_2 are more restricted to the eastern end of the Himalayan orogen in the LGM
345 than during other times, indicating that the LGM precipitation distribution over the South Asia landmass is more
346 concentrated in this region than in other time slice experiments.

347

349 This section describes the cluster analysis based regional climatology of the four investigated Late Cenozoic
350 time slices and illustrates how precipitation and temperature changes from PLIO to PI in tropical and temperate low-
351 and high altitude (i.e. Andes) regions in western South America (Fig. 7-9).

352 LGM and PLIO simulations show the largest simulated deviations (Fig. 7b) from PI temperature and
353 precipitation (Fig. 7a) in western South America. The direction of LGM temperature deviations from PI temperatures is
354 negative and uniform across the region. LGM temperatures are typically 1-3°C below PI temperatures across the region,
355 and 1-7°C below PI values in the Peruvian Andes, which also experience the strongest and most widespread increase in
356 precipitation during the LGM (≤ 1800 mm/a). Other regions, such as much of the northern Andes and tropical South
357 America, experience a decrease of precipitation in the same experiment. PLIO temperature is mostly elevated above PI
358 temperatures by 1-5°C. The Peruvian Andes experience a decrease in precipitation (≤ 2600 mm), while the northern
359 Andes are wetter in the PLIO simulation compared to the PI control simulation.

360 PI, MH, LGM and PLIO precipitation and temperature means for regional subdivisions have been compared.
361 The P_{25} to P_{75} range is smallest for the relatively dry temperate Andes and largest for tropical South America and the
362 tropical Andes (Fig. 8 a-d). P_{max} is lowest in the PLIO in all four regional subdivisions even though P_{md} , P_{25} and P_{75} in
363 the PLIO simulation are similar to the same statistics calculated for PI and MH time slices. P_{md} , P_{25} and P_{75} for the LGM
364 are ca. 50 mm/a lower in tropical South America and ca. 50 mm/a higher in the temperate Andes. Average PLIO
365 temperatures are slightly warmer and LGM temperatures are slightly colder than PI and MH temperatures in tropical
366 and temperate South America (Fig. 8 e and f). These differences are more pronounced in the Andes, however. T_{md} , T_{25}
367 and T_{75} are ca. 5°C higher in the PLIO climate than in PI and MH climates in both temperate and tropical Andes,
368 whereas the same temperatures for the LGM are ca. 2-4°C below PI and MH values (Fig. 8 g and h).

369 For the LGM, the model computes drier-than-PI conditions in tropical South America and tropical Andes,
370 enhanced precipitation in the temperate Andes, and a decrease in temperature that is most pronounced in the Andes. For
371 the PLIO, the model predicts precipitation similar to PI, but with lower precipitation maxima. PLIO temperatures
372 generally increase from PI temperatures, and this increase is most pronounced in the Andes.

373 The climate variability in the region is described by six different clusters (Fig. 9 a-d), which have similar
374 attributes in all time periods. The wettest climate C_1 is also defined by moderate to high precipitation amplitudes, low
375 temperatures and moderate to high u-wind speeds in summer and winter in all time periods (dark blue, Fig. 9 e-h). $C_{2(PI)}$,
376 $C_{2(MH)}$, $C_{3(LGM)}$ and $C_{2(PLIO)}$ are characterized by high temperatures and low seasonal temperature amplitude (dark blue,
377 Fig. 9 e-h), geographically cover the north of the investigated region, and represent a more tropical climate. $C_{5(PI)}$,
378 $C_{5(MH)}$, $C_{6(LGM)}$ and $C_{6(PLIO)}$ are defined by low precipitation and precipitation amplitude, high temperature amplitude and
379 high u-wind speeds in winter (Fig. 9 e-h), cover the low-altitude south of the investigated region (Fig. 9 a-d) and
380 represent dry, extra-tropical climates with more pronounced seasonality. In the PLIO simulation, the lower-altitude east

381 of the region has four distinct climates, whereas the analysis for the other time slice experiments only yield three
382 distinct climates for the same region.

383

384 | 3.3.3 Climate change and palaeoclimate characterization in the St. Elias Range, Southeast Alaska

385 This section describes the changes in climate and the results from the cluster analysis for South Alaska (Fig. 10-12). As
386 is the case for the other study areas, LGM and PLIO simulations show the largest simulated deviations (Fig. 10b) from
387 PI temperature and precipitation (Fig. 10a). The sign of LGM temperature deviations from PI temperatures is negative
388 and uniform across the region. LGM temperatures are typically 1-9°C below PI temperatures, with the east of the study
389 area experiencing largest cooling. PLIO temperatures are typically 1-5°C above PI temperatures and the warming is
390 uniform for the region. In comparison to the PI simulation, LGM precipitation is lower on land, but higher ($\leq 2300\text{mm}$)
391 in much of the coastal regions of South Alaska. Annual PLIO precipitation is mostly higher ($\leq 800\text{mm}$) than for PI.

392 P_{md} , P_{25} , P_{75} , P_{min} and P_{max} for South Alaskan mean annual precipitation do not differ much between PI, MH and
393 PLIO climates, while P_{md} , P_{25} , P_{75} and P_{min} decrease by ca. 20-40 mm/a and P_{max} increases during the LGM (Fig. 11a).
394 The Alaskan PLIO climate is distinguished from the PI and MH climates by its higher (ca. 2°C) regional temperature
395 means, T_{25} , T_{75} and T_{md} (Fig. 11b). Mean annual temperatures, T_{25} , T_{75} , T_{min} and T_{max} are lower in the LGM than in any
396 other considered time period (Fig. 11b), and about 3-5°C lower than during the PI and MH.

397 Distinct climates are present in the PLIO to PI simulations for Southeast Alaska. Climate cluster C_1 is always
398 geographically restricted to coastal southeast Alaska (Fig. 12 a-d) and characterized by the highest precipitation,
399 precipitation amplitude, temperature, and by relatively low temperature amplitude (dark blue, Fig. 12 e-h). Climate C_2 is
400 characterized by moderate to low precipitation, precipitation amplitude, temperature, and by low temperature amplitude.
401 C_2 is either restricted to coastal southeast Alaska (in MH and LGM climates) or coastal southern Alaska (in PI and
402 PLIO climates). Climate C_3 is described by low precipitation, precipitation amplitude, temperature, and moderate
403 temperature amplitude in all simulations. It covers coastal western Alaska and separates climate C_1 and C_2 from the
404 northern C_4 climate. Climate C_4 is distinguished by the highest mean temperature amplitude, by low temperature and
405 precipitation amplitude, and by lowest precipitation.

406 The geographical ranges of PI climates C_1 - C_4 and PLIO climates C_1 - C_4 are similar. $C_{1(\text{PI/PLIO})}$ and $C_{2(\text{PI/PLIO})}$ spread
407 over a larger area than $C_{1(\text{MH/LGM})}$ and $C_{2(\text{MH/LGM})}$. $C_{2(\text{PI/PLIO})}$ are not restricted to coastal southeast Alaska, but also cover the
408 coastal southwest of Alaska. The main difference in characterization between PI and PLIO climates C_1 - C_4 lies in the
409 greater difference (towards lower values) in precipitation, precipitation amplitude and temperature from $C_{1(\text{PLIO})}$ to
410 $C_{2(\text{PLIO})}$ compared to the relatively moderate decrease in those means from $C_{1(\text{PI})}$ to $C_{2(\text{PI})}$.

411

412 | 3.3.4 Climate change and palaeoclimate characterization in the Cascade Range, US Pacific Northwest

413 This section describes the character of regional climatology in the US Pacific Northwest and its change over time
414 (Fig. 13-15). The region experiences cooling of typically 9-11°C on land during the LGM, and warming of 1-5°C
415 during the PLIO (Fig. 13b) when compared to PI temperatures (Fig. 13a). LGM precipitation increases over water,
416 decreases on land by ≤ 800 mm/a in the North and in the vicinity of Seattle and increases on land by ≤ 1400 mm/a on
417 Vancouver Island, around Portland and the Olympic Mountains, whereas PLIO precipitation does not deviate much
418 from PI values over water and varies in the direction of deviation on land. MH temperature and precipitation deviation
419 from PI values are negligible.

420 P_{md} , P_{25} , P_{75} , P_{min} and P_{max} for the Cascade Range do not notably differ between the four time periods (Fig. 14a).
421 The LGM range of precipitation values is slightly larger than that of the PI and MH with slightly increased P_{md} , while
422 the respective range is smaller for simulation PLIO. The T_{md} , T_{25} , T_{75} and T_{max} values for the PLIO climate are ca. 2°C
423 higher than those values for PI and MH (Fig. 14b). All temperature statistics for the LGM are notably (ca. 13°C) below
424 their analogues in the other time periods (Fig. 14b).

425 PI, LGM and PLIO clusters are similar in both their geographical patterns (Fig. 15 a, c, d) and their
426 characterization by mean values (Fig. 15 e, g, h). C_1 is the wettest cluster and shows the highest amplitude in
427 precipitation. The common characteristics of the C_2 cluster are moderate to high precipitation and precipitation
428 amplitude. C_4 is characterized by the lowest precipitation and precipitation amplitudes, and the highest temperature
429 amplitudes. Regions assigned to clusters C_1 and C_2 are in proximity to the coast, whereas C_4 is geographically restricted
430 to more continental settings.

431 In the PI and LGM climates, the wettest cluster C_1 is also characterized by high temperatures (Fig 10 e, g).
432 However, virtually no grid boxes were assigned to $C_{1(LGM)}$. $C_{1(MH)}$ differs from other climate state's C_1 clusters in that it is
433 also described by moderate to high near surface temperature and temperature amplitude (Fig 10 f), and in that it is
434 geographically less restricted and, covering much of Vancouver Island and the continental coastline north of it (Fig 10
435 b). Near surface temperatures are highest for C_2 in PI, LGM and PLIO climates (Fig 10 e, g, h) and low for $C_{2(MH)}$ (Fig
436 10 f). $C_{2(MH)}$ is also geographically more restricted than C_2 clusters in PI, LGM and PLIO climates (Fig 10 a-d). $C_{2(PI)}$,
437 $C_{2(MH)}$ and $C_{2(LGM)}$ have a low temperature amplitude (Fig 10 e-g), whereas $C_{2(PLIO)}$ is characterized by a moderate
438 temperature amplitude (Fig 10 h).

439

440 4. Discussion

441 In the following, we synthesize our results and compare to previous studies that investigate the effects of
442 temperature and precipitation change on erosion. [Since our results do not warrant merited discussion of subglacial](#)
443 [processes without additional work that is beyond the scope of this study, we instead advise caution in interpreting the](#)
444 [presented precipitation and temperature results in an erosional context where the regions are covered with ice. For](#)

445 [convenience, ice cover is indicated on figures 2,3,4,7,10 and 13, and a summary of ice cover used as boundary](#)
446 [conditions for the different time slice experiments is included in the supplemental material.](#) Where possible, we relate
447 the magnitude of climate change predicted in each geographical study area with terrestrial proxy data.

448

449 | **4.1 Synthesis of temperature changes and implications for weathering and erosion**

450

451 | **4.1.1 Temperature changes and implications for weathering and erosion**

452 Changes in temperature can affect physical weathering due to temperature-induced changes in periglacial
453 processes and promote frost cracking and frost creep [e.g., Matsuoka, 2001; Schaller et al., 2002; Matsuoka and
454 Murton, 2008; Delunel et al., 2010; [Andersen et al., 2015](#); Marshall et al., 2015], and also biotic weathering and erosion
455 [e.g. Moulton et al., 1998; Banfield et al., 1999; Dietrich and Perron, 2006]. Quantifying and understanding past
456 changes in temperature is thus vital for our understanding of denudation histories. In the following, we highlight regions
457 in the world where future observational studies might be able to document significant warming or cooling that would
458 influence temperature related changes in physical and chemical weathering over the last ~3 Ma.

459 Simulated MH temperatures show little deviation (typically < 1°C) from PI temperatures in the investigated
460 regions (Fig. 2b), suggesting little difference in MH temperature-related weathering. [The LGM experiences widespread](#)
461 [cooling, which is accentuated at the poles. LGM cooling is accentuated at the poles, in general agreement with studies](#)
462 [such as Otto-Bliesner et al. \[2006\] and Braconnot et al. \[2007\], and , increases in](#) the equator-to-pole pressure gradient
463 and consequently strengthens global atmospheric circulation. Despite this global trend, cooling in coastal South Alaska
464 is higher ($\leq 9^\circ\text{C}$) than in central Alaska ($0\pm 1^\circ\text{C}$). [The larger temperature difference in South Alaska geographically](#)
465 [coincides with ice cover \(Fig. 10b\), and should thus be interpreted in context of a different erosional regime.](#) Cooling in
466 most of the lower-latitude regions in South America and central to southeast Asia is relatively mild. [The greatest](#)
467 [temperature differences in South America are observed for western Patagonia, which was mostly covered by glaciers.](#)
468 The Tibetan plateau experiences more cooling (3-5°C) than adjacent low-altitude regions (1-3°C) during the LGM.

469 The PLIO simulation [is generally warmer, and temperature differences are shows little to no warming in the](#)
470 [tropics and accentuated warming at the poles, as do findings of Salzmann et al. \[2011\] and Robinson \[2009\] and](#)
471 [Ballantyne \[2010\] respectively. This would reduce the equator-to-pole sea and land surface temperature gradient, as](#)
472 [also reported by Dowsett et al. \[2010\], and also weaken global atmospheric circulation. Agreement with proxy-based](#)
473 [reconstructions, as is the case of the relatively little warming in lower latitudes, is not surprising given that sea surface](#)
474 [temperature reconstructions are prescribed in this uncoupled atmosphere simulation. It should be noted that coupled](#)
475 [ocean-atmosphere simulations do predict more low-latitude warming \[e.g. Stepanek and Lohmann 2012; Zhang et al.](#)
476 [2013b\].](#) Warming in simulation PLIO is [present](#) greatest in parts of Canada, [and](#) Greenland and Antarctica (up to

19°C), [which geographically coincides with the presence of ice in the PI reference simulation and thus may be attributed to differences in ice cover. It should therefore also be regarded as areas in which process domain shifted from glacial to non-glacial.](#) and consistent with values based on multi-proxy studies [Ballantyne et al., 2010]. Due to a scarcity of paleo-botanical proxies in Antarctica, reconstruction-based temperature and ice-sheet extent estimates for a PLIO climate have high uncertainties [Salzmann et al., 2011], making model validation difficult. Furthermore, controversy about relatively little warming in the south polar regions compared to the north polar regions remains [e.g. Hillenbrand and Fütterer, 2002; Wilson et al., 2002]. Mid-latitude PLIO warming is mostly in the 1-3°C range with notable exceptions of cooling in the northern tropics of Africa and on the Indian subcontinent, especially south of the ~~Himalayan orogen~~. The warming in simulation PLIO in South Alaska and the US Pacific northwest is mostly uniform and in the range of 1-5°C. [As before, changes in ice cover reveal that the greatest warming may be associated with the absence of glaciers relative to the PI simulation.](#) ~~whereas~~ Warming in South America is concentrated at the Pacific west coast and the Andes between Lima and Chiclayo, and along the Chilean-Argentinian Andes south of Bolivia ($\leq 9^\circ\text{C}$).

Overall, annual mean temperatures in the MH simulation show little deviation from PI values. The more significant temperature deviations of the colder LGM and of the warmer PLIO simulations are accentuated at the poles leading to higher and lower equator-to-pole temperature gradients respectively. The largest temperature-related changes (relative to PI conditions) in weathering and subsequent erosion, [in many cases through a shift in the process domain from glacial to non-glacial or vice versa](#), are therefore to be expected in the LGM and PLIO climates.

4.1.2 Temperature comparison to other studies

[LGM cooling is accentuated at the poles, thus increases the equator-to-pole pressure gradient and consequently strengthens global atmospheric circulation, and is in general agreement with studies such as Otto-Bliesner et al. \[2006\] and Braconnot et al. \[2007\]. The PLIO simulation shows little to no warming in the tropics and accentuated warming at the poles, as do findings of Salzmann et al. \[2011\] and Robinson \[2009\] and Ballantyne \[2010\] respectively. This would reduce the equator-to-pole sea and land surface temperature gradient, as also reported by Dowsett et al. \[2010\], and also weaken global atmospheric circulation. Agreement with proxy-based reconstructions, as is the case of the relatively little warming in lower latitudes, is not surprising given that sea surface temperature reconstructions \(derived from previous coarse resolution coupled ocean-atmosphere models\) are prescribed in this uncoupled atmosphere simulation. It should be noted that coupled ocean-atmosphere simulations do predict more low-latitude warming \[e.g. Stepanek and Lohmann 2012; Zhang et al. 2013b\]. The PLIO warming in parts of Canada and Greenland \(up to 19°C\) and consistent with values based on multi-proxy studies \[Ballantyne et al., 2010\]. Due to a scarcity of palaeobotanical proxies in Antarctica, reconstruction-based temperature and ice-sheet extent estimates for a PLIO climate have high uncertainties](#)

509 | [\[Salzmann et al., 2011\]](#), making model validation difficult. Furthermore, controversy about relatively little warming in
510 | [the south polar regions compared to the north polar regions remains \[e.g. Hillenbrand and Fütterer, 2002; Wilson et al.,](#)
511 | [2002\]. Mid-latitude PLIO warming is mostly in the 1-3°C range with notable exceptions of cooling in the northern](#)
512 | [tropics of Africa and on the Indian subcontinent, especially south of the Himalayan orogen.](#)

513

514 | **4.2 Synthesis of precipitation changes ~~and implications for orogen denudation~~**

515

516 | **[4.2.1 Precipitation and implications for weathering and erosion](#)**

517 | Changes in precipitation affects erosion through river incision, sediment transport, and erosion due to extreme
518 | precipitation events and storms [e.g. Whipple and Tucker, 1999; Hobley et al., 2010]. Furthermore, vegetation type and
519 | cover also co-evolve with variations in precipitation and with changes in geomorphology [e.g. Marston 2010; Roering
520 | et al., 2010]. These vegetation changes in turn modify hillslope erosion by increasing root mass and canopy cover, and
521 | decreasing water-induced erosion via surface runoff [e.g. Gyssels et al., 2005]. Therefore, understanding and
522 | quantifying changes in precipitation in different palaeo-climates is necessary for a more complete reconstruction of
523 | orogen denudation histories. A synthesis of predicted precipitation changes is provided below, and highlights regions
524 | where changes in river discharge and hillslope processes might be impacted by climate change over the last ~3 Ma.

525 | [Most of North Africa is notably wetter during the MH, which is characteristic of the African Humid Period](#)
526 | [\[Sarnthein 1978\]. This pluvial regional expression of the Holocene Climatic Optimum is attributed to sudden changes in](#)
527 | [the strength of the African monsoon caused by orbital-induced changes in summer insolation \[e.g. deMenocal et al.](#)
528 | [2000\]. Southern Africa is characterised by a wetter climate to the east and drier climate to the west of the approximate](#)
529 | [location of the Congo Air Boundary \(CAB\), the migration of which has previously been cited as a cause for](#)
530 | [precipitation changes in East Africa \[e.g. Juninger et al. 2014\].](#) In contrast, simulated MH precipitation rates show little
531 | deviation from the PI in most of the investigated regions, suggesting little difference in MH precipitation-related
532 | erosion. The Himalayan orogen is an exception and shows a precipitation increase of [≤ up to 2000 mm/a](#). The climate's
533 | enhanced erosion potential, that could result from such a climatic change, should be taken into consideration when
534 | palaeo-erosion rates estimated from the geological record in this area are interpreted [e.g. Bookhagen et al., 2005].
535 | Specifically, higher precipitation rates (along with differences in other rainfall-event parameters) could increase the
536 | probability of mass movement events on hillslopes, especially where hillslopes are close to the angle of failure [e.g.
537 | Montgomery, 2001], and modify fluxes to increase shear stresses exerted on river beds and increase stream capacity to
538 | enhance erosion on river beds (e.g. by abrasion).

539 | Most precipitation on land is decreased during the LGM due to large-scale cooling and decreased evaporation
540 | over the tropics, resulting in an overall decrease in inland moisture transport [e.g., Braconnot et al. 2007]. [Coastal](#)-North

541 America, south of the continental ice sheets, is an exception and experiences increases in precipitation. For example,
542 the investigated US Pacific Northwest and the southeastern coast of Alaska are exceptions in that there is experience
543 experience strongly enhanced precipitation of ≤ 1700 mm/a and ≤ 2300 mm/a, respectively. These changes

544 geographically coincide with differences in ice extent. An increase in precipitation in these regions may have had direct
545 consequences on the glaciers' mass balance and equilibrium line altitudes, where the glaciers' effectiveness in erosion is
546 highest [e.g. Egholm et al., 2009; Yanites and Ehlers, 2012]. The differences in the direction of precipitation changes,
547 and accompanying changes in ice cover. Reduced precipitation in other parts of southern Alaska result in a stronger
548 south-to-north drying gradient than in the PI simulation. This could would likely result in more regionally differentiated
549 variations in precipitation-specific erosional processes in the St. Elias Range rather than causing systematic offsets for
550 the LGM. Although precipitation is significantly reduced along much of the Himalayan orogen (≤ 1600 mm/a), which is
551 consistent with findings by, e.g., Braconnot et al. [2007], northeast India experiences strongly enhanced precipitation
552 (≤ 1900 mm/a). This could have large implications for studies of uplift and erosion at orogen syntaxes, where highly
553 localized and extreme denudation has been documented [e.g. Koons et al., 2013; Bendick and Ehlers, 2014].

554 Overall, the PLIO climate is wetter than the PI climate, in particular in the (northern) mid-latitudes, and possibly
555 related to a northward shift of the northern Hadley cell boundary that is ultimately the result of a reduced equator-to-
556 pole temperature gradient [e.g. Haywood et al. 2000, 2013; Dowsett et al. 2010]. A reduction of this gradient by ca. 5°C
557 is indeed present in the PLIO simulation of this study (Fig. 2b). Most of the PLIO precipitation over land increases
558 during the PLIO. This finding agrees well with simulations performed at a lower spatial model resolution [cf. Stepanek
559 and Lohmann, 2012]. PLIO precipitation significantly increases, esp. at the Himalayan orogen by ≤ 1400 mm/a, and
560 decreases from eastern Nepal to Namcha Barwa (≤ 2500 mm/a). Most of the Atacama Desert experiences an increase in
561 precipitation by 100-200 mm/a, which may have to be considered in erosion and uplift history reconstructions for the
562 Andes. A significant increase (~ 2000 mm/a) in precipitation from simulation PLIO to modern conditions is simulated
563 for the eastern margin of the Andean Plateau in Peru and for northern Bolivia. This is consistent with recent findings of
564 a pulse of canyon incision in these locations in the last ~ 3 Ma [Lease and Ehlers, 2013].

565 Overall, the simulated MH precipitation varies least from PI precipitation. The LGM is generally drier than the
566 PI simulation, even though pockets of a wetter-than-PI climate do exist, such as much of coastal North America. Extra-
567 tropical increased precipitation of the PLIO simulation and decreased precipitation of the LGM climate may be the
568 result of decreased and increased equator-to-pole temperature gradients, respectively.

569

570 **4.2.2 Precipitation comparison to other studies**

571 The large scale LGM precipitation decrease on land, related to cooling and decreased evaporation over the
572 tropics, and greatly reduced precipitation along much of the Himalayan orogeny, is consistent with previous studies by,

573 [\(for example\) Braconnot et al. \[2007\]. The large scale PLIO precipitation increase due to a reduced equator-to-pole](#)
574 [temperature gradient, has previously been pointed out by e.g. Haywood et al. \[2000, 2013\] and Dowsett et al. \[2010\]. A](#)
575 [reduction of this gradient by ca. 5°C is indeed present in the PLIO simulation of this study \(Fig. 2b\). This precipitation](#)
576 [increase over land agrees well with simulations performed at a lower spatial model resolution \[cf. Stepanek and](#)
577 [Lohmann, 2012\]. Section 4.4 includes a more in-depth discussion of how simulated MH and LGM precipitation](#)
578 [differences compare with proxy-based reconstructions in South Asia and South America.](#)

579

580 **4.3 Trends in Late Cenozoic changes in regional climatology**

581 This section describes the major changes in regional climatology and highlights their possible implications on
582 erosion rates.

583

584 *Himalaya-Tibet, South Asia*

585 In South Asia, cluster-analysis based categorization and description of climates (Fig. 6) remains similar
586 throughout time. However, the two wettest climates (C₁ and C₂) are geographically more restricted to the eastern
587 Himalayan orogen in the LGM simulation. Even though precipitation over the South Asia region is generally lower, this
588 shift indicates that rainfall on land is more concentrated in this region and that the westward drying gradient along the
589 orogen is more accentuated than during other time periods investigated here. While there is limited confidence in the
590 global Atmospheric General Circulation Model's abilities to accurately represent meso-scale precipitation patterns [e.g.
591 Cohen 1990], the simulation warrants careful consideration of possible, geographically non-uniform offsets in
592 precipitation in investigations of denudation and uplift histories.

593 MH precipitation and temperature in tropical, temperate and high-altitude South Asia is similar to PI
594 precipitation and temperature, whereas LGM precipitation and temperatures are generally lower (by ca. 100 mm/a and
595 1-2°C respectively), possibly reducing precipitation-driven erosion and enhancing frost-driven erosion in areas pushed
596 into a near-zero temperature range during the LGM.

597

598 *Andes, South America*

599 Clusters in South America (Fig. 9), which are somewhat reminiscent of the Köppen and Geiger classification
600 [Kraus, 2001], remain mostly the same over the last 3 Ma. In the PLIO simulation, the lower-altitude east of the region
601 is characterized by four distinct climates, which suggests enhanced latitudinal variability in the PLIO climate compared
602 to PI with respect temperature and precipitation.

603 The largest temperature deviations from PI values are derived for the PLIO simulation in the (tropical and
604 temperate) Andes, where temperatures exceed PI values by 5°C. On the other hand, LGM temperatures in the Andes are

605 ca. 2-4°C below PI values in the same region (Fig 7 g and h). In the LGM simulation, tropical South America
606 experiences ca. 50 mm/a less precipitation, the temperate Andes receive ca. 50 mm/a more precipitation than in PI and
607 MH simulations. These latitude-specific differences in precipitation changes ought to be considered in attempts to
608 reconstruct precipitation-specific palaeo-erosion rates in the Andes on top of longitudinal climate gradients highlighted
609 by, e.g., Montgomery et al. [2001].

610

611 *St. Elias Range, South Alaska*

612 South Alaska is subdivided into two wetter and warmer clusters in the south, and two drier, colder clusters in the
613 north. The latter are characterized by increased seasonal temperature variability due to being located at higher latitudes
614 (Fig. 12). The different equator-to-pole temperature gradients for LGM and PLIO may affect the intensity of the Pacific
615 North American Teleconnection (PNA) [Barnston and Livzey, 1987], which has significant influence on temperatures
616 and precipitation, especially in southeast Alaska, and may in turn result in changes in regional precipitation and
617 temperature patterns and thus on glacier mass balance. Changes in the Pacific Decadal Oscillation, which is related to
618 the PNA pattern, has previously been connected to differences in Late Holocene precipitation [Barron and Anderson,
619 2011]. While this climate cluster pattern appears to be a robust feature for the considered climate states, and hence over
620 the recent geologic history, the LGM sets itself apart from PI and MH climates by generally lower precipitation (20-40
621 mm) and lower temperatures (3-5°C, Fig. 10, 11), which may favour frost driven weathering during glacial climate
622 states [e.g. Andersen et al., 2015; Marshall et al. 2015] in unglaciated areas, whereas glacial processes would have
623 dominated most of this region as it was covered by ice. Simulation PLIO is distinguished by temperatures that exceed
624 PI and MH conditions by ca. 2°C, and by larger temperature and precipitation value ranges, possibly modifying
625 temperature- and precipitation-dependent erosional processes in the region of South Alaska.

626

627 *Cascade Range, US Pacific Northwest*

628 In all time slices, the geographic climate patterns, based on the cluster analysis (Fig. 15), represents an increase
629 in the degree of continentality from the wetter coastal climates to the further inland located climates with greater
630 seasonal temperature amplitude and lower precipitation and precipitation amplitude (Fig 15 e-h). The most notable
631 difference between the time slices is the strong cooling during the LGM, when temperatures are ca. 13°C (Fig. 13, 14)
632 below those of other time periods. Given that the entire investigated region was covered by ice (Fig 13), we can assume
633 a shift to glacially dominated processes. possibly leading to enhanced sediment production driven by frost processes, as
634 proposed for parts of the Pacific Northwest by Marshall et al. [2015].

635

636 **4.4 Comparison of simulated and observed precipitation differences**

637 [The predicted precipitation differences reported in this study were compared with observed \(proxy record\)](#)
638 [palaeoprecipitation change. Proxy based precipitation reconstructions for the MH and LGM are presented for South](#)
639 [Asia and South America for the purpose of assessing ECHAM5 model performance, and for identifying inconsistencies](#)
640 [between neighbouring proxy data. Due to the repeated glaciations, detailed terrestrial proxy records for the time slices](#)
641 [investigated here are not available, to the best of our knowledge, for the Alaskan and Pacific NW USA studies.](#)
642 [Although marine records and records of glacier extent are available in these regions, the results from them do not](#)
643 [explicitly provide estimates of wetter/drier, or colder/warmer conditions that can be spatially compared to the](#)
644 [simulation estimates. For these two areas with no available records, the ECHAM5 predicted results therefore provide](#)
645 [predictions from which future studies can formulate testable hypotheses to evaluate.](#)

646 [The palaeoclimate changes in terrestrial proxy records compiled here are reported as “wetter than today”, “drier](#)
647 [than today” or “the same as today” for each of the study locations, and plotted on top of the simulation-based difference](#)
648 [maps as upward facing blue triangles, downward facing red triangles and grey circles respectively \(Fig. 16, 17\). The](#)
649 [numbers listed next to those indicators are the ID numbers assigned to the studies compiled for this comparison and are](#)
650 [associated with a citation provided in the figure captions.](#)

651 [In South Asia, 14/26 results from local studies agree with the model predicted precipitation changes for the MH.](#)
652 [The model seems able to reproduce the predominantly wetter conditions on much of the Tibetan plateau, but predicts](#)
653 [slightly drier conditions north of Chengdu, which is not reflected in local reconstructions. The modest mismatch](#)
654 [between ECHAM5 predicted and proxy-based MH climate change in south Asia was also documented by Li et al.,](#)
655 [\[2017\], whose simulations were conducted at a coarser \(T106\) resolution. Despite these model-proxy differences, we](#)
656 [note that there are significant discrepancies between the proxy data themselves in neighbouring locations in the MH,](#)
657 [highlighting caution in relying solely upon these data for regional palaeoclimate reconstructions. These differences](#)
658 [could result from either poor age-constraints in the reported values, or systematic errors in the transfer functions used to](#)
659 [convert proxy measurements to palaeoclimate conditions. The widespread drier conditions on the Tibetan Plateau and](#)
660 [immediately north of Laos are confirmed by 7/7 of the palaeoprecipitation reconstructions. 23/39 of the reconstructed](#)
661 [precipitation changes agree with model predictions for South America during the MH. The model predicted wetter](#)
662 [conditions in the central Atacama desert, as well as the drier conditions northwest of Santiago are confirmed by most of](#)
663 [the reconstructions. The wetter conditions in southernmost Peru and the border to Bolivia and Chile cannot be](#)
664 [confirmed by local studies. 11/17 of the precipitation reconstructions for the LGM are in agreement with model](#)
665 [predictions. These include wetter conditions in most of Chile. The most notable disagreement can be seen in northeast](#)
666 [Chile at the border to Argentina and Bolivia, where model predicted wetter conditions are not confirmed by reported](#)
667 [reconstructions from local sites.](#)

668 [Model performance is, in general, higher for the LGM than for the MH and overall satisfactory given that it](#)

669 [cannot be expected to resolve sub-grid scale differences in reported palaeoprecipitation reconstructions. However, as](#)
670 [mentioned above, it should be noted that some locations \(MH of south Asia, and MH of norther Chile\) discrepancies](#)
671 [exist between neighbouring proxy samples and highlight the need for caution in how these data are interpreted. Other](#)
672 [potential sources of error resulting in disagreement of simulated and proxy-based precipitation estimates are the model's](#)
673 [shortcomings in simulating orographic precipitation at higher resolutions, and uncertainties in palaeoclimate](#)
674 [reconstructions at the local sites. In summary, although some differences are evident in both the model-proxy data](#)
675 [comparison and between neighbouring proxy data themselves, the above comparison highlights an overall good](#)
676 [agreement between the model and data for the south Asia and South American study areas. Thus, although future](#)
677 [advances in GCM model parameterisations and new or improved palaeoclimate proxy techniques are likely, the](#)
678 [palaeoclimate changes documented here are found to be in general robust and provide a useful framework for future](#)
679 [studies investigating how these predicted changes in palaeoclimate impact denudation.](#)

680

681 | **4.45 Conclusions**

682 | We present a [statistical](#) cluster-analysis-based description of the geographic coverage of possible distinct
683 regional expressions of climates from four different time slices (Fig. 6, 9, 12, 15). These are determined with respect to
684 a selection of variables that characterize the climate of the region and may be relevant to weathering and erosional
685 processes. While the geographic [distribution of](#) climate [patterns](#) remains similar throughout time (as indicated by results
686 of four different climate states representative for the climate of the last 3 Ma), results for the PLIO simulation suggests
687 more climatic variability east of the Andes (with respect to near-surface temperature, seasonal temperature amplitude,
688 precipitation, seasonal precipitation amplitude and seasonal u-wind and v-wind speeds). Furthermore, the wetter
689 climates in the South Asia region retreat eastward along the Himalayan orogen for the LGM simulation, this is due to
690 decreased precipitation along the western part of the orogen and enhanced precipitation on the eastern end, possibly
691 signifying more localised high erosion rates.

692 Most global trends of the high-resolution LGM and PLIO simulations conducted here are in general agreement
693 with previous studies [Otto-Bliesner et al., 2006; Braconnot et al., 2007; Wei and Lohmann, 2012; Lohmann et al.,
694 2013; Zhang et al., 2013b, 2014; Stepanek and Lohmann, 2012]. The MH does not deviate notably from the PI, the
695 LGM is relatively dry and cool, while the PLIO is comparably wet and warm. While the simulated regional changes in
696 temperature and precipitation usually agree with the sign [\(or direction\)](#) of the simulated global changes, there are
697 region-specific differences in the magnitude and direction. For example, the LGM precipitation of the Tropical Andes
698 does not deviate significantly from PI precipitation, whereas LGM precipitation in the Temperate Andes is enhanced.

699 [Comparisons to local, proxy-based reconstructions of MH and LGM precipitation in South Asia and South](#)
700 [America reveal satisfactory performance of the model in simulating the reported differences. The model performs better](#)

701 [for the LGM than the MH. We note however that compilations of proxy data such as we present here, also identify](#)
702 [inconsistencies between neighbouring proxy data themselves, warranting caution in the extent to which both proxy data](#)
703 [and palaeoclimate models are interpreted for MH climate change in south Asia, and western South America.](#)

704 The changes in regional climatology presented here are manifested, in part, by small to large magnitude changes
705 in fluvial and hillslope relevant parameters such as precipitation and temperature. For the regions investigated here we
706 find that precipitation differences between the PI, MH, LGM, and PLIO are in many areas around +/- 200-600 mm/yr,
707 and locally can reach maximums of +/- 1000-2000 mm/yr (Figs. 4, 7, 10, 13). [In areas where significant precipitation](#)
708 [increases are accompanied by changes in ice extent, such as parts of southern Alaska during the LGM, we would expect](#)
709 [a shift in the erosional regime to glacier dominated processes.](#) Temperature differences between these same time periods
710 are around 1-4 °C in many places, but reach maximum values of 8-10 °C. [Many of these maxima in the temperature](#)
711 [differences geographically coincide with changes in ice sheet extent and must therefore be interpreted as part of a](#)
712 [different erosional process domains. However, we also observe large temperature differences \(~5°C\) in unglaciated](#)
713 [areas that would be affected by hillslope, frost cracking, and fluvial processes.](#) The magnitude of these differences are
714 not trivial, and will likely impact fluvial and hillslope erosion and sediment transport, as well as biotic and abiotic
715 weathering. The regions of large magnitude changes in precipitation and temperature documented here (Figs. 4, 7, 10,
716 13) offer the highest potential for future observational studies interested in quantifying the impact of climate change on
717 denudation and weathering rates.

718

719

720 **Acknowledgements**

721 [The model simulations presented in this study are freely available to interested persons by contacting S. Mutz or T.](#)
722 [Ehlers. We note however that the data files are very large \(~4 TB, and too large to archive in journal supplementary](#)
723 [material\) and require familiarity in reading/plotting NetCDF formatted files. Support from](#) European Research Council
724 (ERC) Consolidator Grant number 615703 provided support for S. Mutz. Additional support is acknowledged from the
725 German science foundation (DFG) priority research program 1803 (EarthShape: Earth Surface Shaping by Biota; grants
726 EH329/14-1 and EH329/17-1). We thank B. Adams and J. Starke for constructive discussions. The DKRZ is thanked
727 for computer time used for some of the simulations presented here. C. Stepanek, M. Werner, and G. Lohmann
728 acknowledge funding by the Helmholtz Climate Initiative Reklim and the Alfred Wegener Institute's research
729 programme Marine, Coastal and Polar Systems.

730

731

732 **Figure Captions**

733

734 **Figure 1** Topography for regions (a) tropical South Asia, (b) temperate South Asia, (c) high altitude South Asia, (d)
735 temperate South America, (e) tropical South America, (f) temperate Andes, (g) tropical Andes-, [SE Alaska and Cas-](#)
736 [cadia](#).

737 **Figure 2** Global PI annual mean near-surface temperatures (a), and deviations of MH, LGM and PLIO annual mean
738 near-surface temperatures from PI values (b). Units are °C and insignificant ($p < 99\%$) differences (as determined by
739 a t-test) are greyed out.

740 **Figure 3** Global PI annual mean precipitation (a), and deviations of MH, LGM and PLIO annual mean near-surface
741 temperatures from PI values (b). Units are mm/yr.

742 **Figure 4** PI annual mean near-surface temperatures (a), and deviations of MH, LGM and PLIO annual mean near-sur-
743 face temperatures from PI values (b) for the South Asia region. Insignificant ($p < 99\%$) differences (as determined
744 by a t-test) are greyed out.

745 **Figure 5** PI, MH, LGM and PLIO annual mean precipitation in (a) tropical South Asia, (b) temperate South Asia, and
746 (c) high-altitude South Asia; PI, MH, LGM and PLIO annual mean temperatures in (d) tropical South Asia, (e) tem-
747 perate South Asia, and (f) high-altitude South Asia. For each time slice, the minimum, lower 25th percentile, median,
748 upper 75th percentile and maximum are plotted.

749 **Figure 6** Geographical coverage and characterization of climate classes C_1 - C_6 based on cluster-analysis of 8 variables
750 (near surface temperature, seasonal near surface temperature amplitude, total precipitation, seasonal precipitation
751 amplitude, u-wind in January and July, v-wind in January and July) in the South Asia region. The geographical cov-
752 erage of the climates C_1 - C_6 is shown on the left for PI (a), MH (b), LGM (c) and PLIO (d); the complementary,
753 time-slice specific characterization of C_1 - C_6 for PI (e), MH (f), LGM (g) and PLIO (h) is shown on the right.

754 **Figure 7** PI annual mean near-surface temperatures (a), and deviations of MH, LGM and PLIO annual mean near-sur-
755 face temperatures from PI values (b) for western South America. Insignificant ($p < 99\%$) differences (as determined
756 by a t-test) are greyed out.

757 **Figure 8** PI, MH, LGM and PLIO annual mean precipitation in (a) tropical South America, (b) temperate South Amer-
758 ica, (c) tropical Andes, and (d) temperate Andes; PI, MH, LGM and PLIO annual mean temperatures in (e) tropical

759 South America, (f) temperate South America, (g) tropical Andes, and (h) temperate Andes. For each time slice, the
760 minimum, lower 25th percentile, median, upper 75th percentile and maximum are plotted.

761 **Figure 9** Geographical coverage and characterization of climate classes C₁- C₆ based on cluster-analysis of 8 variables
762 (near surface temperature, seasonal near surface temperature amplitude, precipitation, seasonal precipitation amp-
763 litude, u-wind in January and July, v-wind in January and July) in western South America. The geographical cover-
764 age of the climates C₁- C₆ is shown on the left for PI (a), MH (b), LGM (c) and PLIO (d); the complementary, time-
765 slice specific characterization of C₁- C₆ for PI (e), MH (f), LGM (g) and PLIO (h) is shown on the right.

766 **Figure 10** PI annual mean near-surface temperatures (a), and deviations of MH, LGM and PLIO annual mean near-sur-
767 face temperatures from PI values (b) for the South Alaska region. Insignificant (p < 99%) differences (as determined
768 by a t-test) are greyed out.

769 **Figure 11** PI, MH, LGM and PLIO annual mean precipitation (a), and mean annual temperatures (b) in South Alaska.
770 For each time slice, the minimum, lower 25th percentile, median, upper 75th percentile and maximum are plotted.

771 **Figure 12** Geographical coverage of climate classes C₁- C₄ based on cluster-analysis of 4 variables (near surface tem-
772 perature, seasonal near surface temperature amplitude, total precipitation, seasonal total precipitation amplitude) in
773 southern Alaska. The geographical coverage of the climates C₁- C₄ is shown on the left for PI (a), MH (b), LGM (c)
774 and PLIO (d); the complementary, time-slice specific characterization of C₁- C₆ for PI (e), MH (f), LGM (g) and
775 PLIO (h) is shown on the right.

776 **Figure 13** PI annual mean near-surface temperatures (a), and deviations of MH, LGM and PLIO annual mean near-sur-
777 face temperatures from PI values (b) for the US Pacific Northwest. Insignificant (p < 99%) differences (as determ-
778 ined by a t-test) are greyed out.

779 **Figure 14** PI, MH, LGM and PLIO annual mean precipitation (a), and annual mean temperatures (b) in the Cascades,
780 US Pacific Northwest. For each time slice, the minimum, lower 25th percentile, median, upper 75th percentile and
781 maximum are plotted.

782 **Figure 15** Geographical coverage and characterization of climate classes C₁- C₄ based on cluster-analysis of 4 variables
783 (near surface temperature, seasonal near surface temperature amplitude, total precipitation, seasonal total precipita-
784 tion amplitude) in the Cascades, US Pacific Northwest. The geographical coverage of the climates C₁- C₄ is shown
785 on the left for PI (a), MH (b), LGM (c) and PLIO (d); the complementary, time-slice specific characterization of C₁-

786 C₆ for PI (e), MH (f), LGM (g) and PLIO (h) is shown on the right.

787 **Figure 16** [Simulated annual mean precipitation deviations of MH \(left\) and LGM \(right\) from PI values in South Asia,](#)
788 [and temporally corresponding proxy-based reconstructions, indicating wetter \(upward facing blue triangles\), drier](#)
789 [\(downward facing red triangles\) or similar \(grey circles\) conditions in comparison with modern climate. MH proxy-](#)
790 [based precipitation differences are taken from Mügler et al. \(2010\) \(66\), Wischnewski et al. \(2011\) \(67\), Mischke et](#)
791 [al. \(2008\), Wischnewski et al. \(2011\), Herzs Schuh et al. \(2009\) \(68\), Yanhong et al. \(2006\) \(69\), Morrill et al. \(2006\)](#)
792 [\(70\), Wang et al. \(2002\) \(71\), Wuennemann et al. \(2006\) \(72\), Zhang et al. \(2011\), Morinaga et al. \(1993\),](#)
793 [Kashiwaya et al. \(1995\) \(73\), Shen et al. \(2005\) \(74\), Liu et al. \(2014\) \(75\), Herzs Schuh et al. \(2006\) \(76\), Zhang and](#)
794 [Mischke \(2009\) \(77\), Nishimura et al. \(2014\) \(78\), Yu and Lai \(2014\) \(79\), Gasse et al. \(1991\) \(80\), Van Campo et](#)
795 [al. \(1996\) \(81\), Demske et al. \(2009\) \(82\), Kramer et al. \(2010\) \(83\), Herzs Schuh et al. \(2006\) \(84\), Hodell et al.](#)
796 [\(1999\)\(85\), Hodell et al. \(1999\) \(86\), Shen et al. \(2006\) \(87\), Tang et al. \(2000\) \(88\), Tang et al. \(2000\) \(89\), Zhou](#)
797 [et al. \(2002\) \(90\), Liu et al. \(1998\) \(91\), Asashi \(2010\)\(92\), Kotila et al. \(2009\) \(93\), Kotila et al. \(2000\) \(94\), Wang](#)
798 [et al. \(2002\) \(95\), Hu et al. \(2014\) \(96\), Hodell et al. \(1999\) \(97\), Hodell et al. \(1999\) \(98\).](#)

799 **Figure 17** [Simulated annual mean precipitation deviations of MH \(left\) and LGM \(right\) from PI values in South Amer-](#)
800 [ica, and temporally corresponding proxy-based reconstructions, indicating wetter \(upward facing blue triangles\),](#)
801 [drier \(downward facing red triangles\) or similar \(grey circles\) conditions in comparison with modern climate. MH](#)
802 [proxy-based precipitation differences are taken from Bird et al. \(2011\) \(1\), Hansen et al \(1994\) \(2\), Hansen et al](#)
803 [\(1994\) \(3\), Hansen et al \(1994\) \(4\), Hansen et al \(1994\) \(5\), Hansen et al \(1994\) \(6\), Hillyer et al. \(2009\) \(7\),](#)
804 [D'Agostino et al. \(2002\) \(8\), Baker et al. \(2001\) \(9\), Schwalb et al \(1999\) \(10\), Schwalb et al \(1999\) \(11\), Schwalb](#)
805 [et al \(1999\) \(12\), Schwalb et al \(1999\) \(13\), Moreno et al \(2009\) \(14\), Pueyo et al \(2011\) \(15\), Mujica et al \(2015\)](#)
806 [\(16\), Fritz et al. \(2004\) \(17\), Gayo et al. \(2012\) \(18\), Latorre et al. \(2006\) \(19\), Latorre et al. \(2003\) \(20\), Quade et al](#)
807 [\(2008\) \(21\), Bobst et al. \(2001\) \(22\), Grosjean et al. \(2001\) \(23\), Betancourt et al. \(2000\) \(24\), Latorre et al. \(2002\)](#)
808 [\(25\), Rech et al. \(2003\) \(26\), Diaz et al. \(2012\) \(27\), Maldonado et al \(2005\) \(28\), Diaz et al. \(2012\) \(29\), Lamy et](#)
809 [al. \(2000\) \(30\), Kaiser et al. \(2008\) \(31\), Maldonado et al. \(2010\) \(32\), Villagrán et al. \(1990\) \(33\), Méndez et al.](#)
810 [\(2015\) \(34\), Maldonado et al. \(2006\) \(35\), Lamy et al. \(1999\) \(36\), Jenny et al. \(2002\) \(37\), Jenny et al. \(2002b\)](#)
811 [\(38\), Villa-Martínez et al. \(2003\) \(39\), Bertrand et al. \(2008\) \(40\), De Basti et al. \(2008\) \(41\), Lamy et al. \(2009\)](#)
812 [\(42\), Lamy et al. \(2002\) \(43\), Szeicz et al. \(2003\) \(44\), de Porras et al. \(2012\) \(45\), de Porras et al. \(2014\) \(46\),](#)
813 [Markgraf et al. \(2007\) \(47\), Siani et al. \(2010\) \(48\), Gilli et al. \(2001\) \(49\), Markgraf et al. \(2003\) \(50\), Stine et al.](#)
814 [\(1990\) \(51\).](#)

815

817 **References**

818

819 Abe-Ouchi, A., Saito, F., Kageyama, M., Bracannot, P., Harrison, S. P., Lambeck, K., Otto-Bliesner, B. L., Peltier,
820 W.R., Tarasov, L., Peterschmitt, J.-Y., Takahashi, K.: Ice-sheet configuration in the CMUP5/PMIP3 Last Glacial
821 Maximum experiments. *Geosci. Model Dev.*, 8, 3621-3637, doi:10.5194/gmd-8-3621-2015, 2015

822 [Andersen, J., Egholm, D.L., Knudsen, M.F., Jansen, J., Nielsen, S.B., The periglacial engine of mountain erosion – Part](#)
823 [1: Rates of frost cracking and frost creep., *Earth Surface Dynamics*, 3\(4\), 447-462, 2015.](#)

824 Arnold, L., Breon, F.M., and Brewer, S: The earth as an extrasolar planet: the vegetation spectral signature today and
825 during the last Quaternary climatic extrema, *Int. J. Astrobiol.*, 8, 81–94. [http://dx.doi.org/10.1017/](http://dx.doi.org/10.1017/S1473550409004406)
826 [S1473550409004406](http://dx.doi.org/10.1017/S1473550409004406), 2009.

827 [Asahi, K.: Equilibrium-line altitudes of the present and Last Glacial Maximum in the eastern Nepal](#)
828 [Himalayas and their implications for SW monsoon climate, *Quatern. Int.*, 212, 26-34,](#)
829 [doi:10.1016/j.quaint.2008.08.004](http://dx.doi.org/10.1016/j.quaint.2008.08.004), 2010.

830 Bahrenberg, G., Giese, E., and Nipper, J.: Multivariate Statistik. *Statistische Methoden in der Geographie 2*, Stuttgart,
831 1992.

832 [Baker, P. A., Seltzer, G. O., Fritz, S. C., Dunbar, R. B., Grove, M. J., Tapia, P. M., Cross L., Rowe H. D., and](#)
833 [Baroda, J. P.: The History of South America Tropical Precipitation for the Past 25,000 Years, *Earth and*](#)
834 [Atmospheric Sciences](#), 291, 640-643, doi:10.1126/science.291.5504.640, 2001.

835 Ballantyne, A.P., Greenwood, D.R., Sinninghe Damste, J.S., Csank, A.Z., Eberle, J.J., and Rycczynski, N.:
836 Significantly warmer Arctic surface temperatures during the Pliocene indicated by multiple independent proxies,
837 *Geology* 38 (7), 603–606, 2010.

838 Banfield, J.F., Barker, W.W., Welch, S.A., and Taunton, A.: Biological impact on mineral dissolution: application of
839 the lichen model to understanding mineral weathering in the rhizosphere, *Proceedings of the National Academy of*
840 *Sciences*, 96, 3404-3411, 1999.

841 [Barnston, A. G. and Livezey, R. E.: Classification, Seasonality and Persistence of Low-Frequency](#)
842 [Atmospheric Circulation Patterns, *Mon. Weather Rev.*, 115, 1083-1126, doi:10.1175/1520-](#)
843 [0493\(1987\)1151083:CSAPOL2.0.CO;2](http://dx.doi.org/10.1175/1520-0493(1987)1151083:CSAPOL2.0.CO;2), 1987.

844 [Barron, J.A., and Anderson, L.: Enhanced Late Holocene ENSO/PDO expression along the margins of the](#)
845 [eastern North Pacific. *Quaternary International*, 235, 3-12, 2011.](#)

846 Bendick, R., and Ehlers, T.A.: Extreme localized exhumation at syntaxes initiated by subduction geometry, *Geophys.*
847 *Res. Lett.*, 41(16), 2014GL061026, doi:10.1002/2014GL061026, 2014.

848 [Bertrand, S., Charlet F., Charlier B., Renson V., and Fagel N.: Climate variability of southern Chile since the](#)
849 [Last Glacial Maximum: a continuous sedimentological records from Lago Puyehue \(40°S\), *J. Paleolimnol.*](#)

850 | [39, 179-195, doi:10.1007/s10933-007-9117-y, 2008.](#)

851 | [Betancourt, J. L., Latorre C., Rech J. A., Quade J., and Rylander K.A.: A 22,000 Year Record of Monsoonal](#)
852 | [Precipitation from Northern Chile's Atacama Desert, *Science*, 289, 1542-1546, doi: 10.1126/](#)
853 | [science.289.5484.1542, 2000.](#)

854 | Bigelow, N. H., Brubaker, L. B., Edwards, M. E., Harrison, S. P., Prentice, I. C., Anderson, P. M., Andreev, A. A.,
855 | Bartlein, P. J., Christensen, T. R., Cramer, W., Kaplan, J. O., Lozhkin, A. V., Matveyeva, N. V., Murray, D. V.,
856 | McGuire, A. D., Razzhivin, V. Y., Ritchie, J. C., Smith, B., Walker, D. A., Gajewski, K., Wolf, V., Holmqvist, B.
857 | H., Igarashi, Y., Kremenetskii, K., Paus, A., Pisaric, M. F. J., and Vokova, V. S.: Climate change and Arctic ecosys-
858 | tems I. Vegetation changes north of 55°N between the last glacial maximum, mid-Holocene and present. *Journal of*
859 | *Geophysical Research - Atmospheres*, 108(D19), doi: 10.1029/2002JD002558, 2003.

860 | [Bird, B. W., Abbott M. B., Rodbell D. T., and Vuille M.: Holocene tropical South American hydroclimate re-](#)
861 | [vealed from a decadal resolved lake sediment \$\delta^{18}O\$ record, *Earth Planet. Sc. Lett.*, 310, 192-202,](#)
862 | [doi:10.1016/j.epsl.2011.08.040, 2011.](#)

863 | [Bobst, A. L., Lowenstein, T. K., Jordan, T. E., Godfrey, L. V., Ku, T.-L., and Luo, S.: A 106 ka paleoclimate](#)
864 | [record from drill core of the Salar de Atacama, northern Chile, *Palaeogeogr. Palaeocl.*, 173, 21-42,](#)
865 | [doi:10.1016/S0031-0182\(01\)00308, 2001.](#)

866 | Braconnot, P., Otto-Bleisner, B., Harrison, S.P., Joussaume, S., Peterschmitt, J.-Y., Abe-Ouchi, A., Crucifix, M.,
867 | Driesschaert, E., Fichet, T., Hewitt, C.D., Kagayama, M., Kitoh, A., Loutre, M.-F., Marti, O., Merkel, U.,
868 | Ramstein, G., Valdes, P., Weber, L., Yu, Y., and Zhao, Y.: Results of PMIP2 coupled simulations of the mid-
869 | Holocene and Last Glacial maximum, part 1: experiments and large-scale features, *Clim Past* 3:261–277, 2007.

870 | Böhner, J.: General climatic controls and topoclimatic variations in Central and High Asia, *Boreas*, 35(2), 279-295,
871 | 2006.

872 | Bookhagen, B., Thiede, R.C., and Strecker, M.R.: Late Quaternary intensified monsoon phases control landscape
873 | evolution in the northwest Himalaya, *Geology*, 33(2), 149-152. doi: 10.1130/G20982.1, 2005.

874 | Boos, W. R., and Kuang, Z.: Dominant control of the South Asian monsoon by orographic insulation versus plateau
875 | heating, *Nature*, 463, 218-222, 2010.

876 | Braun, J.: A simple model for regolith formation by chemical weathering: Regolith Formation, *Journal of Geophysical*
877 | *Research Earth's Surface*, DOI: 10.1002/2016JF003914, 2016.

878 | Caves, J.: Late Miocene Uplift of the Tian Shan and Altai and Reorganization of Central Asia Climate, *GSA*
879 | [Today](#), doi:10.1130/gsatg305a.1, 2017.

880 | CLIMAP Project Members: Seasonal Reconstruction of the Earth's Surface at the Last Glacial Maximum.
881 | *Map and Chart Series*, Vol. 36, Geological Society of America, 18 pp., 1981.

882 | Cohen, S.J.: Bringing the global warming issue close to home: The challenge of regional impact studies. *Bulletin of the*
883 | *American Meteorological Society*, 71: 520 – 526., 1990.

- 886 | [D'Agostino, K., Seltzer, G., Baker, P., Fritz, S., and Dunbar, R.: Late-Quaternary lowstands of Lake Titicaca: evidence from high-resolution seismic data, *Palaeogeogr. Palaeoclimatol.*, 179, 97-111, doi:10.1016/S0031-0182\(01\)00411-4, 2002.](#)
- 887 |
- 888 |
- 889 | [De Batist, M., Fagel N., Loutre M. F., and Chapron E.: A 17,900-year multi-proxy lacustrine record of Lago Puyehue \(Chilean Lake District\): introduction, *J. Paleolimnol.*, 39, 151-161, doi:10.1007/s10933-007-9113-2, 2007.](#)
- 890 |
- 891 |
- 892 | [de Porras, M. E., Maldonado, A., Abarzua, A. M., Cardenas, M. L., Francois, J. P., Martel-Cea, A., Stern, C. R., Mendez, C., and Reyes, O.: Postglacial vegetation, fire and climate dynamics at Central Chilean Patagonia \(Lake Shaman, 44°S\), *Quaternary Sci. Rev.*, 50, 71-85, doi:10.1016/j.quascirev.2012.06.015; 2012.](#)
- 893 |
- 894 |
- 895 |
- 896 | [de Porras, M. E., Maldonado, A., Quintana, F. A., Martel-Cea, A., Reyes, O., and Méndez, C.: Environmental and climatic changes in central Chilean Patagonia since the Late Glacial \(Mallín El Embudo, 44° S\), *Clim. Past*, 10, 1063–1078, doi:10.5194/cp-10-1063-2014, 2014.](#)
- 897 |
- 898 |
- 899 | Delunel, R., van der Beek, P. A., Carcaillet, J., Bourlès, D. L., and Valla, P.G.: Frost-cracking control on catchment denudation rates: Insights from in situ produced ¹⁰Be concentrations in stream sediments (Ecrins–Pelvoux massif, French Western Alps), *Earth and Planetary Science Letters*, 293(1–2), 72–83, doi:10.1016/j.epsl.2010.02.020, 2010.
- 900 |
- 901 |
- 902 |
- 903 | [DeMenocal, P., Ortiz, J., Guilderson, T., Adkins, J., Samthein, M., Baker, L., and Yarusinsky, M.: Abrupt onset and termination of the African Humid Period:: rapid climate responses to gradual insolation forcing, *Quaternary Sci. Rev.*, 19, 347-361, doi:10.1016/S0277-3791\(99\)00081-5, 2000.](#)
- 904 |
- 905 |
- 906 | [Demske, D., Tarasov, P. E., Wünnemann, B., and Riedel, F.: Late glacial and Holocene vegetation, Indian monsoon and westerly circulation in the Trans-Himalaya recorded in the lacustrine pollen sequence from Tso Kar, Ladakh, NW India, *Palaeogeogr. Palaeoclimatol.*, 279, 172-185, doi:10.1016/j.palaeo.2009.05.008, 2009.](#)
- 907 |
- 908 |
- 909 |
- 910 | [Diaz, F.P., Latorre, C., Maldonado, A., Quade, J., and Betancourt, J.L.: Rodent middens reveal episodic, long-distance plant colonizations across the hyperarid Atacama Desert over the last 34,000 years, *J. Biogeogr.*, 39, 510-525, doi:10.1111/j.1365-2699.2011.02617.x, 2012.](#)
- 911 |
- 912 |
- 913 | Dietrich, W. E., and Perron, J.T.: The search for a topographic signature of life, *Nature*, 439(7075), 411–418, doi:10.1038/nature04452, 2006.
- 914 |
- 915 | Dietrich, S., Werner, M., Spanghel, T., and Lohmann, G.: Influence of orbital forcing and solar activity on water isotopes in precipitation during the mid and late Holocene, *Clim. Past*, 9, 13-26. doi:10.5194/cp-9-13-2013, 2013.
- 916 |
- 917 |
- 918 | Dettman, D.L., Fang, X.M., Garzzone, C.N., and Li, J.J.: Uplift-driven climate change at 12 Ma: a long delta O-18 record from the NE margin of the Tibetan plateau. *Earth and Planetary Science Letters*, 214(1-2), 267-277, 2003.
- 919 |
- 920 | Dowsett, H.J., Robinson, M., Haywood, A., Salzmann, U., Hill, D., Sohl, L., Chandler, M., Williams, M., Foley, K., and Stoll, D.: The PRISM3D paleoenvironmental reconstruction. *Stratigraphy*, 7, 123–139, 2010.
- 921 |
- 922 | [Egholm, D.L., Nielsen, S.B., Pedersen, V.K., Lesemann, J.: Glacial effects limiting mountain height, *Nature*, 460\(7257\).](#)

923 | [884-887, 2009.](#)

924 | Ehlers, T.A., and Poulsen, C.J.: Influence of Andean uplift on climate and paleoaltimetry estimates, *Earth and Planet-*
925 *ary Science Letters*, 281(3-4), 238-248, 2009.

926 Etheridge, D.M., Steele, L., Langenfelds, R., Francey, R., Barnola, J., and Morgan, V.: Natural and anthropogenic
927 changes in atmospheric CO₂ over the last 1000 years from air in Antarctic ice and firn, *J Geophys Res* 101:4115–
928 4128, 1996.

929

930 Etheridge, D.M., L. Steele, R. Francey, and R. Langenfelds (1998), Atmospheric methane between 1000 a.d. and
931 present: evidence of anthropogenic emissions and climatic variability. *J Geophys Res*, 103:15979–15993
932

933 Feng, R., Poulsen, C.J., Werner, M., Chamberlain, C.P., Mix, H.T., and Mulch, A.: Early Cenozoic evolution of topo-
934 graphy, climate, and stable isotopes in precipitation in the North American Cordillera, *American Journal of Science*,
935 313(7), 613–648, 2013.

936 | [Feng, R., Poulsen, C.J., Werner, M., 2016. Tropical circulation intensification and tectonic extension recorded](#)
937 [by Neogene terrestrial d18O records of the western United States. *Geology* 44. doi:10.1130/G38212.1](#)
938

939 | [Feng, R., Poulsen, C.J., 2016. Refinement of Eocene lapse rates, fossil-leaf altimetry, and North American](#)
940 [Cordilleran surface elevation estimates. *Earth Planet. Sci. Lett.* doi:10.1016/j.epsl.2015.12.022](#)
941

942 | [Fritz, S. C., Baker, P. A., Lowenstein, T. K., Seltzer, G. O., Rigsby, C. A., Dwyer, G. S., Tapia, P. M., Arnold,](#)
943 [K. K., Ku, T. L., and Luo, S: Hydrologic variation during the last 170,000 years in the southern hemisphere](#)
944 [tropics of South America, *Quaternary Res.*, 61, 95 – 104, doi:10.1016/j.yqres.2003.08.007, 2004.](#) Gasse, F.,
945 Arnold, M., Fontes, J. C., Fort, M., Gibert, E., Huc, A., Li, B., Li, Y., Liu, Q., Melleres, F., Van Campo, E.,
946 Wang, F., and Zhang, Q.: A 13,000-year climate record from western Tibet, *Nature*, 353, 742-745,
947 [doi:10.1016/j.quaint.2006.02.001, 1991.](#)

948 | [Gayo E. M., Latorre, C., Santoro, C. M., Maldonado, A., and De Pol-Holz, R.: Hydroclimate variability in the](#)
949 [low-elevation Atacama Desert over the last 2500 yr, *Clim. Past*, 8, 287-306, doi:10.5194/cp-8-287-2012,](#)
950 [2012.](#)

951 | Gierz, P., Lohmann, G., and Wei, W.: Response of Atlantic Overturning to future warming in a coupled atmosphere-
952 ocean-ice sheet model, *Geophysical Research Letters*, 42, 6811-6818, doi:10.1002/2015GL065276, 2015.

953 | [Gilli, A., Ariztegui, D., Bradbury, J. P., Kelts, K. R., Markgraf, V., and McKenzie, J. A.: Tracking abrupt cli-](#)
954 [mate change in the Southern Hemisphere: a seismic stratigraphic study of Lago Cardiel, Argentina](#)
955 [\(49°S\), *Terra Nova*, 13, 443-448, doi:10.1046/j.1365-3121.2001.00377.x , 2001.](#)

956 Glotzbach, C., van der Beek, P., Carcaillet, J., and Delunel, R.: Deciphering the driving forces of erosion rates on mil-
957 lennial to million-year timescales in glacially impacted landscapes: An example from the Western Alps, *Journal of*
958 *Geophysical Research: Earth Surface*, 118, 1491-1515, 2013.

959 Gong, X., Knorr, G., Lohmann, G., and Zhang, X.: Dependence of abrupt Atlantic meridional ocean circulation changes
960 on climate background states, *Geophysical Research Letters*, 40 (14), 3698-3704, doi:10.1002/grl.50701, 2013.

961 | [Grosjean, M., Van Leeuwen, J., Van der Knaap, W., Geyh, M., Ammann, B., Tanner, W., Messerli, B.,](#)

- 962 | [Núñez, L., Valero-Garcés, B., and Veit, H. : A 22,000 14C year BP sediment and pollen record of climate](#)
963 | [change from Laguna Miscanti \(23°S\), northern Chile, *Global Planet. Change*, 28, 35–51, doi:10.1016/](#)
964 | [S0921-8181\(00\)00063-1, 2001.](#)
- 965 | Gysels, G., Poesen, J., Bochet, E., and Li, Y.: Impact of plant roots on the resistance of soils to erosion by water: a re-
966 | view, *Progress in Physical Geography*, 29, 189–217. <http://doi.org/10.1191/0309133305pp443ra>, 2005.
- 967 | [Hansen, B. C. S., Seltzer, G. O., and Wright Jr., H.E.: Late Quaternary vegetational change in the central](#)
968 | [Peruvian Andes, *Palaeogeogr. Palaeocl.*, 109, 263-285, doi:10.1016/0031-0182\(94\)90179-1, 1994.](#)
- 969 | Harris, I., Jones, P.D., Osborn, T.J., and Lister, D.H.: Updated high-resolution grids of monthly climatic observations -
970 | the CRU TS3.10 Dataset, *International Journal of Climatology*, doi:10.1002/joc.3711, 2013.
- 971 | Harrison, S. P., Yu, G., Takahara, H., and Prentice, I. C.: Palaeovegetation - Diversity of temperate plants in east Asia.
972 | *Nature* 413, 129-130, 2001.
973 |
- 974 | Harrison, S.P., Bartlein, P.J., Brewer, S., Prentice, I.C., Boyd, M., Hessler, I., Holmgren, K., Izumi, K., and Willis, K.:
975 | Climate model benchmarking with glacial and mid-Holocene climates, *Climate Dynamics*, 43, 671-688. doi
976 | 10.1007/s00382-013-1922-6, 2013.
- 977 | Haywood, A.M., Valdes, P.J., and Sellwood, B.W.: Global scale palaeoclimate reconstruction of the middle Pliocene
978 | climate using the UKMO GCM: initial results. *Global and Planetary Change*, 25 (3–4), 239–256, 2000.
- 979 | Haywood, A.M., Dowsett, H.J., Otto-Bliesner, B., Chandler, M.A., Dolan, A.M., Hill, D.J., Lunt, D.J., Robinson, M.M.,
980 | Rosenbloom, N., Salzmann, U., and Sohl, L.E.: Pliocene Model Intercomparison Project (PlioMIP): experimental
981 | design and boundary conditions (Experiment 1), *Geoscientific Model Development* (3), 227-242, 2010.
982 |
- 983 | Haywood, A.M., Hill, D.J., Dolan, A.M., Otto-Bliesner, B., Bragg, F., Chan, W.-L., Chandler, M.A., Contoux, C., Jost,
984 | A., Kamae, Y., Lohmann, G., Lunt, D.J., Abe-Ouchi, A., Pickering, S.J., Ramstein, G., Rosenbloom, N.A., Sohl, L.,
985 | Stepanek, C., Yan, Q., Ueda, H., and Zhang, Z.: Large-scale features of Pliocene climate: results from the Pliocene
986 | Model Intercomparison Project, *Clim. Past*, 9, 191-209. doi:10.5194/cp-9-191-2013, 2013.
987 |
- 988 | Herman, F., Seward, D., Valla, P.G., Carter, A., Kohn, B., Willett, S.D., and Ehlers, T.A.: Worldwide acceleration of
989 | mountain erosion under a cooling climate, *Nature*, 504, 423–426. doi:10.1038/nature12877, 2013.
- 990 | [Herzschuh, U., Kuerschner, H., and Mischke, S.: Temperature variability and vertical vegetation belt shifts](#)
991 | [during the last ~50,000 yr in the Qilian Mountains \(NE margin of the Tibetan Plateau, China\), *Quaternary*](#)
992 | [Res., 66, 133-146, doi:10.1016/j.yqres.2006.03.001, 2006a.](#)
- 993 | [Herzschuh, U., Winter, K., Wuennemann, B., and Li, S.: A general cooling trend on the central Tibetan](#)
994 | [Plateau throughout the Holocene recorded by the lake Zigetang pollen spectra, *Quatern. Int.*, 154, 113-](#)
995 | [121, doi:10.1016/j.quaint.2006.02.005, 2006b.](#)
- 996 |
- 997 | [Herzschuh, U., Kramer A., Mischke S., and Zhang C.: Quantitative climate and vegetation trends since the](#)
998 | [late glacial on the northeastern Tibetan Plateau deduced from Koucha lake pollen spectra, *Quaternary*](#)
999 | [Res., 71, 162-171, doi:10.1016/j.yqres.2008.09.003, 2009.](#)

- 1000 Hillenbrand, C.-D., and Fütterer, D.K.: Neogene to Quaternary deposition of opal on the continental rise west of the
1001 Antarctic Peninsula, ODP Leg 178, Sites 1095, 1096, and 1101. In: Barker, P.F., Camerlenghi, A., Acton, G.D.,
1002 Ramsay, A.T.S. (Eds.), Proceedings of the Ocean Drilling Programme, Scientific Results, 178. Texas A and M Uni-
1003 versity, College Station, Texas, pp. 1–40 (CD-ROM), 2002.
- 1004 [Hillyer, R., Valencia, B. G., Bush, M.B., Silman, M.R., and Steinitz-Kannan, M.: A 24,700-yr paleolimnological](#)
1005 [history from the Peruvian Andes, *Quaternary Res.*, 71, 71-82, doi:10.1016/j.yqres.2008.06.006, 2009.](#)
- 1006 Hobley, D.E., Sinclair, H.D., and Cowie, P.A.: Processes, rates, and time scales of fluvial response in an ancient post-
1007 glacial landscape of the northwest Indian Himalaya. *Geological Society of America Bulletin*, 122, 1569-1584, 2010.
- 1008 [Hodell, D. A., Brenner, M., Kanfoush, S. L., Curtis, J. H., Stoner, J. S., Song, X., Wu, Y., and Whitmore, T. J.:](#)
1009 [Paleoclimate of southwestern China for the past 50,000 yr inferred from lake sediment records, *Quatern-*](#)
1010 [ary Res., 52, 369-380, doi:10.1006/qres.1999.2072, 1999.](#)
- 1011 [Hu, G., Yi, C.-L., Zhang, J.-F., Liu, J.-L., Jiang, T., and Qin, X.: Optically stimulated luminescence dating of a](#)
1012 [moraine and a terrace in Laohugou valley, western Qilian Shan, northeastern Tibet, *Quaternary Interna-*](#)
1013 [tional 321, 37-49, doi:10.1016/j.quaint.2013.12.019, 2014.](#)
- 1014 Insel, N., Poulsen, C.J., and Ehlers, T.A.: Influence of the Andes Mountains on South American moisture transport,
1015 convection, and precipitation, *Climate Dynamics*, 35 (7-8), 1477-1492, 2010.
- 1016 Jeffery, M.L., Ehlers, T.A., Yanites, B.J., and Poulsen, C.J.: Quantifying the role of paleoclimate and Andean Plateau
1017 uplift on river incision: PALEOCLIMATE ROLE IN RIVER INCISION, *Journal of Geophysical Research: Earth*
1018 *Surface*, 118(2), 852–871, doi:10.1002/jgrf.20055, 2013.
- 1019 [Jenny, B., Valero-Garces, B. L., Urrutia, R., Kelts, K., Veit, H., and Geyh, M.: Moisture changes and](#)
1020 [fluctuations of the Westerlies in Mediterranean Central Chile during the last 2000 years: The Laguna](#)
1021 [Aculeo record \(33°50' S\), *Quatern. Int.*, 87, 3-18, doi:10.1016/S1040-6182\(01\)00058-1, 2002a.](#)
- 1022 [Jenny, B., Valero-Garcés, B.L., Villa-Martínez, R., Urrutia, R., Geyh, M. A., and Veit, H.: Early to Mid-Holo-](#)
1023 [cene Aridity in Central Chile and the Southern Westerlies: The Laguna Aculeo Record \(34°S\), *Quaternary*](#)
1024 [Res., 58, 160–170, doi:10.1006/qres.2002.2370, 2002b.](#)
- 1025 Jungclauss, J. H., Lorenz, S. J., Timmreck, C., Reick, C. H., Brovkin, V., Six, K., Segschneider, J., Giorgetta, M.A.,
1026 Crowley, T.J., Pongratz, J., Krivova, N.A., Vieira, L.E., Solanski, S.K., Klocke, D., Botzet, M., Esch, M., Gayler,
1027 V., Haak, H., Raddatz, T.J., Roeckner, E., Schnur, R., Widmann, H., Claussen, M., Stevens, B., and Marotzke, J.:
1028 Climate and carbon-cycle variability over the last millennium. *Climate of the Past*, 6, 723-737. doi:10.5194/cp-6-723-
1029 2010, 2010.
- 1030 [Junginger, A., Roller, S., Olaka, L. A., and Trauth, M. H.: The effects of solar irradiation changes on the mi-](#)
1031 [gration of the Congo Air Boundary and water levels of paleo-Lake Suguta, Northern Kenya Rift, during the](#)
1032 [African Humid Period \(15–5 ka BP\), *Palaeogeogr. Palaeoclimatol.*, 396, 1-16, doi:10.1016/](#)
1033 [j.palaeo.2013.12.007, 2014.](#)
- 1034 [Kaiser, J., Schefuss, E., Lamy, F., Mohtadi, M., and Hebbeln, D.: Glacial to Holocene changes in sea surface](#)
1035 [temperature and coastal vegetation in north central Chile : high versus low latitude forcing, *Quaternary*](#)

- 1036 | [Sci. Rev., 27, 2064–2075, doi:10.1016/j.quascirev.2008.08.025, 2008.](#)
- 1037 Kalnay, E., Kanamitsu, M., Kistler, R., Collins, W., Deaven, D., Gandin, L., Iredell, M., Saha, S., White, G., Woollen,
1038 J., Zhu, Y., Chelliah, M., Ebisuzaki, W., Higgins, W., Janowiak, J., Mo, K.C., Ropelewski, C., Wang, J., Leetmaa,
1039 A., Reynolds, R., Jenne, R., and Joseph, D.: The NCEP/NCAR 40-year reanalysis project. *Bulletin of the American*
1040 *Meteorological Society*, 77(3), 437-471, 1996.
- 1041 | [Kashiwaya, K., Masuzawa, T., Morinaga, H., Yaskawa, K., Yuan, B. Y., Liu, J. Q., and Gu, Z.: Changes in](#)
1042 [hydrological conditions in the central Qing-Zang \(Tibetan\) Plateau inferred from lake bottom sediments.](#)
1043 [Earth Planet. Sc. Lett., 135, 31-39, doi:10.1016/0012-821X\(95\)00136-Z, 1995.](#)
- 1044 | [Kent-Corson, M., Sherman, L., Mulch, A. and Chamberlain, C.: Cenozoic topographic and climatic response](#)
1045 [to changing tectonic boundary conditions in Western North America. Earth Planet. Sc. Lett., 252\(3-4\),](#)
1046 [453-466, doi:10.1016/j.epsl.2006.09.049, 2006.](#)
- 1047 Kistler, R., Collins, W., Saha, S., White, G., Woollen, J., Kalnay, E., Chelliah, M., Ebisuzaki, W., Kanamitsu, M.,
1048 Kousky, V., Van den Dool, H., Jenne, R., and Fiorino, M.: The NCEP–NCAR 50–Year Reanalysis: Monthly Means
1049 CD–ROM and Documentation. *Bulletin of the American Meteorological Society*, 82(2), 247–267, 2001.
- 1050 Kirchner, J.W., Finkel, R.C., Riebe, C.S., Granger, D.E., Clayton, J.L., King, J.G., and Megahan, W.F.: Mountain
1051 erosion over 10 yr, 10 k.y., and 10 m.y. time scales, *Geology*, 29 (7), 591-594, 2001.
- 1052 Knorr, G., Butzin, M., Micheels, A., and Lohmann, G.: A Warm Miocene Climate at Low Atmospheric CO₂ levels.
1053 *Geophysical Research Letters*, 38, L20701, doi:10.1029/2011GL048873, 2011.
- 1054 Koons, P.O., Zeitler, P.K., and Hallet, B.: 5.14 Tectonic Aneurysms and Mountain Building, in *Treatise on Geomor-*
1055 *phology*, pp. 318–349, Elsevier, 2013.
- 1056 | [Kotlia, B. S., Sharma, C., Bhalla, M. S., Rajagopalan, G., Subrahmanyam, K., Bhattacharya, A., and](#)
1057 [Valdiya, K. S.: Paleoclimatic conditions in the late Pleistocene Wadda Lake, eastern Kumaun Himalaya](#)
1058 [\(India\), Palaeogeogr. Palaeocl., 162, 105-118, doi:10.1016/S0031-0182\(00\)00107-3, 2000.](#)
- 1059 | [Kramer, A., Herzschuh, U., Mischke, S., and Zhang, C.: Late glacial vegetation and climate oscillations on](#)
1060 [the southeastern Tibetan Plateau inferred from the lake Naleng pollen profile. Quaternary Res., 73, 324-](#)
1061 [335, doi:10.1016/j.yqres.2009.12.003, 2010.](#)
- 1062 Kraus, H.: Die Atmosphäre der Erde. Eine Einführung in die Meteorologie. Berlin, 2001.
- 1063 Kutzbach, J.E., Guetter, P.J., Ruddiman, W.F., and Prell, W.L.: Sensitivity of Climate to Late Cenozoic Uplift in
1064 Southern Asia and the American West - Numerical Experiments, *Journal of Geophysical Research-Atmospheres*,
1065 94(D15), 18393-18407, 1989.
- 1066 Kutzbach, J.E., Prell, W.L., and Ruddiman, W.F.: Sensitivity of Eurasian Climate to Surface Uplift of the Tibetan Plat-
1067 eau, *Journal of Geology*, 101(2), 177-190, 1993.
- 1068 | [Lamy, F. and Kaiser, J.: Past Climate Variability in South America and Surrounding Regions, Chapter 6:](#)

- 1069 | [Glacial to Holocene Paleoceanographic and Continental Paleoclimate Reconstructions Based on ODP Site 1233/GeoB 3313 Off southern Chile, 2009.](#)
- 1071 | [Lamy, F., Hebbeln, D., and Wefer, G.: High Resolution Marine Record of Climatic Change in Mid-latitude Chile during the Last 28,000 Years Based on Terrigenous Sediment Parameters, *Quaternary Res.*, 51, 83-93, doi:10.1006/qres.1998.2010, 1999.](#)
- 1072 |
- 1073 |
- 1074 | [Lamy, F., Klump, J., Hebbeln, D., and Wefer, G.: Late Quaternary rapid climate change in northern Chile, *Terra Nova*, 12, 8-13, doi:10.1046/j.1365-3121.2000.00265.x, 2000.](#)
- 1075 |
- 1076 | [Lamy, F., Rühlemann, C., Hebbeln, D. and Wefer, G.: High- and low-latitude climate control on the position of the southern Peru-Chile Current during the Holocene, *Paleoceanography*, 17, 16-1–16-10, doi:10.1029/2001PA000727, 2002.](#)
- 1077 |
- 1078 |
- 1079 | [Latorre, C., Betancourt, J., Rylander, K., and Quade, J.: Vegetation invasions into absolute desert: A 45 000 yr rodent midden record from the Calama-Salar de Atacama basins, northern Chile \(lat 22° - 24°S\), *Geol. Soc. Am. Bull.*, 114, 349–366, doi:10.1130/0016-7606\(2002\)114<0349:VIIADA>2.0.CO;2, 2002.](#)
- 1080 |
- 1081 |
- 1082 | [Latorre, C., Betancourt, J.L., Rylander, K.A., Quade, J., and Matthei, O.: A vegetation history from the arid prepuna of northern Chile \(22-23°S\) over the last 13500 years, *Palaeogeogr. Palaeoclimatol.*, 194, 223-246, doi:10.1016/S0031-0182\(03\)00279-7, 2003.](#)
- 1083 |
- 1084 |
- 1085 | [Latorre, C., Betancourt, J.L., and Arroyo, M.T.K.: Late Quaternary vegetation and climate history of a perennial river canyon in the Río Salado basin \(22°S\) of northern Chile, *Quaternary Res.*, 65, 450-466, doi:10.1016/j.yqres.2006.02.002, 2006.](#)
- 1086 |
- 1087 |
- 1088 | [Lechler, A. and Niemi, N.: Sedimentologic and isotopic constraints on the Paleogene paleogeography and paleotopography of the southern Sierra Nevada, California, *Geology*, 39\(4\), 379-382, doi:10.1130/g31535.1, 2011.](#)
- 1089 |
- 1090 |
- 1091 | [Lechler, A., Niemi, N., Hren, M. and Lohmann, K.: Paleoelevation estimates for the northern and central proto-Basin and Range from carbonate clumped isotope thermometry, *Tectonics*, 32\(3\), 295-316, doi:10.1002/tect.20016, 2013.](#)
- 1092 |
- 1093 |
- 1094 | Lease, R.O., and Ehlers, T.A.: Incision into the Eastern Andean Plateau During Pliocene Cooling, *Science*, 341(6147), 774–776, doi:10.1126/science.1239132, 2013.
- 1095 |
- 1096 | Legates, D.R., and Willmott, C.J.: Mean Seasonal and Spatial Variability in Gauge-Corrected, Global Precipitation, *International Journal of Climatology* 10(2), 111-127. doi: 10.1002/joc.3370100202, 1990.
- 1097 |
- 1098 | Li, J., Ehlers, T.A., Werner, M., Mutz, S.G., Steger, C., Paeth, H.: Late quaternary climate, precipitation $\delta^{18}\text{O}$, and Indian monsoon variations over the Tibetan Plateau. *Earth and Planetary Science Letters* 457, 412-422, 2017.
- 1099 |
- 1100 | [Liu, X., Colman, S. M., Brown, E. T., An, Z., Zhou, W., Jull, A. J. T., Huang, Cheng, Y., P., Liu, W., and Xu, H.: A climate threshold at the eastern edge of the Tibetan plateau, *Geophys. Res. Lett.*, doi: 10.1002/2014GL060833, 2014.](#)
- 1101 |
- 1102 |
- 1103 | [Licht, A., Quade, J., Kowler, A., de los Santos, M., Hudson, A., Schauer, A., Huntington, K., Copeland, P., and Lawton, T.: Impact of the North American monsoon on isotope paleoaltimeters: Implications for the paleoaltimetry of the American southwest, *Am. J. Sci.*, 317\(1\), 1-33, doi:10.2475/01.2017.01, 2017.](#)
- 1104 |
- 1105 |

- 1106 Lohmann, G., Pfeiffer, M., Laepple, T., Leduc, G., and Kim, J.-H.: A model-data comparison of the Holocene global
1107 sea surface temperature evolution. *Clim. Past*, 9, 1807-1839, doi:10.5194/cp-9-1807-2013, 2013.
1108
- 1109 Lorenz, S.J., and Lohmann, G.: Acceleration technique for Milankovitch type forcing in a coupled atmosphere-ocean
1110 circulation model: method and application for the Holocene. *Climate Dynamics* (2004) 23: 727. doi:10.1007/
1111 s00382-004-0469-y, 2004.
1112
- 1113 [Maldonado, A. and Villagrán, C.: Climate variability over the last 9900 cal yr BP from a swamp forest pollen
1114 record along the semiardi coast of Chile. *Quaternary Res.*, 66, 146-258, doi:10.1016/j.yqres.2006.04.003,
1115 2006.](#)
- 1116 [Maldonado, A. J., Betancourt, J. L., Latorre, C., and Villagrán, C.: Pollen analyses from a 50000-yr rodent
1117 midden series in the southern Atacama Desert \(25°30' S\), *J. Quaternary Sci.*, 20, 493-507,
1118 doi:10.1002/jqs.936, 2005.](#)
- 1119 [Maldonado, A., Méndez, C., Ugalde, P., Jackson, D., Seguel, R., and Latorre, C.: Early Holocene climate
1120 change and human occupation along the semiarid coast of north-central Chile. *J. Quaternary Sci.*, 25,
1121 985–988, doi:10.1002/jqs.1385, 2010.](#)
- 1122 [Markgraf, V., Bradbury, J. P., Schwalb, A., Burns, S., Stern, C., Ariztegui, D., Gilli, D., Anselmetti, F. S.,
1123 Stine, S., and Maidana, N.: Holocene palaeoclimates of southern Patagonia: limnological and
1124 environmental history of Lago Cardiel, Argentina, *Holocene*, 13, 581–591,
1125 doi:10.1191/0959683603hl648rp, 2003.](#)
- 1126 [Markgraf, V., Whitlock, C., and Haberle, S.: Vegetation and fire history during the last 18,000 cal yr B.P. in
1127 Southern Patagonia: Mallín Pollux, Coyhaique, Province Aisén \(45°41'30" S, 71°50'30" W, 640 m
1128 elevation\), *Palaeogeogr. Palaeocl.*, 254, 492–507, doi:10.1016/j.palaeo.2007.07.008, 2007.](#)
- 1129 [Maroon, E. A., Frierson, D. M. W., and Battisti, D. S.: The tropical precipitation response to Andes
1130 topography and ocean heat fluxes in an aquaplanet model, *J. Climate*, 28, 381–398, doi:10.1175/JCLI-D-
1131 14-00188.1, 2015.](#)
- 1132 [Maroon, E. A., Frierson, D. M. W., Kang, S. M., and Scheff, J.: The precipitation response to an idealized
1133 subtropical continent, *J. Climate*, 29, 4543–4564, doi:10.1175/JCLI-D-15-0616.1, 2016.](#)
- 1134 Marshall, J.A., Roering, J.J., Bartlein, P.J., Gavin, D.G., Granger, D.E., Rempel, A.W., Praskievicz, S.J., and Hales,
1135 T.C.: Frost for the trees: Did climate increase erosion in unglaciated landscapes during the late Pleistocene? *Science
1136 Advances*, 1, 1-10, 2015.
- 1137 Marston, R.A.: Geomorphology and vegetation on hillslopes: Interactions, dependencies, and feedback loops, *Geomor-
1138 phology*, 116(3–4), 206–217. doi:http://doi.org/10.1016/j.geomorph.2009.09.028, 2010.
- 1139 Matsuoka, N., and Murton, J.: Frost weathering: Recent advances and future directions. *Permafr. Periglac. Process.* 19,
1140 195–210, 2008.
- 1141 Matsuoka, N.: Solifluction rates, processes and landforms: A global review. *Earth Science Reviews* 55, 107–134, 2001.
- 1142 Maussion, F., Scherer, D., Mölg, T., Collier, E., Curio, J., and Finkelnburg, R.: Precipitation seasonality and variability
1143 over the Tibetan Plateau as resolved by the High Asia Reanalysis, *J. Climate*, 27, 1910-1927, doi:10.1175/JCLI-D-
1144 13-00282.1, 2014
- 1145 [Méndez, C., Gil, A., Neme, G., Nuevo Delaunay, A., Cortegoso, V., Huidobro, C., Durán, and Maldano, A.:
1146 Mid Holocene radiocarbon ages in the Subtropical Andes \(~29° - 35° S\), climatic change an implicaton for
1147 human space organization, *Quatern. Int.*, 356, 15-26, doi:10.1016/j.quaint.2014.06.059, 2015.](#)

- 1148 Mesinger, F., DiMego, G., Kalnay, E., Mitchell, K., Shafran, P.C., Ebisuzaki, W., Jovic, D., Woollen, J., Rogers, E.,
1149 Berbery, E.H., Ek, M.B., Fan, Y., Grumbine, R., Higgins, W., Li, H., Lin, Y., Manikin, G., Parrish, D., and Shi, W.:
1150 North American Regional Reanalysis, *Bulletin of the American Meteorological Society*, 87, 343–
1151 360.[doi:10.1175/BAMS-87-3-343](https://doi.org/10.1175/BAMS-87-3-343), 2006.
- 1152 [Methner, K., Fiebig, J., Wacker, U., Umhoefer, P., Chamberlain, C. and Mulch, A.: Eocene-Oligocene proto-](#)
1153 [Cascades topography revealed by clumped \(\$\Delta 47\$ \) and oxygen isotope \(\$\delta 18O\$ \) geochemistry \(Chumstick](#)
1154 [Basin, WA, USA\), *Tectonics*, 35\(3\), 546-564, doi:10.1002/2015tc003984, 2016.](#)
- 1155 [Mischke S., Kramer M., Herzs Schuh U., Shang H., Erzinger J., and Zhang C.: Reduced early holocene](#)
1156 [moisture availability in the Bayan Har Mountains, northeastern Tibetan Plateau, inferred from a multi-](#)
1157 [proxy lake record, *Palaeogeogr. Palaeoclimatol.*, 267, 59-76, doi:10.1016/j.palaeo.2008.06.002, 2008.](#)
- 1158 Molnar, P., Boos, W.R., and Battisti, D.S.: Orographic Controls on Climate and Paleoclimate of Asia: Thermal and
1159 Mechanical Roles for the Tibetan Plateau, *Annual Review of Earth and Planetary Sciences*, 38, 77-102, 2010.
- 1160 Molnar, P., and England, P.: Late Cenozoic uplift of mountain ranges and global climate change: chicken or egg?,
1161 *Nature*, 346, 29-34, 1990.
- 1162 Montgomery, D.R.: Slope distributions, threshold hillslopes, and steady-state topography, *American Journal of Science*,
1163 301, 432-454, 2001.
- 1164 Montgomery, D.R., Balco, G., and Willett, S.D.: Climate, tectonics, and the morphology of the Andes, *Geology*, 29(7),
1165 579-582, 2001.
- 1166 Moon, S., Chamberlain, C.P., Blisniuk, K., Levine, N., Rood, D.H., Hilley, G.E.: Climatic control of denudation in the
1167 deglaciated landscape of the Washington Cascades, *Nature Geoscience*, 4, 469-473, 2011.
- 1168 [Moreno, A., Santoro, C. M., and Latorre, C.: Climate change and human occupation in the northernmost](#)
1169 [Chilean Altiplano over the last ca. 11500 cal. a BP, *Quaternary Sci.*, 24, 373–382, doi:10.1002/jqs.1240,](#)
1170 [2009.](#)
- 1171 [Morinaga, H., Itota, C., Isezaki, N., Goto, H., Yaskawa, K., Kusakabe, M., Liu, J., Gu, Z., Yuan, B., and Cong,](#)
1172 [S.: Oxygen-18 and carbon-13 records for the last 14,000 years from lacustrine carbonates of Siling-Co](#)
1173 [\(lake\) in the Qinghai-Tibetan Plateau, *Geophys. Res. Lett.*, 20, 2909-2912, doi:10.1029/93GL02982,](#)
1174 [1993.](#)
- 1175 [Morrill, C., Overpeck, J. T., Cole, J. E., Liu, K., Shen, C., and Tang, L.: Holocene variations in the Asian mon-](#)
1176 [soon inferred from the geochemistry of lake sediments in central Tibet, *Quaternary Res.*, 65, 232-243,](#)
1177 [doi:10.1016/j.yqres.2005.02.014, 2006.](#)
- 1178 Moulton, K.L., and Berner, R.A.: Quantification of the effect of plants on weathering: studies in Iceland, *Geology*, 26,
1179 895-898, 1998.
- 1180 [Muegler, I., Gleixner, G., Guenther, F., Maeusbacher, R., Daut, G., Schuett, B., Berking, J., Schwalb, A.,](#)
1181 [Schwark, L., Xu, B., Yao, T., Zhu, L., and Yi, C.: A multi-proxy approach to reconstruct hydrological](#)
1182 [changes and Holocene climate development of Nam Co, Central Tibet, *J. Paleolimnol.*, 43, 625-648,](#)
1183 [doi:10.1007/s10933-009-9357-0, 2010.](#)

- 1184 [Mujica, M. I., Latorre, C., Maldonado, A., González-Silvestre, L., Pinto, R., De Pol-Holz, R., and Santoro, C.](#)
1185 [M.: Late Quaternary climate change, relict populations and present-day refugia in the northern Atacama](#)
1186 [Desert: a case study from Quebrada La Higuera \(18° S\). *J. Biogeogr.*, 42, 76–88, doi:10.1111/jbi.12383,](#)
1187 [2015.](#)
- 1188 [Mulch, A., Sarna-Wojcicki, A., Perkins, M. and Chamberlain, C.: A Miocene to Pleistocene climate and](#)
1189 [elevation record of the Sierra Nevada \(California\), *P. Natl. Acad. Sci. USA*, 105\(19\), 6819-6824,](#)
1190 [doi:10.1073/pnas.0708811105, 2008.](#)
- 1191
- 1192 [Mulch, A., Chamberlain, C., Cosca, M., Teyssier, C., Methner, K., Hren, M. and Graham, S.: Rapid change in](#)
1193 [high-elevation precipitation patterns of western North America during the Middle Eocene Climatic Op-](#)
1194 [timum \(MECO\), *Am. J. Scie.*, 315\(4\), 317-336, doi:10.2475/04.2015.02, 2015.](#)
- 1195 Mutz, S.G., Ehlers, T.A., Li, J., Steger, C., Peath, H., Werner, M., Poulsen, C.J.: Precipitation $\delta^{18}\text{O}$ over the South Asia
1196 Orogen from ECHAM5-wiso Simulation: Statistical Analysis of Temperature, Topography and Precipitation.
1197 *Journal of Geophysical Research-Atmospheres*, 121(16),9278-9300, doi: 10.1002/2016JD024856, 2016.
- 1198 [Nishimura, M., Matsunaka, T., Morita, Y., Watanabe, T., Nakamura, T., Zhu, L., Nara, W. F., Imai, A., Izutsu,](#)
1199 [Y., and Hasuike, N.: Paleoclimatic changes on the southern Tibetan Plateau over the past 19,000 years](#)
1200 [recorded in lake Pumoyum Co. and their implications for the southwest monsoon evolution, *Palaeogeogr.*](#)
1201 [Palaeocl., 396, 75-92, doi:10.1016/j.palaeo.2013.12.015, 2014.](#)
- 1202 Otto-Bliesner, B.L., Brady, C.B., Clauzet, G., Tomas, R., Levis, S., and Kothavala, Z.: Last Glacial Maximum and
1203 Holocene Climate in CCSM3. *Journal of Climate*, 19, 2526-2544, 2006.
- 1204 Paeth, H.: Key Factors in African Climate Change Evaluated by a Regional Climate Model, *Erdkunde*, 58, 290-315,
1205 2004.
- 1206 [Peel, M.C., Finlayson, B.L., McMahon, T.A.: Updated world map of the Koppen- Geiger climate classification.](#)
1207 [*Hydrol. Earth Syst. Sci.*, 11, 1633–1644, 2007.](#)
- 1208
- 1209 Pfeiffer, M., and Lohmann, G.: Greenland Ice Sheet influence on Last Interglacial climate: global sensitivity studies
1210 performed with an atmosphere-ocean general circulation model. *Climate of the Past*, 12, pp. 1313-1338,
1211 doi:10.5194/cp-12-1313-2016, 2016.
- 1212 Pickett, E.J., Harrison, S.P., Flenley, J., Grindrod, J., Haberle, S., Hassell, C., Kenyon, C., MacPhail, M., Martin, H.,
1213 Martin, A.H., McKenzie, M., Newsome, J.C., Penny, D., Powell, J., Raine, J.I., Southern, W., Stevenson, J., Sutra,
1214 J.-P., Thomas, I., van der Kaars, S., Ward, J.: Pollen-based reconstructions of biome distributions for Australia,
1215 South-East Asia and the Pacific (SEAPAC region) at 0, 6000 and 18,000 14C years B.P.. *Journal of Biogeography*,
1216 31, 1381–1444, doi: 10.1111/j.1365-2699.2004.01001.x, 2004.
- 1217
- 1218 [Pingel, H., Mulch, A., Alonso, R., Cottle, J., Hynek, S., Poletti, J., Rohrmann, A., Schmitt, A., Stockli, D. and](#)
1219 [Strecker, M.: Surface uplift and convective rainfall along the southern Central Andes \(Angastaco Basin,](#)
1220 [NW Argentina\), *Earth Planet. Sc. Lett.*, 440, 33-42, doi:10.1016/j.epsl.2016.02.009, 2016.](#)
- 1221
- 1222 Prentice, I. C., Jolly, D., and BIOME 6000 Participants. (2000). Mid-Holocene and glacial-maximum vegetation geo-
1223 graphy of the northern continents and Africa. *Journal of Biogeography* 27, 507-519.

- 1224
- 1225 [Pueyo, J. J., Sáez, A., Giralt, S., Valero-Garcés, B.L., Moreno, A., Bao, R., Schwalb, A., Herrera, C., Klo-](#)
- 1226 [sowska, B., and Taberner, C.: Carbonate and organic matter sedimentation and isotopic signatures in](#)
- 1227 [Lake Chungará, Chilean Altiplano, during the last 12.3 kyr, *Palaeogeogr. Palaeocl.*, 307, 339-355,](#)
- 1228 [doi:10.1016/j.palaeo.2011.05.036, 2011.](#)
- 1229 [Quade, J., Rech, J. A., Betancourt, J. L., Latorre, C., Quade, B., Rylander, K. A., and Fisher, T.: Paleowet-](#)
- 1230 [lands and regional climate change in the central Atacama Desert, northern Chile, *Quaternary Res.*, 69,](#)
- 1231 [343-360, doi:10.1016/j.yqres.2008.01.003, 2008.](#)
- 1232 Raymo, M.E., and Ruddiman, W.F.: Tectonic forcing of late cenozoic climate. *Nature*, 359(6391), 117-122, 1992.
- 1233 [Rech, J. A., Pigati, J. S., Quade, J., and Betancourt, J. L.: Re-evaluation of mid-Holocene deposits at](#)
- 1234 [Quebrada Puripica, northern Chile, *Palaeogeogr. Palaeocl.*, 194, 207-222, doi:0.1016/S0031-](#)
- 1235 [0182\(03\)00278-5, 2003.](#)
- 1236 Robinson, M.M.: New quantitative evidence of extreme warmth in the Pliocene Arctic, *Stratigraphy* 6, 265–275, 2009.
- 1237 Roeckner, E., Bäuml, G., Bonaventura, L., Brokopf, R., Esch, M., Giorgetta, M., Hagemann, S., Kirchner, I., Korn-
- 1238 blueh, L., Manzini, E., Rhodin, A., Schlese, U., Schulzweida, U., and Tompkins, A.: The atmospheric general circu-
- 1239 lation model ECHAM5. Part I: Model description. Rep. 349Rep., 127 pp, Max Planck Institute for Meteorology,
- 1240 Hamburg, 2003.
- 1241 Roering, J.J., Marshall, J., Booth, A.M., Mort, M., and Jin, Q.: Evidence for biotic controls on topography and soil pro-
- 1242 duction, *Earth and Planetary Science Letters*, 298(1–2), 183–190, doi:10.1016/j.epsl.2010.07.040, 2010.
- 1243 Salzmann, U., Williams, M., Haywood, A.M., Johnson, A.L.A., Kender, S., and Zalasiewicz, J.: Climate and environ-
- 1244 ment of a Pliocene warm world. *Palaeogeography, Palaeoclimatology, Palaeoecology*, 309 (1-8), 2011.
- 1245 [Sarnthein, M.: Sand deserts during glacial maximum and climatic optimum, *Nature*, 272, 43–46,](#)
- 1246 [doi:10.1038/272043a0, 1978.](#)
- 1247 Sarnthein, M., Gersonde, R., Niebler, S., Pflaumann, U., Spielhagen, R., Thiede, J., Wefer, G., Weinelt, M.: Overview
- 1248 of Glacial Atlantic Ocean Mapping (GLAMAP 2000), *Paleoceanography*, 18(2), doi:10.1029/2002PA000769,
- 1249 2003.
- 1250 Schäfer-Neth C., and Paul, A.: The Atlantic Ocean at the last glacial maximum: objective mapping of the GLAMAP
- 1251 sea-surface conditions. In: Wefer G, Mulitza S, Ratmeyer V (eds) *The South Atlantic in the late quaternary: recon-*
- 1252 *struction of material budgets and current systems.* Springer, Berlin, pp 531–548, 2003.
- 1253 Schaller, M., von Blanckenburg, F., Veldkamp, A., Tebbens, L.A., Hovius, N., and Kubik, P.W.: A 30 000 yr record of
- 1254 erosion rates from cosmogenic ^{10}Be in Middle European river terraces, *Earth and Planetary Science Letters*,
- 1255 204(1), 307–320, 2002.
- 1256 Schaller, M., and Ehlers T.A.: Limits to quantifying climate driven changes in denudation rates with cosmogenic radio-
- 1257 nuclides, *Earth and Planetary Science Letters*, v. 248, pp. 153-167. doi:10.1016/j.epsl.2006.05.027, 2006.

- 1258 [Schwalb, A., Burns, S., and Kelts, K.: Holocene environments from stable isotope stratigraphy of ostracods](#)
1259 [and authigenic carbonate in Chilean Altiplano Lakes, *Palaeogeogr. Palaeocl.*, 148, 153-168, doi:10.1016/](#)
1260 [S0031-0182\(98\)00181-3, 1999.](#)
- 1261 [Shen J., Liu X. Q., Wang S. M., and Matsumoto R.: Palaeoclimatic changes in the Qinghai, Lake area during](#)
1262 [the last 18,000 years, *Quatern. Int.*, 136, 131-140, doi:10.1016/j.quaint.2004.11.014, 2005.](#)
- 1263 [Shen C., Liu K., Tang L., and Overpeck J. T.: Quantitative relationships between modern pollen rain and cli-](#)
1264 [mate in the Tibetan Plateau. *Rev. Palaeobot. Palyno.*, 140, 61–77, doi:10.1016/j.revpalbo.2006.03.001,](#)
1265 [2006.](#)
- 1266 [Siani, G., Colin, C., Michel, E., Carel, M., Richter, T., Kissel, C., and Dewilde, F.: Late Glacial to Holocene](#)
1267 [terrigenous sediment record in the Northern Patagonian margin: Paleoclimate implications, *Palaeogeogr.*](#)
1268 [Palaeocl., 297, 26-36, doi:10.1016/j.palaeo.2010.07.011, 2010.](#)
- 1269 Simmons, A.J., Burrige, D.M., Jarraud, M., Girard, C., and Wergen, W.: The ECMWF Medium-Range prediction
1270 models development of the numerical formulations and the impact of increased resolution, *Meteorology and Atmo-*
1271 *spheric Physics*, 40(1-3), 28-60, 1989.
- 1272 Sohl, L.E., Chandler, M.A., Schmunk, R.B., Mankoff, K., Jonas, J.A., Foley, K.M., and Dowsett, H.J.: PRISM3/GISS
1273 topographic reconstruction, *U.S. Geological Survey Data Series*, 419, 6p., 2009.
- 1274
- 1275 Sowers T., Alley, R.B., and Jubenville, J.: Ice core records of atmospheric N₂O covering the last 106,000 years. *Sci-*
1276 *ence*, 301:945–948, 2003.
- 1277
- 1278 Stepanek, C., and Lohmann, G.: Modelling mid-Pliocene climate with COSMOS , *Geosci. Model Dev.* , 5 , pp. 1221-
1279 1243 . doi:10.5194/gmd-5-1221-2012, 2012.
- 1280 [Stine, S. and Stine M.: A record from Lake Cardiel of climate change in southern South America, *Nature*,](#)
1281 [345, 705-708, doi:10.1038/345705a0,1990.](#)
- 1282 [Szeicz, J. M., Haberle, S. G., and Bennett, K. D.: Dynamics of North Patagonian rainforests from fine-resolu-](#)
1283 [tion pollen, charcoal and tree-ring analysis, *Chonos Archipelago, Southern Chile, Austral Ecol.*, 28, 413–](#)
1284 [422, doi:10.1046/j.1442-9993.2003.01299.x , 2003.](#)
- 1285 Takahashi, K., and Battisti, D.: Processes controlling the mean tropical pacific precipitation pattern. Part I: The Andes
1286 and the eastern Pacific ITCZ. *Journal of Climate*, 20(14), 3434-3451, 2007a.
- 1287 Takahashi, K., and Battisti, D.: Processes controlling the mean tropical pacific precipitation pattern. Part II: The SPCZ
1288 and the southeast pacific dry zone. *Journal of Climate*, 20(23), 5696-5706, 2007b.
- 1289 [Tang, L., Shen, S., Liu, K., and Overpeck, J. T.: Changes in south Asian monsoon: new high-resolution pa-](#)
1290 [leoclimatic records from Tibet, China, *Chinese Sci. Bull.*, 45, 87-91, doi:10.1007/BF02884911, 2000.](#)
- 1291 Thiede, R.C., and Ehlers, T.A.: Large spatial and temporal variations in Himalayan denudation. *Earth and Planetary*
1292 *Science Letters*, 374, 256-257. doi:10.1016/j.epsl.2013.03.004, 2013.

- 1293 Thomas, A.: The climate of the Gongga Shan range, Sichuan Province, PR China. *Arctic and Alpine Research*, 29(2),
1294 226-232, 1997.
- 1295 Uppala, S.M., Kållberg, P.W., Simmons, A.J., Andrae, U., da Costa Bechtold, V., Fiorino, M., Gibson, J.K., Haseler, J.,
1296 Hernandez, A., Kelly, G.A., Li, X., Onogi, K., Saarinen, S., Sokka, N., Allan, R.P., Andersson, E., Arpe, K.,
1297 Balmaseda, M.A., Beljaars, A.C.M., van de Berg, L., Bidlot, J., Bormann, N., Caires, S., Chevallier, F., Dethof, A.,
1298 Dragosavac, M., Fisher, M., Fuentes, M., Hagemann, S., Hólm, E., Hoskins, B.J., Isaksen, I., Janssen, P.A.E.M.,
1299 Jenne, R., McNally, A.P., Mahfouf, J.-F., Morcrette, J.-J., Rayner, N.A., Saunders, R.W., Simon, P., Sterl, A.,
1300 Trenberth, K.E., Untch, A., Vasiljevic, D., Viterbo, P., and Woollen, J.: The ERA-40 re-analysis. *Quart. J. R.*
1301 *Meteorol. Soc.*, 131, 2961-3012, 2005.
- 1302
- 1303 von Blanckenburg, F., Bouchez, J., Ibarra, D.E., and Maher, K.: Stable runoff and weathering fluxes into the oceans
1304 over Quaternary climate cycles, *Nature Geoscience*, 8(7), 538–542, doi:10.1038/ngeo2452, 2015.
- 1305 Valla, P.G., Shuster, D.L., and van der Beek, P.A.: Significance increase in relief of European Alps during mid-Pleisto-
1306 cene glaciations. *Nature Geoscience*, 4, 688–692. doi:10.1038/ngeo1242, 2011.
- 1307 [Van Campo, E., Cour, P., and Huang, S.: Holocene environmental changes in Bangong Co basin \(Western](#)
1308 [Tibet\). Part 2: The pollen record, *Palaeogeogr. Palaeoclimatol., 120*, 49-63, doi:10.1016/0031-0182\(95\)00033-](#)
1309 [X, 1996.](#)
- 1310
- 1311 [Villagrán, C. and Varela, J.: Palynological Evidence for Increased Aridity on the Central Chilean Coast during](#)
1312 [the Holocene, *Quaternary Res.*, 34, 198–207, doi:10.1016/0033-5894\(90\)90031-F, 1990.](#)
- 1313 [Villa-Martínez, R., Villagrán, C., and Jenny, B.: The last 7500 cal yr B.P. of westerly rainfall in Central Chile](#)
1314 [inferred from a high-resolution pollen record from Laguna Aculeo \(34°S\), *Quaternary Res.*, 60, 284-293,](#)
1315 [doi:https://doi.org/10.1016/j.yqres.2003.07.007, 2003.](#)
- 1316 Wei, W., and Lohmann, G.: Simulated Atlantic Multidecadal Oscillation during the Holocene. *Journal of Climate*, 25,
1317 6989–7002. doi: http://dx.doi.org/10.1175/JCLI-D-11-00667.1, 2012.
- 1318 [Wang, R.L., Scarpitta, S. C., Zhang, S. C., and Zheng, M. P.: Later Pleistocene/Holocene climate conditions](#)
1319 [of Qinghai-Xizhang Plateau \(Tibet\) based on carbon and oxygen stable isotopes of Zabuye Lake sedi-](#)
1320 [ments, *Earth Planet. Sc. Lett.*, 203, 461-477, doi:10.1016/S0012-821X\(02\)00829-4, 2002.](#)
- 1321 Whipple, K.X., Kirby, E., and Broecklehurst, S.H.: Geomorphic limits to climate-induced increases in topographic re-
1322 lief. *Nature*, 401, 39-43. doi:10.1038/43375, 1999.
- 1323 Whipple, K.X., and Tucker, G.E.: Dynamics of the stream-power river incision model: Implications for height limits of
1324 mountain ranges, landscape response timescales, and research needs, *Journal of Geophysical Research-Solid Earth*,
1325 104, 17661-17674, 1999.
- 1326 Whipple, K. X.: The influence of climate on the tectonic evolution of mountain belts, *Nat. Geosci.*, 2, doi:10.1038/
1327 ngeo413, 2009.
- 1328 Wilks, D.S.: Statistical methods in the atmospheric sciences - 3rd ed. Academic Press, Oxford, 2011.

- 1329 Willett, S.D., Schlunegger, F., and Picotti, V.: Messinian climate change and erosional destruction of the central
1330 European Alps. *Geology*, 34(8), 613-616, 2006.
- 1331 Wilson, G.S., Barron, J.A., Ashworth, A.C., Askin, R.A., Carter, J.A., Curren, M.G., Dalhuisen, D.H., Friedmann, E.I.,
1332 Fyodorov-Davidov, D.G., Gilichinsky, D.A., Harper, M.A., Harwood, D.M., Hiemstra, J.F., Janecek, T.R., Licht,
1333 K.J., Ostroumov, V.E., Powell, R.D., Rivkina, E.M., Rose, S.A., Stroeven, A.P., Stroeven, P., van der Meer, J.J.M.,
1334 Wizevich, M.C.: The Mount Feather Diamicton of the Sirius Group: an accumulation of indicators of Neogene Ant-
1335 arctic glacial and climatic history, *Palaeogeography, Palaeoclimatology, Palaeoecology*, 182 (1–2), 117–131, 2002.
- 1336 [Wischnewski, J., Mischke, S., Wang, Y., and Herzsuh, U.: Reconstructing climate variability on the](#)
1337 [northeastern Tibetan Plateau since the last lateglacial – a multi-proxy, dual-site approach comparing](#)
1338 [terrestrial and aquatic signals, *Quaternary Science Reviews*, 30, 82-97,](#)
1339 [doi:10.1016/j.quascirev.2010.10.001, 2011.](#)
- 1340 [Wünnemann, B., Mischke, S., and Chen, F.: A Holocene sedimentary record from Bosten lake, China, *Pa-*
1341 \[laeogeogr. Palaeocl., 234, 223-238, doi:10.1016/j.palaeo.2005.10.016, 2006.\]\(#\)](#)
- 1342 [Yanhong, W., Lücke, A., Zhangdong, J., Sumin, W., Schleser, G.H., Battarbee, R.W., and Weilan, X.: Holo-](#)
1343 [cene climate development on the central Tibetan Plateau: A sedimentary record from Cuoe Lake, *Palaeo-*](#)
1344 [geogr. Palaeocl., 234, 328-340, doi:10.1016/j.palaeo.2005.09.017, 2006](#)
- 1345 Yanites, B.J., and Ehlers, T.A.: Global climate and tectonic controls on the denudation of glaciated mountains. *Earth*
1346 *and Planetary Science Letters*, 325, 63-75, 2012.
- 1347 [Yu, L. and Lai, Z.: Holocene climate change inferred from stratigraphy and OSL chronology of Aeolian sedi-](#)
1348 [ments in the Qaidam Basin, northeastern Qinghai-Tibetan Plateau, *Quaternary Res.*, 81, 488-499,](#)
1349 [doi:10.1016/j.yqres.2013.09.006, 2014.](#)
- 1350 [Zhang, C. and Mischke, S.: A lateglacial and Holocene lake record from the Nianbaoyeze Mountains and in-](#)
1351 [ferences of lake, glacier and climate evolution on the eastern Tibetan Plateau, *Quaternary Sci. Rev.*, 28,](#)
1352 [1970-1983, doi:10.1016/j.quascirev.2009.03.007, 2009.](#)
- 1353 [Zhang, J., Chen, F., Holmes, J. A., Li, H., Guao, X., Wang, J., Li, S., Lu, Y., Zhao, Y., and Qiang, M.: Holo-](#)
1354 [cene monsoon climate documented by oxygen and carbon isotopes from lake sediments and peat bogs](#)
1355 [in China: a review and synthesis, *Quaternary Sci. Rev.*, 30, 1973-1987, doi:10.1016/](#)
1356 [j.quascirev.2011.04.023, 2011.](#)
- 1357 Zhang, X., Lohmann, G., Knorr, G., and Xu X.: Different ocean states and transient characteristics in Last Glacial Max-
1358 imum simulations and implications for deglaciation. *Clim. Past*, 9, 2319-2333, doi:10.5194/cp-9-2319-2013, 2013a.
- 1359 Zhang, R., Yan, Q., Zhang, Z.S., Jiang, D., Otto-Bliesner, B.L., Haywood, A.M., Hill, D.J., Dolan, A.M., Stepanek, C.,
1360 Lohmann, G., Contoux, C., Bragg, F., Chan, W.-L., Chandler, M.A., Jost, A., Kamae, Y., Abe-Ouchi, A., Ramstein,
1361 G., Rosenbloom, N.A., Sohl, L., and Ueda, H.: East Asian monsoon climate simulated in the PlioMIP. *Clim. Past*, 9,
1362 2085-2099, doi:10.5194/cp-9-2085-2013, 2013b.
- 1363
- 1364 Zhang, X., Lohmann, G., Knorr, G., and Purcell C.: Abrupt glacial climate shifts controlled by ice sheet changes.

1365 *Nature*, 512 (7514), 290-294, doi:10.1038/nature13592, 2014.

1366 Zhisheng, A., Kutzbach, J.E., Prell, W.L., and Porter, S.C.: Evolution of Asian monsoons and phased uplift of the South
1367 Asian plateau since Late Miocene times. *Nature*, 411(6833), 62-66, 2001.

1368 [Zhou, W. J., Lu, X. F., Wu, Z. K., Deng, L., Jull, A. J. T., Donahue, D. J., and Beck, W.: Peat record reflecting
1369 Holocene climate change in the Zoigê Plateau and AMS radiocarbon dating, *Chinese Sci. Bull.*, 47, 66-
1370 70, doi:10.1360/02tb9013, 2002.](#)

1371
1372
1373
1374
1375
1376
1377
1378
1379
1380
1381
1382
1383
1384
1385
1386
1387
1388
1389
1390
1391
1392
1393
1394
1395
1396
1397
1398
1399
1400
1401
1402
1403
1404
1405
1406
1407
1408
1409
1410
1411
1412
1413
1414
1415
1416
1417
1418

1419
1420
1421
1422
1423
1424
1425
1426
1427
1428
1429
1430
1431
1432
1433
1434
1435
1436
1437
1438
1439
1440
1441
1442
1443
1444
1445
1446
1447
1448
1449
1450
1451
1452
1453
1454
1455
1456
1457
1458
1459
1460
1461
1462
1463
1464
1465
1466
1467
1468
1469
1470
1471
1472
1473
1474
1475
1476
1477

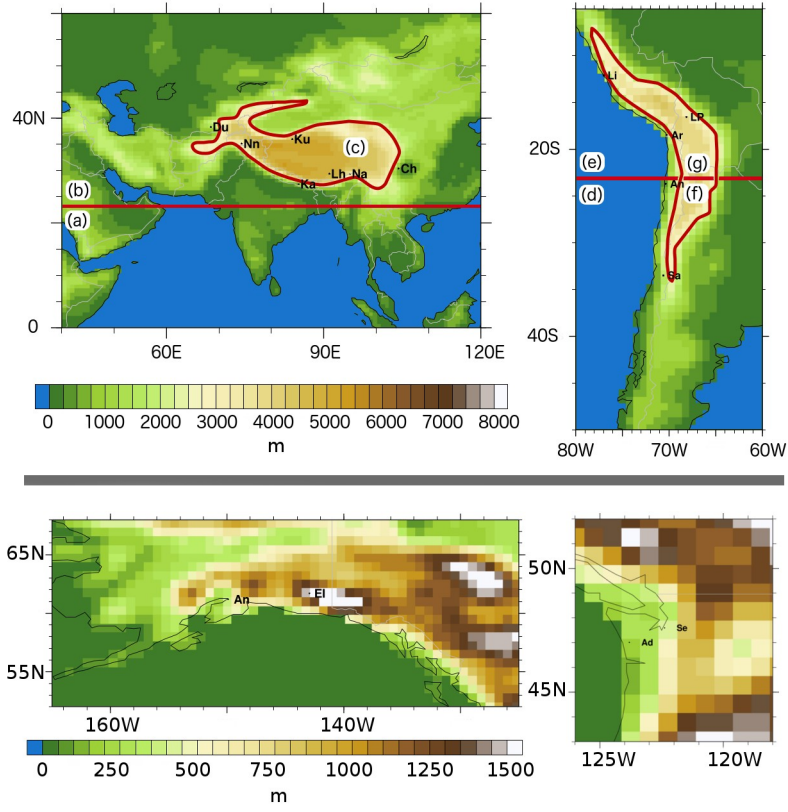


Figure 1

1478
1479
1480
1481
1482
1483
1484
1485
1486
1487
1488
1489
1490
1491
1492
1493
1494
1495
1496
1497
1498
1499
1500
1501
1502
1503
1504
1505
1506
1507
1508
1509
1510
1511
1512
1513
1514
1515
1516
1517
1518
1519
1520
1521
1522
1523
1524
1525
1526
1527
1528
1529
1530
1531
1532
1533
1534
1535
1536
1537

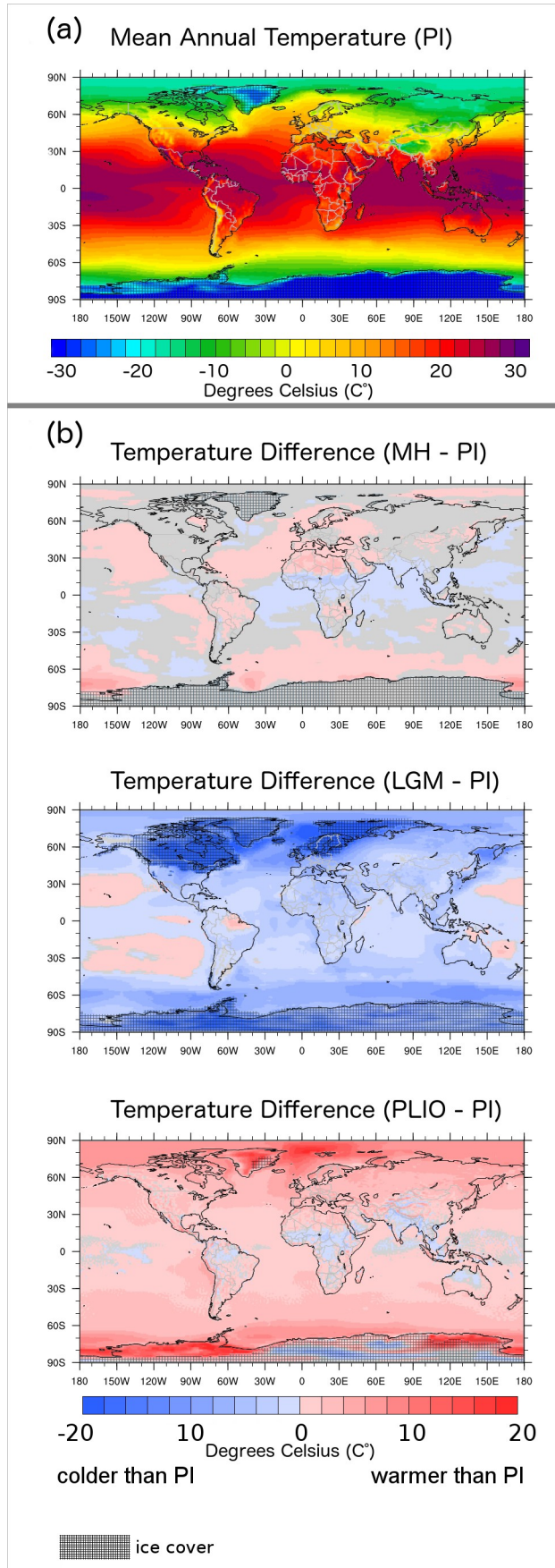


Figure 2

1538
1539
1540
1541
1542
1543
1544
1545
1546
1547
1548
1549
1550
1551
1552
1553
1554
1555
1556
1557
1558
1559
1560
1561
1562
1563
1564
1565
1566
1567
1568
1569
1570
1571
1572
1573
1574
1575
1576
1577
1578
1579
1580
1581
1582
1583
1584
1585
1586
1587
1588
1589
1590
1591
1592
1593
1594
1595
1596
1597

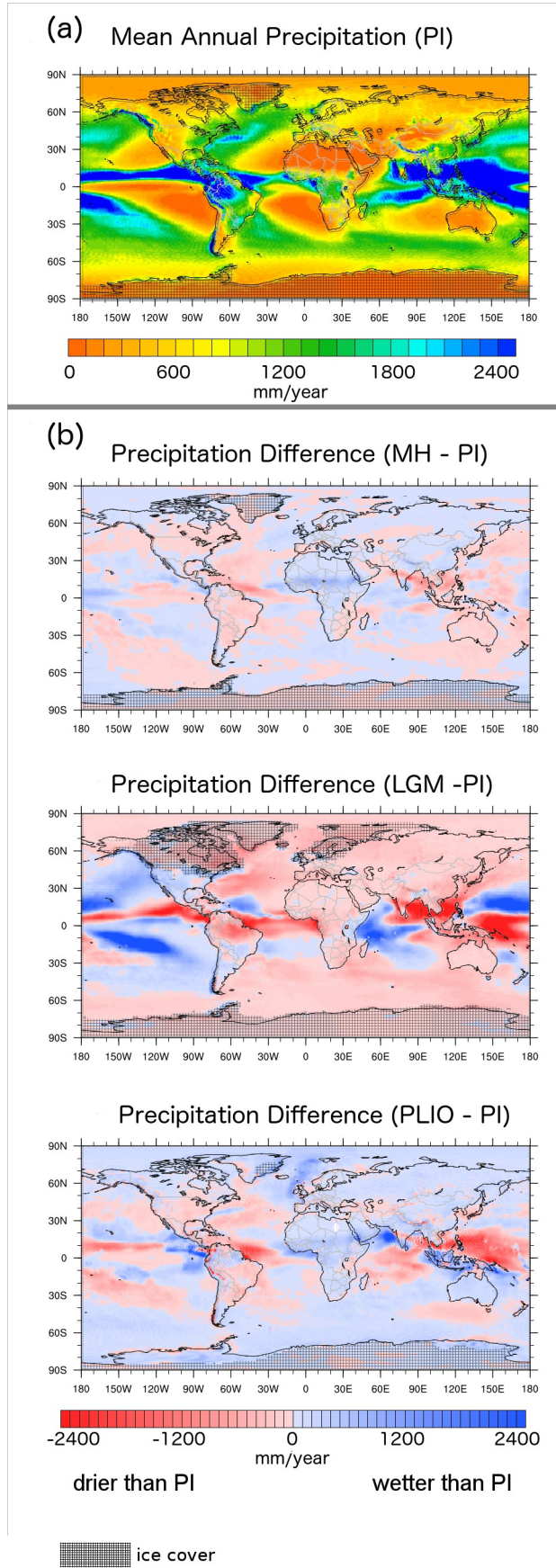


Figure 3

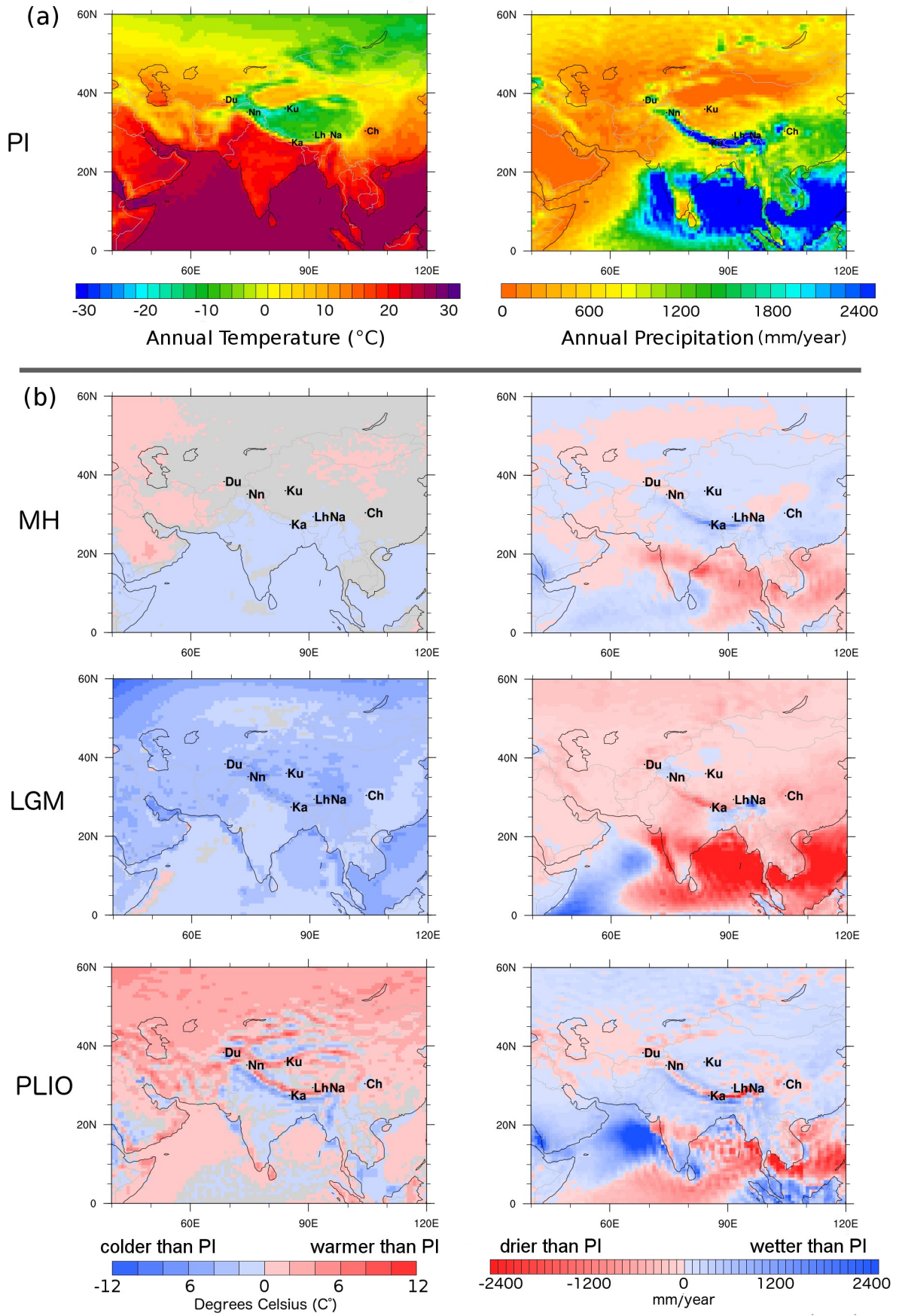


Figure 4

1601
1602
1603
1604
1605
1606
1607
1608
1609
1610
1611
1612
1613
1614
1615
1616
1617
1618
1619
1620
1621
1622
1623
1624
1625
1626
1627
1628
1629
1630
1631
1632
1633
1634
1635
1636
1637
1638
1639
1640
1641
1642
1643
1644
1645
1646
1647
1648
1649
1650
1651
1652
1653
1654
1655
1656
1657
1658
1659
1660

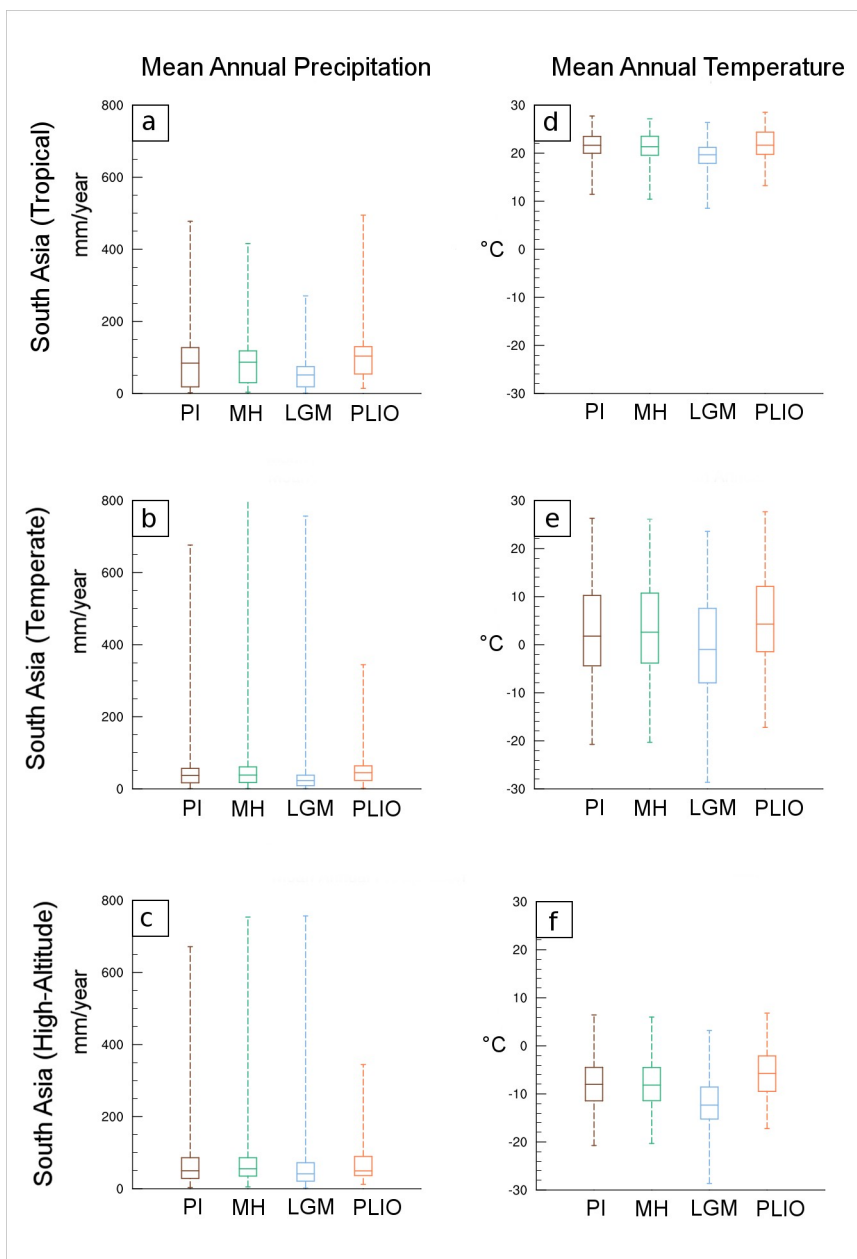


Figure 5

1661
 1662
 1663
 1664
 1665
 1666
 1667
 1668
 1669
 1670
 1671
 1672
 1673
 1674
 1675
 1676
 1677
 1678
 1679
 1680
 1681
 1682
 1683
 1684
 1685
 1686
 1687
 1688
 1689
 1690
 1691
 1692
 1693
 1694
 1695
 1696
 1697
 1698
 1699
 1700
 1701
 1702
 1703
 1704
 1705
 1706
 1707
 1708
 1709
 1710
 1711
 1712
 1713
 1714
 1715
 1716
 1717
 1718
 1719
 1720

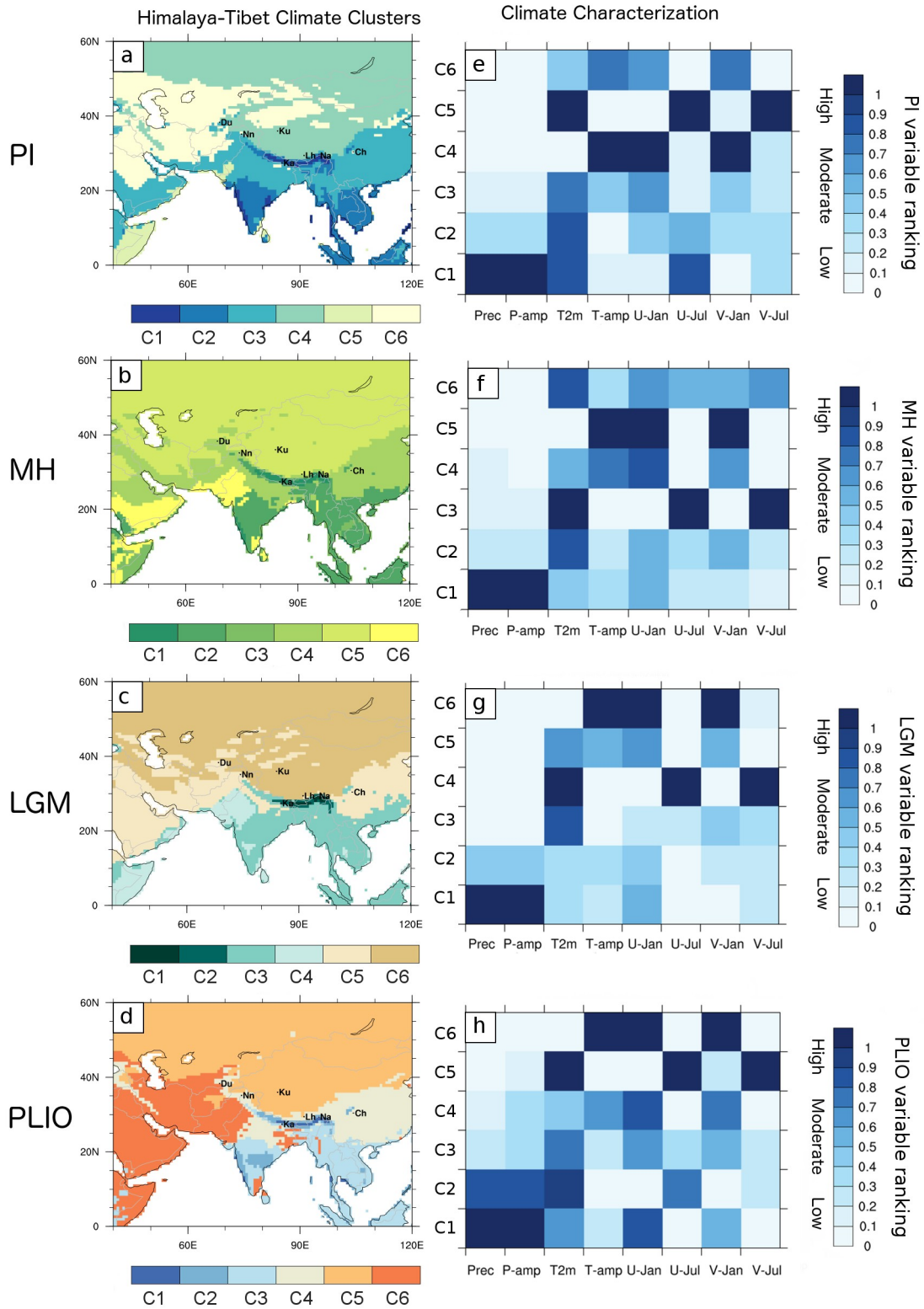


Figure 6

1721
 1722
 1723
 1724
 1725
 1726
 1727
 1728
 1729
 1730
 1731
 1732
 1733
 1734
 1735
 1736
 1737
 1738
 1739
 1740
 1741
 1742
 1743
 1744
 1745
 1746
 1747
 1748
 1749
 1750
 1751
 1752
 1753
 1754
 1755
 1756
 1757
 1758
 1759
 1760
 1761
 1762
 1763
 1764
 1765
 1766
 1767
 1768
 1769
 1770
 1771
 1772
 1773
 1774
 1775
 1776
 1777
 1778
 1779
 1780

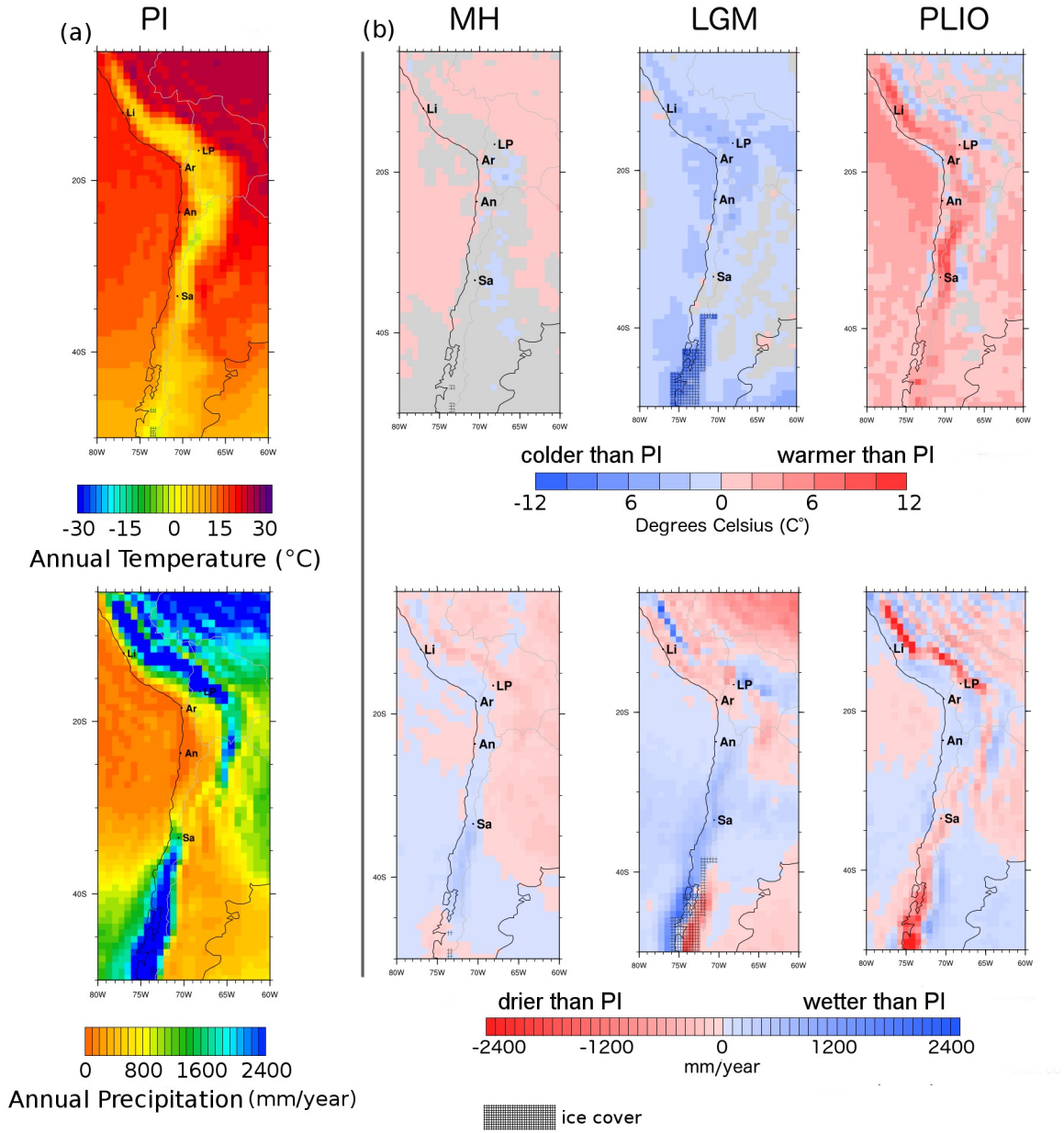


Figure 7

1781
1782
1783
1784
1785
1786
1787
1788
1789
1790
1791
1792
1793
1794
1795
1796
1797
1798
1799
1800
1801
1802
1803
1804
1805
1806
1807
1808
1809
1810
1811
1812
1813
1814
1815
1816
1817
1818
1819
1820
1821
1822
1823
1824
1825
1826
1827
1828
1829
1830
1831
1832
1833
1834
1835
1836
1837
1838
1839
1840

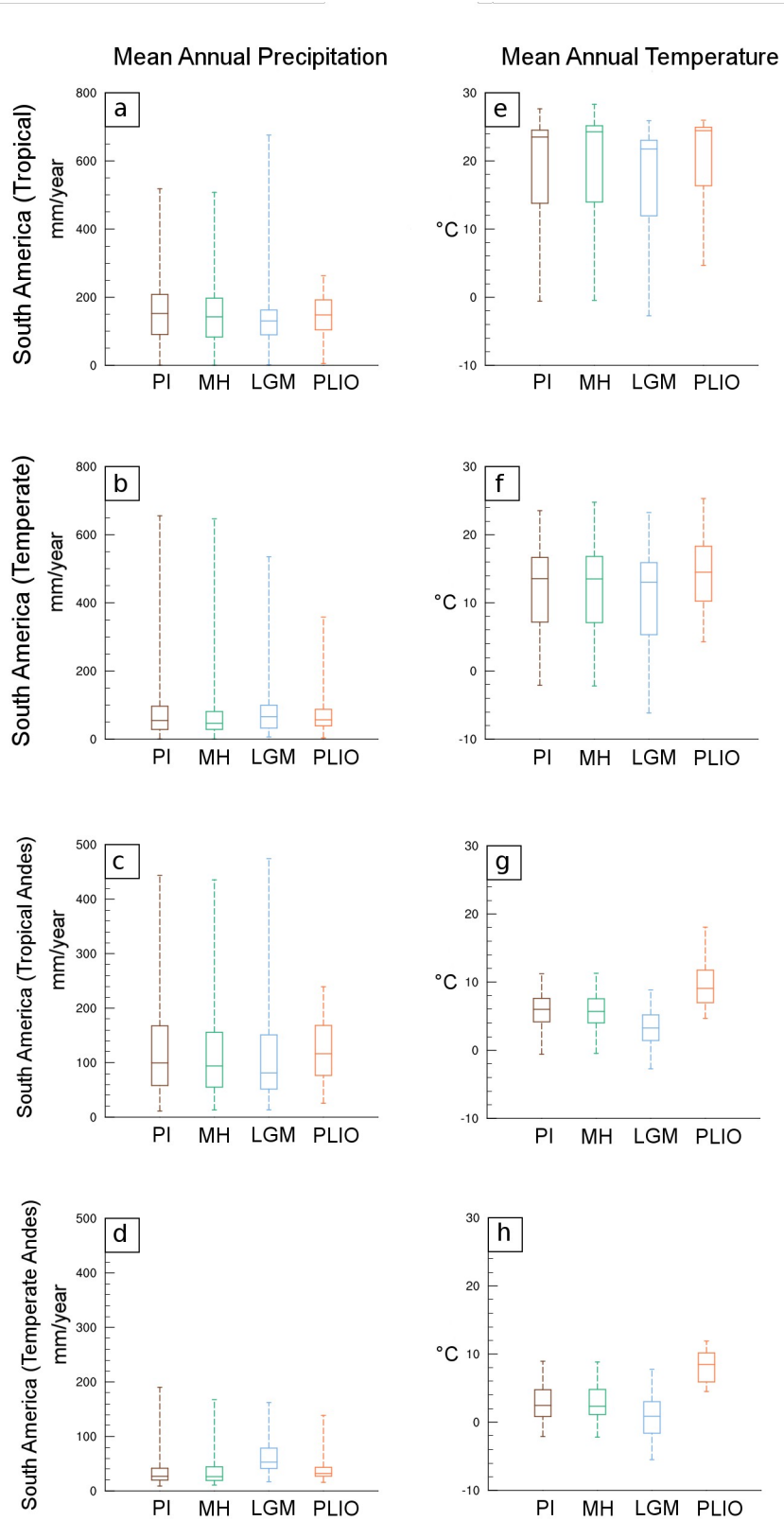


Figure 8

1841
1842
1843
1844
1845
1846
1847
1848
1849
1850
1851
1852
1853
1854
1855
1856
1857
1858
1859
1860
1861
1862
1863
1864
1865
1866
1867
1868
1869
1870
1871
1872
1873
1874
1875
1876
1877
1878
1879
1880
1881
1882
1883
1884
1885
1886
1887
1888
1889
1890
1891
1892
1893
1894
1895
1896
1897
1898
1899
1900

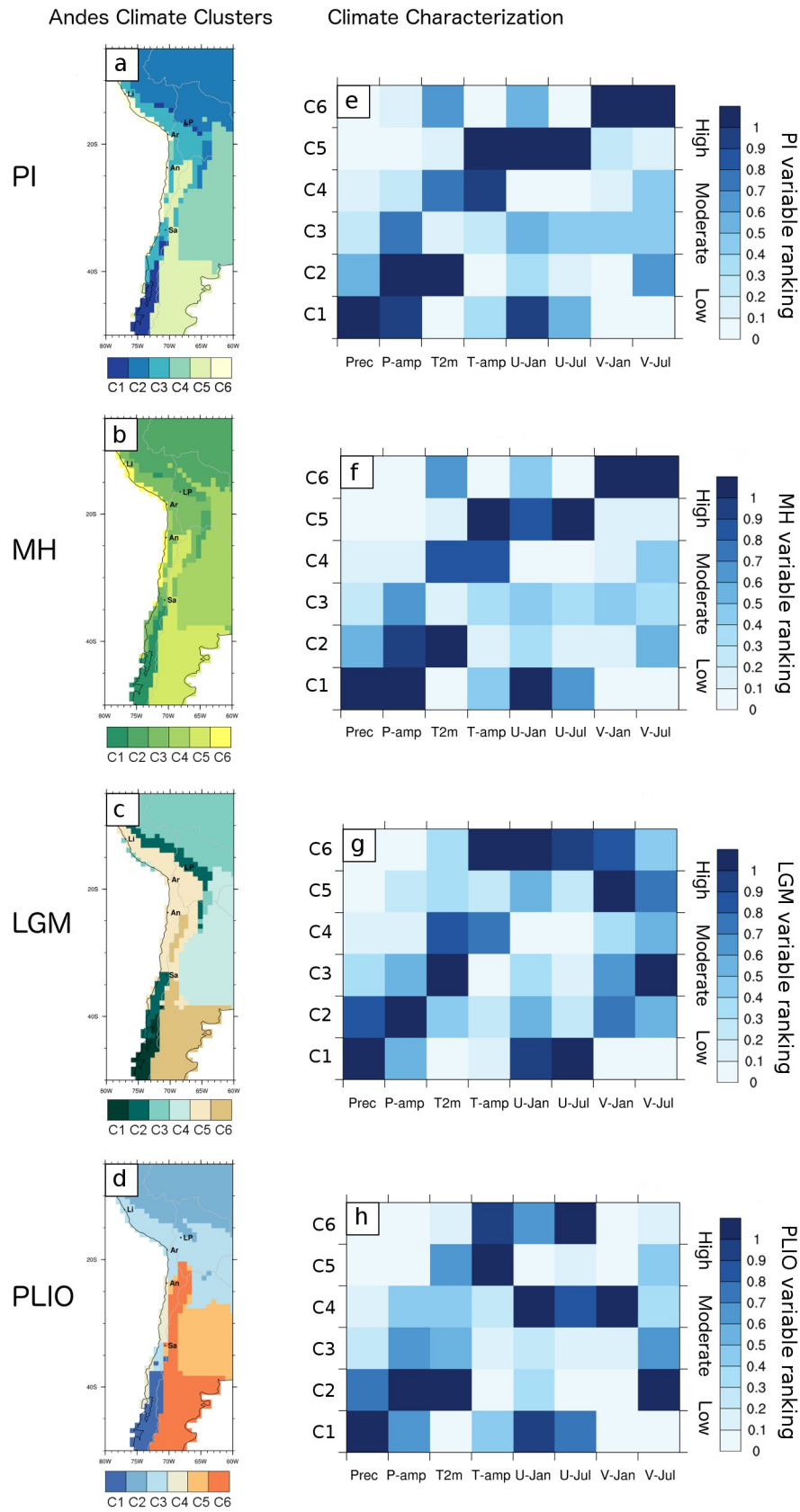


Figure 9

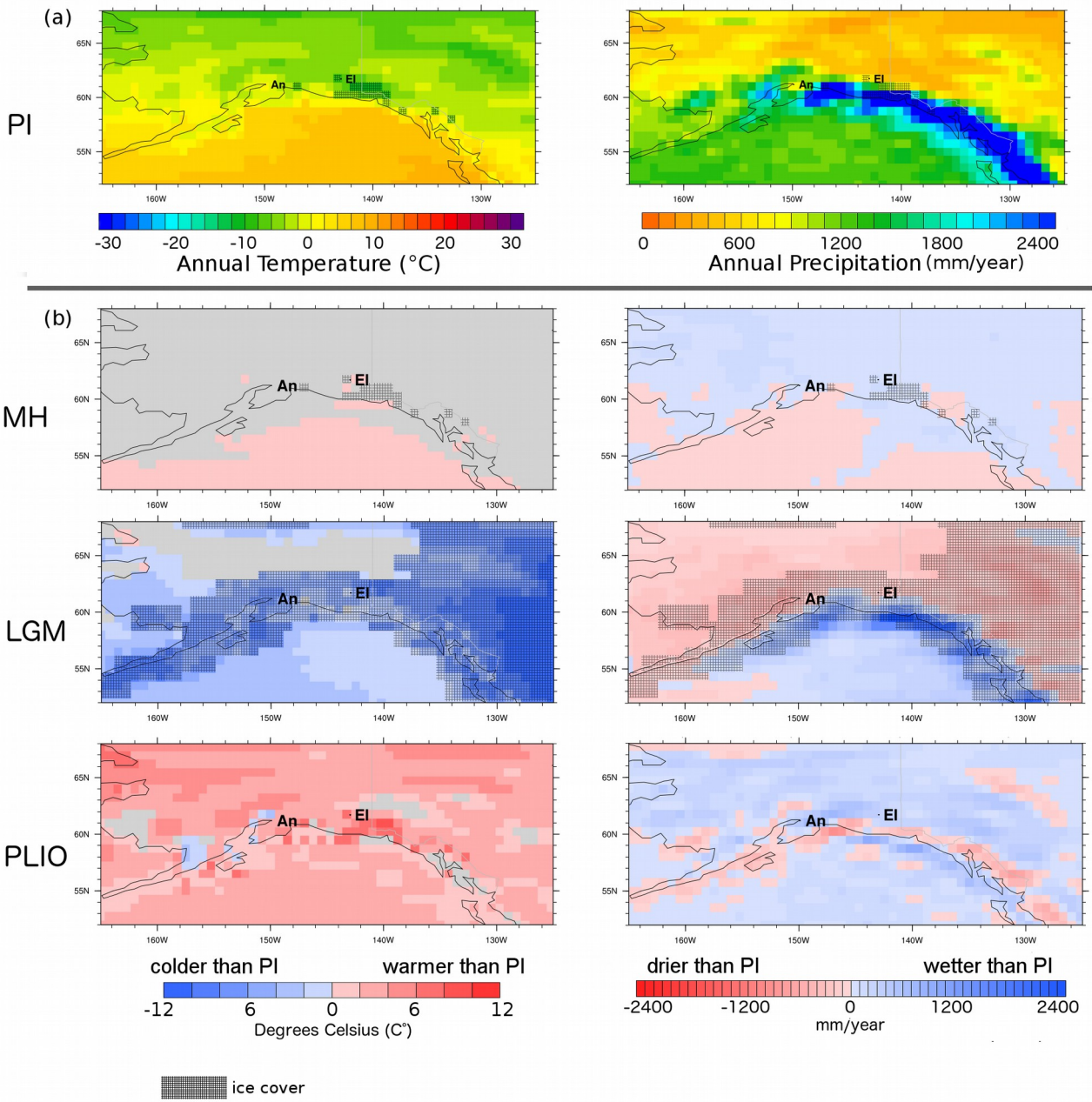


Figure 10

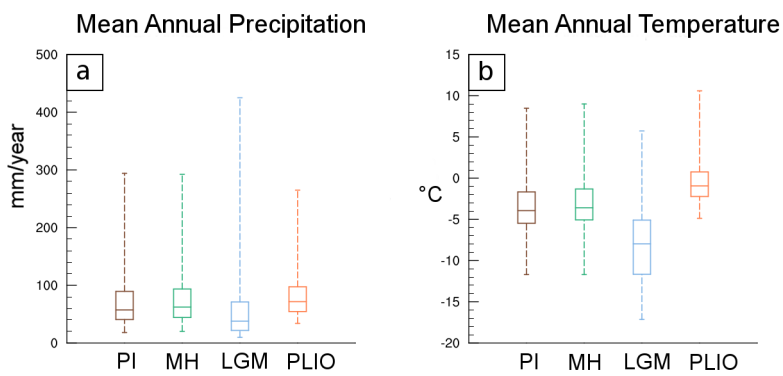


Figure 11

1902
1903
1904
1905
1906
1907
1908
1909
1910
1911
1912
1913
1914
1915
1916
1917
1918
1919

1920
1921
1922
1923
1924
1925
1926
1927
1928
1929
1930
1931
1932
1933
1934
1935
1936
1937
1938
1939
1940
1941
1942
1943
1944
1945
1946
1947
1948
1949
1950
1951
1952
1953
1954
1955
1956
1957
1958
1959
1960
1961
1962
1963
1964
1965
1966
1967
1968
1969
1970
1971
1972
1973
1974
1975
1976
1977
1978
1979

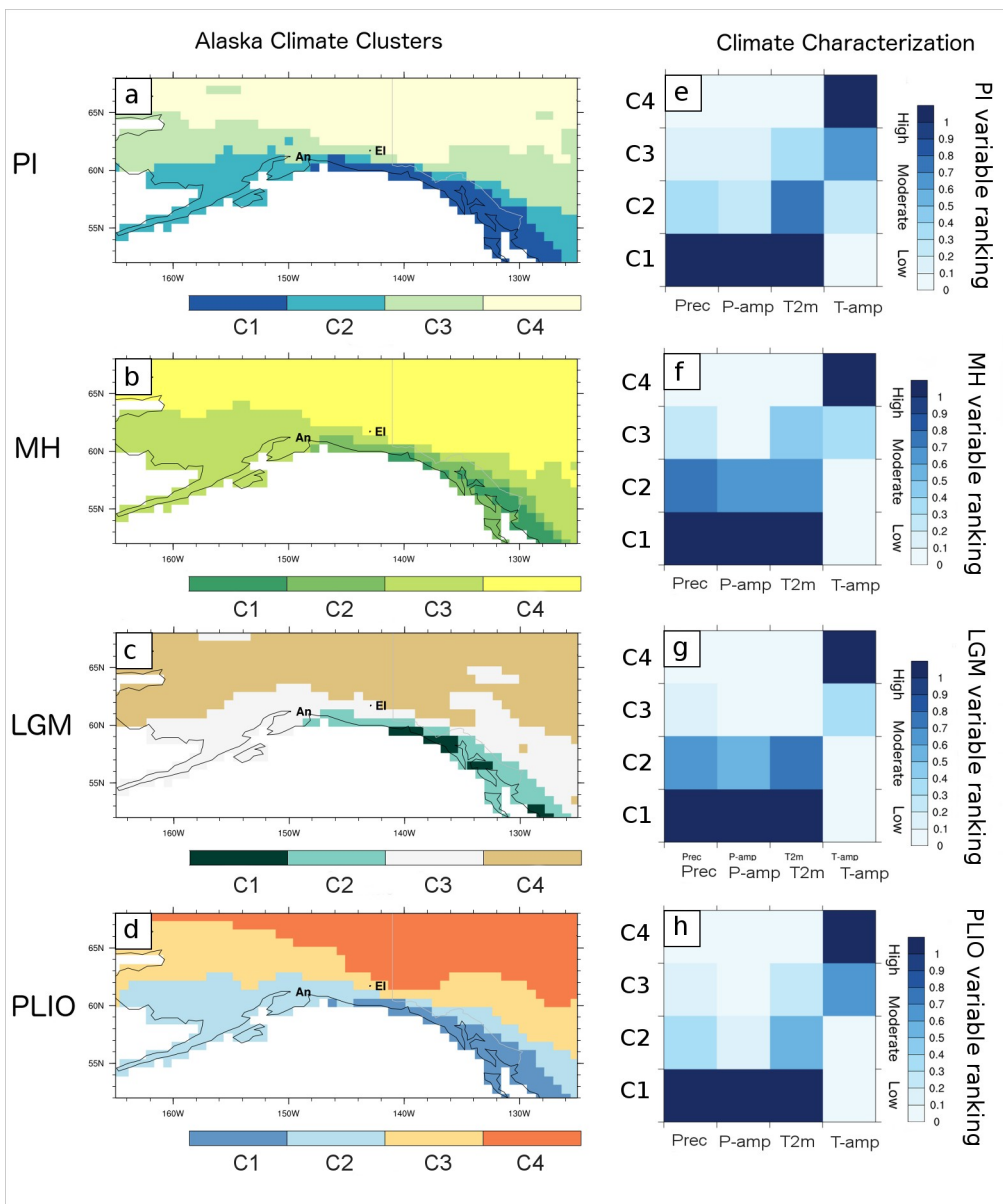


Figure 12

1980
1981
1982
1983
1984
1985
1986
1987
1988
1989
1990
1991
1992
1993
1994
1995
1996
1997
1998
1999
2000
2001
2002
2003
2004
2005
2006
2007
2008
2009
2010
2011
2012
2013
2014
2015
2016
2017
2018
2019
2020
2021
2022
2023
2024
2025
2026
2027
2028
2029
2030
2031
2032
2033
2034
2035
2036
2037
2038
2039

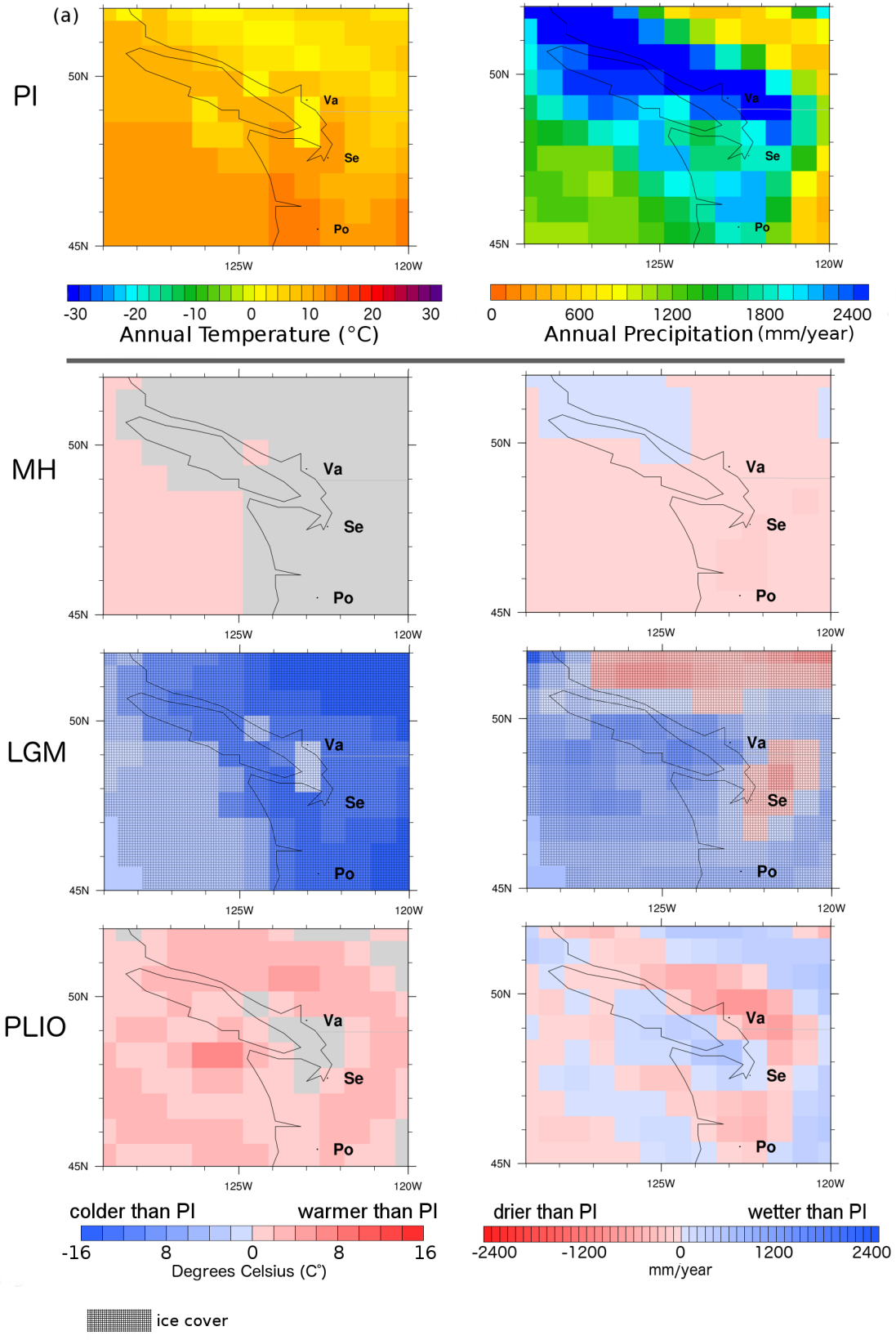


Figure 13

2040
2041
2042
2043
2044
2045
2046
2047
2048
2049
2050
2051
2052
2053
2054
2055
2056
2057
2058
2059
2060
2061
2062
2063
2064
2065
2066
2067
2068
2069
2070
2071
2072
2073
2074
2075
2076
2077
2078
2079
2080
2081
2082
2083
2084
2085
2086
2087
2088
2089
2090
2091
2092
2093
2094
2095
2096
2097
2098
2099

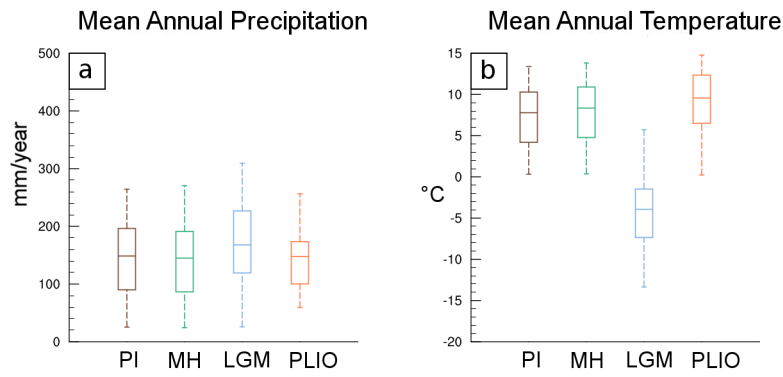


Figure 14

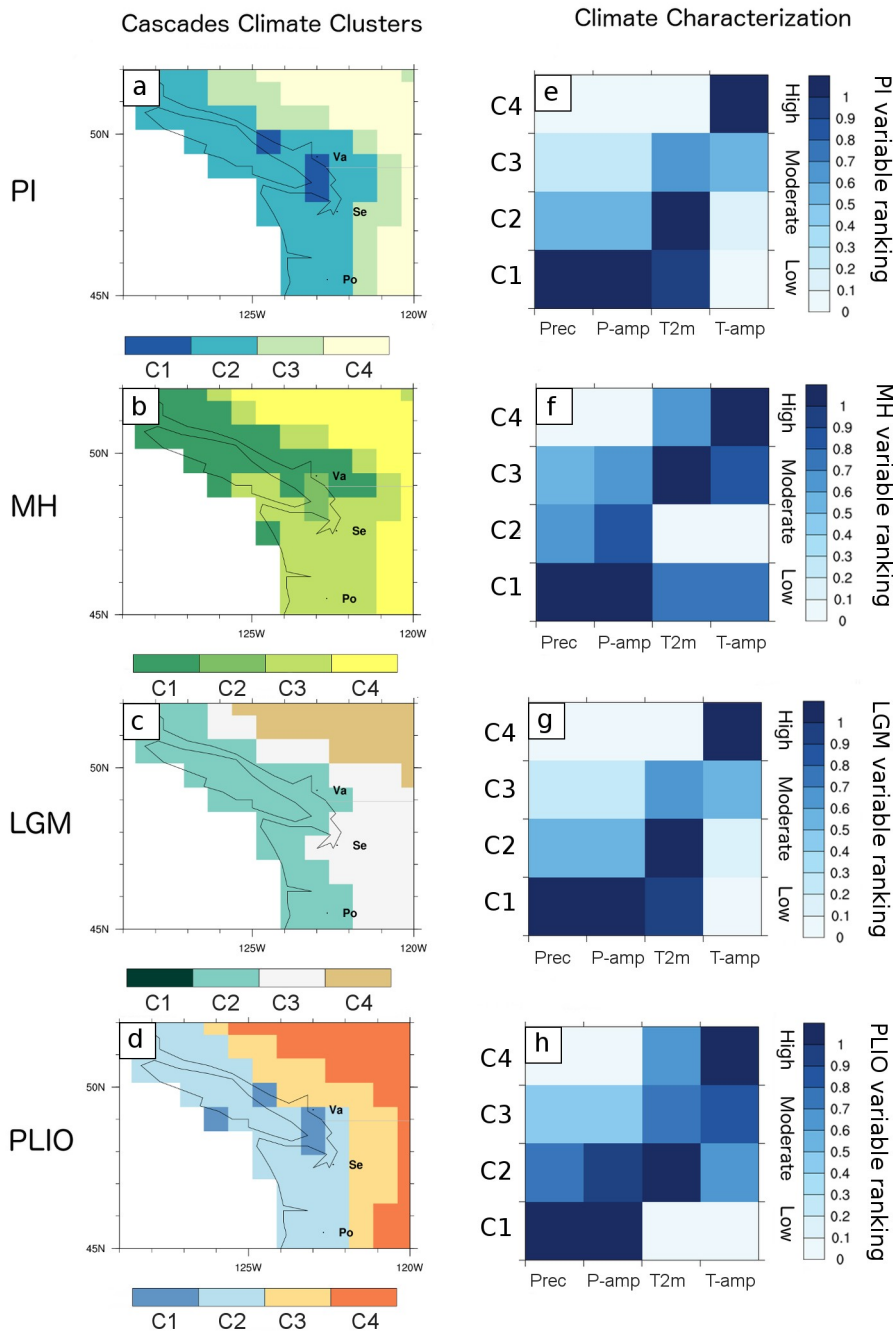


Figure 15

2100
2101
2102
2103
2104
2105
2106
2107

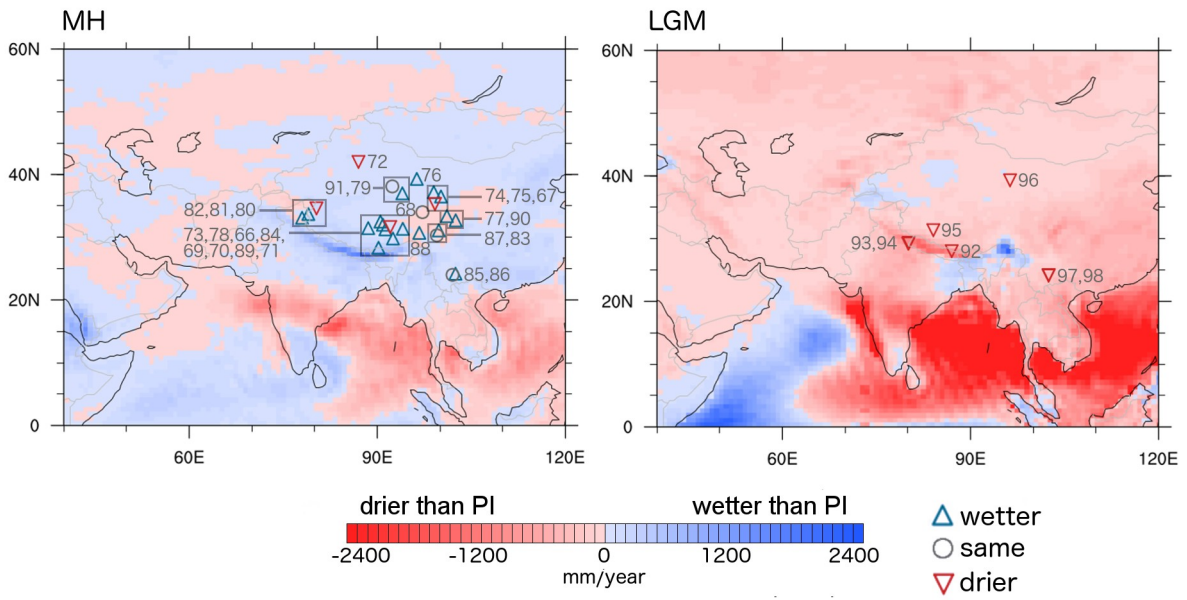


Figure 16

2108
2109
2110
2111
2112
2113
2114
2115
2116
2117
2118
2119
2120
2121
2122
2123
2124
2125
2126
2127
2128
2129
2130
2131
2132
2133
2134
2135
2136
2137
2138
2139
2140
2141
2142
2143
2144
2145
2146
2147

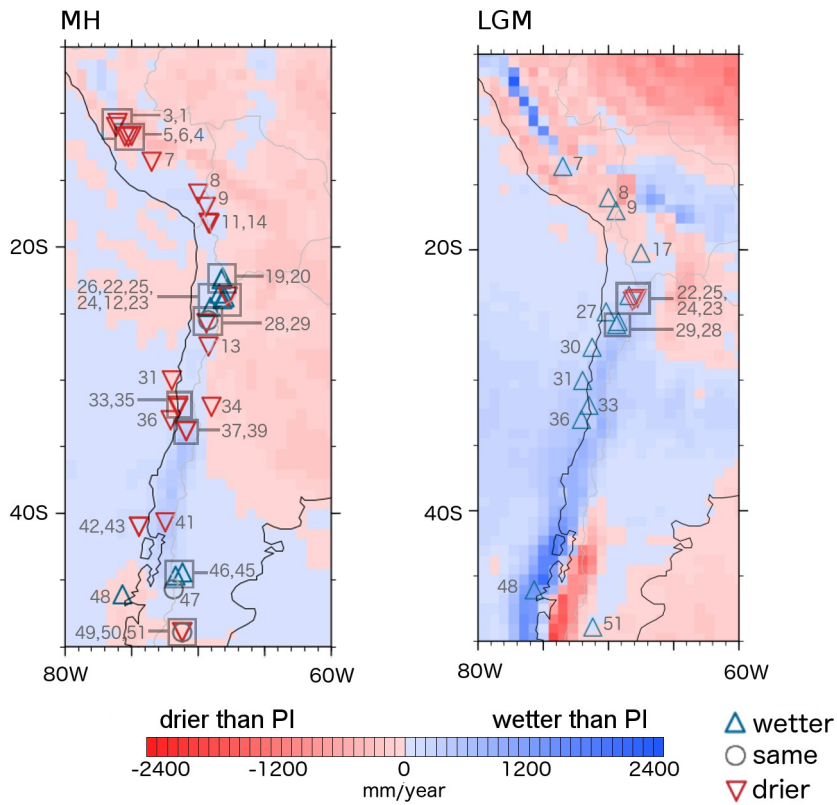
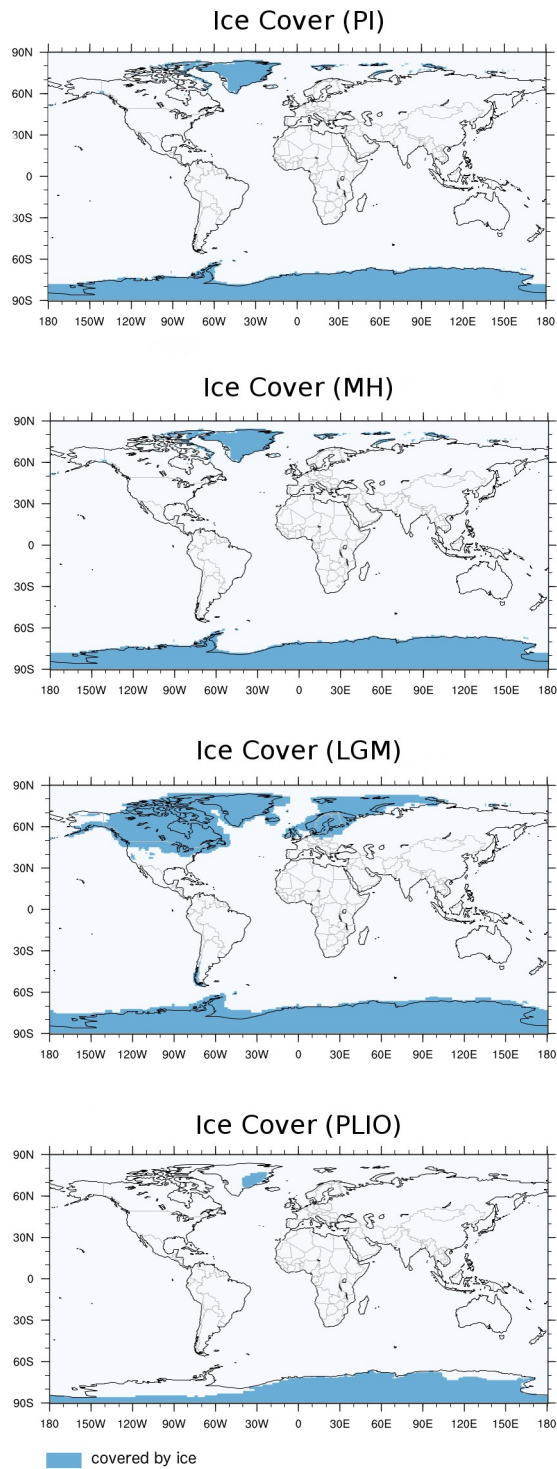


Figure 17

2148
2149
2150
2151
2152
2153
2154
2155
2156
2157
2158
2159
2160
2161
2162
2163
2164
2165
2166
2167
2168
2169
2170
2171
2172
2173
2174
2175
2176
2177
2178
2179
2180
2181
2182
2183
2184
2185
2186
2187
2188
2189
2190
2191
2192
2193
2194
2195



Supplemental Figure S1